Cyclic Nucleotide Regulated Calcium Signaling in Vascular and Jurkat T Cells

LEUNG, Yuk Ki

A Thesis submitted in Partial Fulfillment
of the Requirements for the Degree of
Doctor of Philosophy
in
Physiology

The Chinese University of Hong Kong

August 2010

ProQuest LLC.
789 East Eisenhower Parkway
P.O. Box 1346
Ann Arbor, MI 48106 - 1346

Thesis/Assessment Committee

Professor Yung, Wing Ho (Chair)

Professor Yao, Xiao Qiang (Thesis Supervisor)

Professor Kong, Siu Kai (Committee Member)

Professor Ballard, Heather J (External Examiner)

Abstract of thesis entitled:

Cyclic Nucleotide Regulated Calcium Signaling in Vascular and Jurkat T Cells

Submitted by LEUNG, Yuk Ki

for the degree of Doctor of Philosophy

at the Chinese University of Hong Kong in August 2010

Thromboxane A_2 (TxA_2)-induced smooth muscle contraction has been implicated in cardiovascular, renal and respiratory diseases. This contraction can partly be attributed to TxA_2-induced Ca^{2+} influx, which activates the Ca^{2+}-calmodulin-MLCK pathway. This study aims to identify the channels that mediate TxA_2-induced Ca^{2+} influx in vascular smooth muscle cells. Application of U-46619, a thromboxane A_2 mimic, resulted in a constriction in endothelium-denuded small mesenteric artery segments. The constriction relied on the presence of extracellular Ca^{2+}, because removal of extracellular Ca^{2+} abolished the constriction. This constriction was partially inhibited by a L-type Ca^{2+} channel inhibitor nifedipine (0.5-1 μM). The remaining component was inhibited by L-*cis*-diltiazem, a selective inhibitor for CNG channels, in a dose-dependent manner. Another CNG channel blocker LY83583 [6-(phenylamino)-5,8-quinolinedione] had similar effect. In primary cultured smooth muscle cells derived from rat aorta, application of U46619 (100 nM) induced a rise in cytosolic Ca^{2+}, which was inhibited by L-*cis*-diltiazem. Immunoblot experiments confirmed the presence of CNGA2 protein in vascular smooth muscle cells. These data suggest a functional role of CNG channels in U-46619-induced Ca^{2+} influx and contraction of smooth muscle cells.

cAMP-elevating agents such as adenosine and epinephrine (after binding to β-adrenergic receptor) contribute to local vascular dilation and some of these dilations are endothelium-dependent. Previous intracellular Ca^{2+} imaging studies in mouse microvessel endothelial cells reported that addition of adenosine or epinephrine induced a Ca^{2+} influx which is blocked by CNG channel blockers such as L-*cis*-diltiazem or LY83583. Inside-out patch clamp studies confirmed the existence of a cAMP-activated current in endothelial cells, strongly suggesting a functional role of CNG, in particular CNGA2, channels in endothelial cells. The current study went further to show that similar Ca^{2+} influx in response to adenosine or epinephrine occurred in endothelial cells in freshly isolated mouse aortic strips and was again blocked by L-*cis*-diltiazem. By measuring the isometric force developed in mouse aortic strips, we showed that CNGA2 channel-mediated Ca^{2+} influx in endothelial cells contributed to the endothelium-dependent vascular dilatation in response to adenosine and epinephrine.

In Jurkat T cells, cyclic nucleotides regulated Ca^{2+} mobilization in a different way. Fluorescence-imaging studies showed that cGMP inhibited store-operated Ca^{2+} influx and histamine-induced Ca^{2+} rise in Jurkat T cells through activation of PKG.

In conclusion, cyclic nucleotides play a vital role in the regulation of intracellular Ca^{2+} concentration in vascular cells and Jurket T cells.

論文擇要

心血管，腎臟和呼吸系統疾病均被認爲與血栓素 A2（TXA2）引起的平滑肌收縮有關。部分這種收縮是由 TxA2 所引起的細胞鈣內流，通過鈣調蛋白-肌球蛋白輕鏈激酶所造成。這項研究旨在找出血栓素 A2 引起的血管平滑肌細胞鈣離子內流所使用的離子通道。實驗中使用的 U－46619 是一種血栓素 A2 的類似物，在剝脫內皮的動脈血管上，它能引起動脈血管收縮。這收縮依賴細胞外鈣離子的存在，去除細胞外的鈣離子令血管無法收縮。L -型鈣離子通道阻滯劑硝苯地平（nifedipine）(0.5-1μM）能抑制一部分血栓素 A2 引起的血管收縮。其餘部分能被一種環化核苷酸門控的離子通道(CNG-Cyclic nucleotide-gated channels) 的選擇性抑製劑 L-cis-diltiazem 所抑制，該抑制隨著劑量加大而擴大。另一個環化核苷酸門控的離子通道阻滯劑 LY83583 也有類似的效果。用大鼠主動脈原代培養的平滑肌細胞的實驗證明 U46619（100 nM）能引發細胞內鈣離子上升，這鈣離子上升也能被 L-cis-diltiazem 抑制。免疫印跡實驗證實了 CNGA2 蛋白存在於血管平滑肌細胞上。這些數據顯示 U－46619 會引起 CNG 通道的開放，導致細胞鈣離子內流，進而收縮平滑肌細胞。

另一方面，環一磷酸腺苷(cAMP)提升劑，如腺苷(Adenosine)，腎上腺素(Epinephrine)（在結合 beta-腎上腺素受體後）有助於血管擴張，這些擴張在某些血管是內皮依賴性的。過去在細胞層面的研究顯示，腺苷或腎上腺素誘導小鼠微血管內皮細胞的鈣離子內流，可能被 CNG 通道的抑製劑 L-cis-diltiazem 或 LY83583 所抑制。膜片鉗研究也證實內皮細胞存在一個由環一磷酸腺苷激活的電流，這是一個強烈的證據顯示 CNG 通道，特別是 CNGA2 通道，影響着內皮細胞的功能。目前的研究還進一步表明，類似的腺苷或腎上腺素引起的細胞鈣離子內流的反應同樣地發生在剛取出的小鼠主動脈血管內皮細胞上，而 L-cis-diltiazem 大大抑制了這種鈣離子湧入的反應。通過量度血管的張力，我們發現透過開放 CNGA2 通道造成的內皮細胞鈣離子內流是腺苷，腎上腺素引起的血管舒張的主要原因。

在 Jurkat 細胞中，環化核苷酸以不同的方式調節細胞內鈣離子的濃度。利用熒光測定法鈣顯影技術的研究顯示，環一磷酸鳥苷（cGMP）透過激活蛋白激酶 G (PKG)，抑制鈣儲備耗竭操縱型鈣內流和組織胺 (histamine) 引起的鈣內流。

總括而言，環化核苷酸在調節血管細胞和 T 淋巴細胞內鈣離子的濃度方面扮演着重要的角色。

Acknowledgements

I owe my deepest gratitude to my supervisor, Prof. Xiaoqiang Yao, whose encouragement, guidance, support and patience in the past few years enabled me to develop an understanding in the cardiovascular research field and experience the process of transforming an idea to a research project and finally to a thesis. Besides making himself always available for discussion and advices, he also strived to create a friendly atmosphere in the laboratory that encouraged knowledge exchange and questioning.

I would also like to express my heartfelt thanks to Prof. Yu Huang for his valuable advices and support in both my research work and personal life. His stimulating discussion has greatly enriched the content of the project.

Special thanks to Prof. Heather Ballard (Physiology Department, University of Hong Kong), Prof. Siu-Kai Kong (Department of Biochemistry, Chinese University of Hong Kong and Prof. Wing-Ho Yung (School of Biomedical Science, Chinese University of Hong Kong) for serving on the thesis committee.

Great thanks also go to Dr. Bing Shen for his inspiring discussion, critical comments and technical support in the research work. Dr. Anna Kwan is another important person that has made a significant contribution to this thesis.

I gratefully thank all labmates in the department of Physiology, in particular Mr. Chi-Wai Lau, Dr. Jacqueline Ngai and Dr. Xin Ma, for their generous help in my laboratory work.

Financially, the research work was supported by Hong Kong RGC 4526/06M.

Last but not least, I would like to thank my parents for their unflagging love and support throughout my life and study. You are the best parents.

Abbreviations

AC	adenylate cyclase
Ach	acetylcholine
ATP	adenosine-5'-triphosphate
BAPTA	1,2-bis(o-aminophenoxy)ethane-N,N,N',N'-tetraacetic acid
$[Ca^{2+}]_i$	cytosolic Ca2+ concentration
CaM	calmodulin
cAMP	cyclic adenosine monophosphate
cGMP	cyclic guanosine monophosphate
CNG	cyclic nucleotide gated channels
CRAC	Ca^{2+} release-activated Ca^{2+} channel
COX	cyclooxygenase
DAG	diacylglycerol
DMEM	Dulbecco's Modified Eagle Medium
eNOS	endothelial nitric oxide synthase
EGTA	ethylene glycol tetraacetic acid
EDCF	endothelium-derived contacting factor
GEF	guanine nucleotide exchange factor
IP_3	inositol trisphosphate
L-NAME	N(G)-nitro-L-arginine methyl ester
LY 83583	6-(phenylamino)-5,8-quinolinedione
KHS	Krebs-Henseleit solution
MLCK	myosin light chain kinase
MLCP	myosin light chain phosphatase
MYPT1	myosin phosphatase target subunit 1
NECA	N6-Ethyl-carboxamido Adenosine
NFAT	nuclear factors of activated T cells
NO	nitric oxide
NPSS	Normal physiological saline solution
ODQ	1H-[1,2,4]Oxadiazolo[4,3-a]quinoxalin-1-one
OSN	olfactory sensory neuron
PDE	phosphodiesterase
PKA	protein kinase A
PKG	protein kinase G
pGC	particulate guanylyl cyclase
PLC	phospholipase C
PVDF	polyvinylidene difluoride

ROCC	receptor-operated calcium channel
ROK	Rho-associated kinase
RyR	ryanodine receptors
SDS-PAGE	sodium dodecyl sulfate polyacrylamide gel electrophoresis
SERCA	sarcoplasmic/endoplasmic reticulum Ca^{2+} ATPase
sGC	soluble guanylyl cyclase
SHR	spontaneously hypertensive rat
siRNA	small interfering RNA
SMC	smooth muscle cell
SNAP	*S*-nitroso-*N*-acetylpenicillamine
SOCC	store-operated calcium channel
SOCE	store-operated calcium entry
SR	sarcoplasmic reticulum
TCR	T cell receptor
TEMED	N,N,N',N'-tetramethyl-ethylenediamine
TP receptor	thromboxane-prostanoid receptor
TRP	transient receptor potential
TRPC	canonical transient receptor potential
Tween 20	polyoxyethyleneesorbitan monolaurate
TxA_2	thromboxane A_2
U46619	9,11-dideoxy-11α,9α-epoxymethanoprostaglandin F2α
U73122	1-[6-[((17β)-3-Methoxyestra-1,3,5[10]-trien-17-yl)amino]hexyl]-1H-pyrrole-2,5-dione
U73343	1-[6-[((17β)-3-Methoxyestra-1,3,5[10]-trien-17-yl)amino]hexyl]-2,5-pyrrolidinedione
VOCC	voltage-operated calcium channel
WKY	Wistar Kyoto rat

Table of Content

Tables and Figures

Chapter 1

General Introduction

1.1 Cardiovascular system

The cardiovascular system consists of two sets of blood vessels, the systemic and pulmonary circulations, joined together at the heart. The systemic circulation begins at the left ventricle, the aorta branch off to arteries, arterioles and capillaries to perfuse every cell in the body, and then drains back to the right atrium through a set of veins. Distribution of blood flow among tissues is controlled primarily at the level of arterioles while nutrients, metabolic wastes and gaseous exchange take place in capillaries. As different organs serve different functions in the body, their blood supply and hence responsiveness of the vascular bed to different agents varies. Arterial blood pressure and resistance may be adjusted according to their metabolic needs, under the influence of sympathetic and parasympathetic nervous system, and by hormonal control.

1.1.1 Structure of blood vessels

Except capillaries which only consist of an endothelium, blood vessel walls may be divided into three layers, a tunica intima consisting of an endothelium and in some large arteries, layers of smooth muscle cells; a tunica media consisting of a smooth muscle layer sandwiched between two elastic laminae; and a tunica adventitia of connective tissue containing fibroblasts and nerve endings. Gap junctions which allow direct communication between cells in the form of ions and small molecules exist among endothelial cells, between endothelial cells and smooth muscle cells (myoendothelial gap junctions) and among smooth muscle cells, with decreasing extent. Myoendothelial gap junctions exist in some arteries and the extent of

connection seems to be inversely correlated with artery size (Takano et al. 2005). Endothelial cells serve as a barrier between circulating blood and other cells in the body, release vasoactive agents in response to neurohumoral and physical stimuli, and interact with other cells through gap junction or the extracellular matrix, to regulate the vascular tone. The vasoactive agents may act on the underlying smooth muscle cells affecting their contractility and proliferation, or modulate the activity of platelets and leukocytes. Smooth muscle layer of arterioles is extensively innervated by sympathetic and to a lesser extent parasympathetic nerve fibers. Smooth muscle cells are spindle-shaped and interconnected by gap junctions that facilitate synchronized contraction. Myogenic tone of vascular smooth muscle adjusts the contractility of the vessel in response to intravascular pressure.

1.1.2 Vascular smooth muscle cells

Up to 90% of the cell volume of smooth muscle cells (SMCs) is occupied by the contractile machinery including the myofilaments, intermediate filaments and the associated dense bodies (Gabella, 1981).

Vascular smooth muscle contractility is influenced by the sympathetic nervous system, circulating hormones and vasoactive metabolites released from endothelial cells.

1.1.2.1 Smooth muscle cell contraction mechanism

SMC undergoes slow and sustained contraction which is dependent on an increase in cytosolic Ca^{2+} concentration ($[Ca^{2+}]_i$), which may result from Ca^{2+} influx through ion channels or Ca^{2+} release from intracellular stores such as the endoplasmic or sarcoplasmic reticulum, or a combination of both. Elevation of

intracellular Ca^{2+} activates Ca^{2+}/calmodulin-dependent myosin light chain kinase (MLCK) which then phosphorylates myosin light chains (MLC20) in the presence of ATP. Phosphorylation of MLC20, the regulatory subunit on myosin head, leads to the formation of a cross-bridge between the myosin head and the actin filament, and hence muscle contraction. Myosin light chain phosphatase (MLCP) dephosphorylates MLC20 and relaxes the muscle. Ca^{2+} sensitization enables sustained muscle contraction at nearly basal level of $[Ca^{2+}]_i$. As the phosphorylation status of MLC20 reflects the activities of both MLCK and MLCP, Ca^{2+} sensitization may be achieved by inhibition of MLCP or sensitization of MLCK. Rho kinase catalyzes phosphorylation of MYPT1, the myosin phosphatase target subunit of MLCP, at several sites, the major ones are Thr696 and Thr853 (Kawano et al., 1999), causing inhibition of the MLCP activity. Besides the regulation by MYPT1, phosphorylation of CPI-17 at Thr38 also exerts an inhibitory effect on MLCP. Both protein kinase C and Rho kinase have been shown to phosphorylate CPI-17 (Dimopoulos et al., 2007). Elevated intracellular Ca^{2+} level increase the activity of Ca^{2+}-ATPase located on the plasma membrane and the sarchoplasmic reticulum leading to extrusion of Ca^{2+} to extracellular region or reuptake of Ca^{2+} to internal stores, bring the cytosolic Ca^{2+} concentration back to the resting low level.

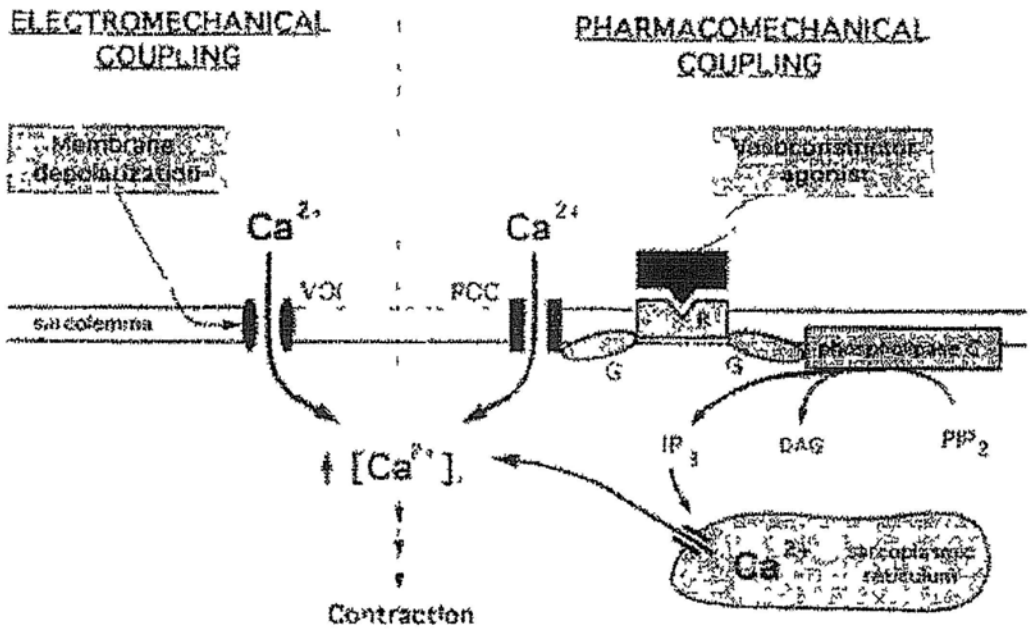

Figure 1-1 General mechanism of smooth muscle cell activation.

VOC, voltage-operated Ca^{2+} channel; ROC, receptor-operated Ca^{2+} channel; R, agonist specific receptor; G, GTP-binding protein; PIP2, phosphatidyl inositol biphosphate; InsP3, inositol triphosphate; DAG, diacylglycerol. Adapted from Mohrman & Heller, 1997

1.1.2.2 Ca^{2+}-permeable channels on smooth muscle cells

Currently known Ca^{2+}-permeable channels present on SMCs may be classified into voltage-operated (VOCC), receptor-operated (ROCC), store-operated (SOCC) and mechanosensitive (Davis et al., 1992) types. L-type and T-type Ca^{2+} channels are the major VOCC identified in SMC, with L-type dominant in large arteries and increasing importance of T-type towards small resistance arteries (Braunstein et al., 2009, Morita et al., 1999). Gustafsson et al. found that in small mesenteric arterioles with a diameter <40 mm, L-type Ca^{2+} channels are absent and T-type Ca^{2+} channels play a dominant role in depolarization-induced contraction (2001). Compared to T-type Ca^{2+} channels, L-type Ca^{2+} channels have a higher single channel

conductance, activate at a more positive potential and for a longer time while T-type Ca^{2+} channels are characterized by a low voltage activation threshold and rapid inactivation during depolarization. Mechanosensitive Ca^{2+} channels include TRP channels.

1.1.2.3 Sarcoplasmic reticulum (SR) and its role in smooth muscle cell

SR plays an important role in the Ca^{2+} homeostasis in smooth muscle cells. SR accounts for ~5% of cell volume of SMC in aorta and pulmonary artery, but falls to ~2% in mesenteric arteries. It may be classified as peripheral SR, near the plasma membrane and are often found to be in close proximity to caveolae, or central SR, which are located away from the membrane. Some of the currently known stimulations for Ca^{2+} release from SR include increased IP_3 generated from stimulation of specific receptors, calcium-induced-calcium release involving the activation of ryanodine receptors by increased $[Ca^{2+}]_i$, Ca^{2+} store depletion and increase in nicotinic acid adenine dinucleotide phosphate. Depending on the localization and amplitude, such Ca^{2+} release may give rise to Ca^{2+} sparks (local) or Ca^{2+} waves (global) which may act on contraction proteins directly, act on ryanodine receptors to elicit more Ca^{2+} release, or differentially activate several types of Ca^{2+} activated ion channels on the plasma membrane. In smooth muscle cells, the two major types of Ca^{2+} activated ion channels on plasma membrane are Cl_{Ca} and K_{Ca} channels. K_{Ca} channels include BK, SK and IK channels with BK channels having the largest conductance and sensitive to both Ca^{2+} and voltage. Activation of K^+ channels will produce spontaneous transient outward currents leading to membrane hyperpolarization and muscle relaxation. Cl_{Ca} channels have a higher affinity for Ca^{2+} than BK channels and less sensitive to voltage. Activation of Cl^- channels produces

transient inward currents and membrane depolarization which may lead to the opening of VOCC and increase muscle contractility. Thus, SR, as an internal store of Ca^{2+}, may increase muscle contraction by a Ca^{2+} amplification mechanism or reduce excitability and limit contraction through a Ca^{2+} spark/spontaneous transient outward current coupling mechanism.

1.1.3 Endothelial cell

Endothelial cells are involved in vaso-regulation and in normal circumstances, play an anti-thrombotic and anti-adhesive role.

During inflammation, the property of endothelial cells changes profoundly by the action of cytokines to the one that promotes the formation of thrombus and adhesion of platelets and leukocytes. Permeability to macromolecules also increases significantly.

The main agents affecting vascular tone that are released by endothelial cells include endothelium derived relaxing factors such as NO, prostaglandins, endothelium derived hyperpolaring factor (EDHF) and endothelium derived constricting factors (EDCF). Upon stimulation, a change in intracellular Ca^{2+} is often required to activate the synthesis and release of these agents. Ca^{2+} homeostasis is a dynamic equilibrium between Ca^{2+} in and out through the various calcium pumps and channels on plasma membrane and internal calcium stores. Global and localized increase in $[Ca^{2+}]_i$ in endothelial cells may lead to different or even opposing vascular responses. Transient increase in calcium may be a result of the opening of ligand-gated calcium channels or a Ca^{2+} release from internal stores while a sustained rise in Ca^{2+} level must be maintained by Ca^{2+} influx. Receptor-coupled and stretch-activated Ca^{2+} channels are abundant on endothelial cells, but voltage-gated

Ca^{2+} channels are rare and seem to be reported in microvascular endothelial cells only. The presence of T-type channels ($Ca_V3.2$) was reported on endothelial cells of the terminal arteriole from the rat mesenteric fat pad by Jensen et al (2009) and another subtype of T-type channels (Cav3.1) was found on pulmonary microvascular endothelial cells (Zhou & Wu, 2006). Rate of Ca^{2+} entry may also be affected by channels other than Ca^{2+} channels through their effect on membrane potential. The resting membrane potential of endothelial cells is largely determined by K^+ channels, including K_{ir}, BK_{Ca}, IK_{Ca}, SK_{Ca}, K_{ATP}, K_v and shear stress activated K^+ channels (Adams & Hill, 2004). Same as in other cell types, Ca^{2+} may release from internal stores by the stimulation of IP_3 receptor or RyR receptors. Global increase in $[Ca^{2+}]_i$ in endothelial cells was shown to stimulate Ca^{2+}-dependent nitric oxide synthase (eNOS). NO diffuses to the underlying smooth muscle cells causing vasodilatation through a complicated process involving the elevation of cGMP, PKG and activation of K^+ channels. This process underlies many of the endothelium-dependent vasodilations including those induced by acetylcholine, bradykinin and change in flow rate.

1.1.3.1 Endothelium-derived contacting factor (EDCF)

Activation of cyclooxygenase, which is dependent on an increase in cytosolic Ca^{2+} level, plays a dominant role in the release of EDCF. Response to EDCF is augmented by inhibitors of NO synthases and inhibited chronically by exposure to NO (Vanhoutte et al., 2005). TP (thromboxane-prostanoid) receptors on smooth muscle cells are central to this EDCF response as antagonists of TP receptors prevented the endothelium-dependent contractions. Endoperoxides, TxA_2, $PGF_{2\alpha}$ and PGI_2 can act on TP receptors.

The aorta of adult spontaneously hypertensive rats (SHR) has an abnormally high level of COX-1 expression while the expression of which is still normal in prehypertensive rats of the same strain, suggesting premature aging of the endothelium in SHR. The expression level of prostacyclin synthase in endothelial cells increases with age and is higher in SHR. Though the expression levels of TP receptor in arteries of SHRs and WKYs are similar, TP receptors in SHRs are hyperresponsive to endoperoxides and prostacyclin (Vanhoutte, 2009).

In diabetic patients, the release of endothelium-derived vascular prostanoids is enhanced by the production of oxygen-derived free radicals in high-glucose environment.

1.1.4 Thromboxane A_2

Thromboxane A_2 (TxA_2) is a prostanoid produced predominantly in platelets, but also from endothelial cells, from the metabolism of arachidonic acid by COX and TxA synthase. An elevation in intracellular Ca^{2+} concentration stimulates phospholipase A_2 which frees arachidonic acid from membrane phospholipids, and activates the constitutively expressed COX-1 in endothelial cells (Heymes et al., 2000, Vanhoutte et al., 2008). COX-1 was suggested to be the predominant isoform in endothelial cells and the major source of EDCF (Vanhoutte, 2009). COX-2 is an inducible enzyme and activation of which is often associated with various cardiovascular risk factors such as cytokines, cholesterol, hypoxia or vascular injury (Smith *et al.*, 2000). In endothelial cells, the expression of COX-2 is normally very low, but may be upregulated rapidly by many biochemical stimuli, including lipopolysaccharide, cytokines, growth factors (Ristimäki et al., 1994; Hla & Neilson, 1992; Vane et al., 1994) and lysophosphatidylcholine (Zembowicz et al., 1995), and

steady laminar shear stress (Topper et al., 1996). In healthy blood vessels, endothelial cells contain much more COXs than the surrounding SMC (DeWitt et al., 1983). The principal metabolite of arachidonic acid is prostacyclin (Feletou et al., 2010). TxA_2 consists of a six-membered ring with a half life of only about 30s (Hamberg et al., 1975). Functionally, TxA_2 acts on the TP receptor to promote platelet aggregation (Arita et al., 1989) and induces smooth-muscle contraction (Wilson et al., 2005, Tosun et al., 1998).

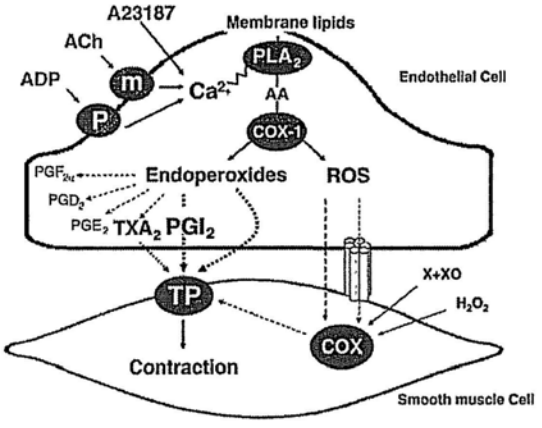

Figure 1-2 COX involvement in endothelium-dependent contraction and TxA_2 production in endothelial cells

AA, arachidonic acid; Ach, acetycholine; ADP, adenosine diphosphate; H_2O_2, hydrogen peroxide; m, muscarinic receptors; P, purinergic receptors; PGD_2, prostaglandin D_2; PGE_2, prostaglandin E_2; $PGF_{2\alpha}$, prostaglandin F2α; PGI_2, prostacyclin; PLA_2, phospholipase A_2; ROS, reactive oxygen species; TxA_2, thromboxane A_2; X + XO, xanthine plus xanthine oxidase.

Adapted from Eva H.C. Tang and Paul M. Vanhoutte, 2009.

TxA_2 had also been linked to various cardiovascular diseases. Its synthesis is increased in a number of inflammatory diseases, myocardial infarction and vascular

disease related to hypertension, diabetes, and atherosclerosis (Chamorro, 2009). TxA_2 receptors exist in both endothelial and smooth muscle cells, and the receptor number is increased in atherosclerotic plaque (Chamorro, 2009).

1.1.4.1 TP receptors

TxA_2 is the preferential physiological ligand of TP receptor, but PGH_2 and other prostaglandins can also activate this receptor with various potencies (Gluais et al., 2005). Activation of the G-protein coupled TP receptors on smooth muscle cells induces muscle contraction, proliferation and migration. TP receptors exist on endothelial cells as well and activation of it affects SMC contractility (Liu et al., 2009). The gene code for the TP receptor in human was cloned in 1991 (Hirata et al., 1991). Two isoforms of thromboxane A_2 receptors exists, TPα and TPβ, being two alternatively spliced variants of a single gene product (Raychowdhury et al., 1994), have been identified in human. They differ only in the cytoplasmic carboxyl terminal tail distal to Arg 328 (Raychowdhury et al., 1994) and have similar ligand binding characteristics.

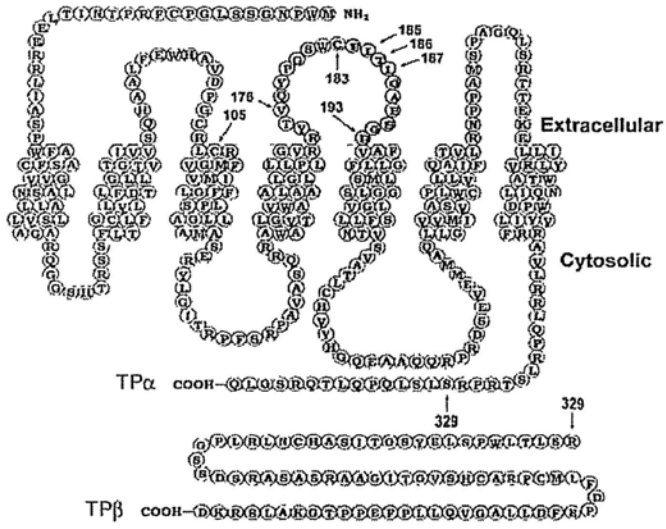

Figure 1-3 Putative structures of the TPα and TPβ receptor proteins

Adapted from Huang et al., 2004.

Reverse transcriptase-polymerase chain reaction experiments performed by Miggin et al. (1998) on 17 different cell/tissue types of physiologic relevance to TxA_2 showed that, except for the liver hepatoblastoma HepG2 cell line which expresses only TPα mRNA, both types of TP receptors are expressed in all the other cell types, with TPα mRNA predominating over TPβ mRNA. The level of expression of TPα mRNA is similar across cell types, but that of TPβ varies considerably. Both isoforms are expressed in smooth muscle cells with similar level of expression of both in foetal aortic SMC but significantly more TPα than TPβ in adult aortic SMC (Miggin et al. 1998).

1.1.4.2 TP receptor signal transduction pathway

At least nine G proteins were shown to couple to TP receptors, including G_q, G_{i2}, G_s, G_{11}, G_{12}, G_{13}, G_{15}, G_{16} and G_h (Shenker et al., 1991; Kinsella et al.,1997; Offermans et al., 1994; Djellas et al.,1999; Feng et al.,1996; Hwang et al.,1995; Vezza et al.,1999). Differential G protein coupling to TPα and TPβ in the same cell type and to the same isoform in different tissues has been observed. This not only affects the subsequent signaling pathway, but the conformation of the TP receptor and hence agonist efficacy would be affected (Nakahata, 2008). The α-isoform on platelets was shown to enhance adenylyl cyclase activity while the β-isoform inhibits it (Hirata et al., 1996, Muck et al., 1998).

In cultured adult rat aortic SMC, stimulation of TP receptors was shown to cause an increase in phospholipase C activity and hence the production of IP_3 which mobilizes intracellular free Ca^{2+}. The elevation of intracellular Ca^{2+} level was rapid, transient and independent on extracellular Ca^{2+}. A phospholipase C inhibitor, U-73122 (1-[6-[[17 beta-3-methoxyestra-1,3,5(10)-trien-17-yl]amino]hexyl]-1H-

pyrrole-2,5-dione), was able to reduce the Ca^{2+} release by 53% (Dorn & Becker, 1993). In tissue studies, Tosun *et al* found that thromboxane A_2 receptor-mediated contraction in rat aorta is resulted from Ca^{2+} influx through both L-type and non-L-type channels, and Ca^{2+} sensitization, although the identity of the non-L-type Ca^{2+} channel is unclear (Tosun et al. 1998). In rat caudal arterial smooth muscle, TP receptor activation is coupled to the activation of a $G_{12/13}$ protein which in turn stimulates a guanine nucleotide exchange factor (GEF). The GEF then activates GTPase Rho A which will cause phosphorylation of the myosin targeting subunit of the myosin light chain phosphatase (MLCP) at Thr-855 through Rho-associated kinase (ROK), resulting in inhibition of MLCP and Ca^{2+} sensitization (Wilson et al . 2005). ROK may also mediate Ca^{2+} influx through a non-selective cation channel (Villalba et al., 2008).

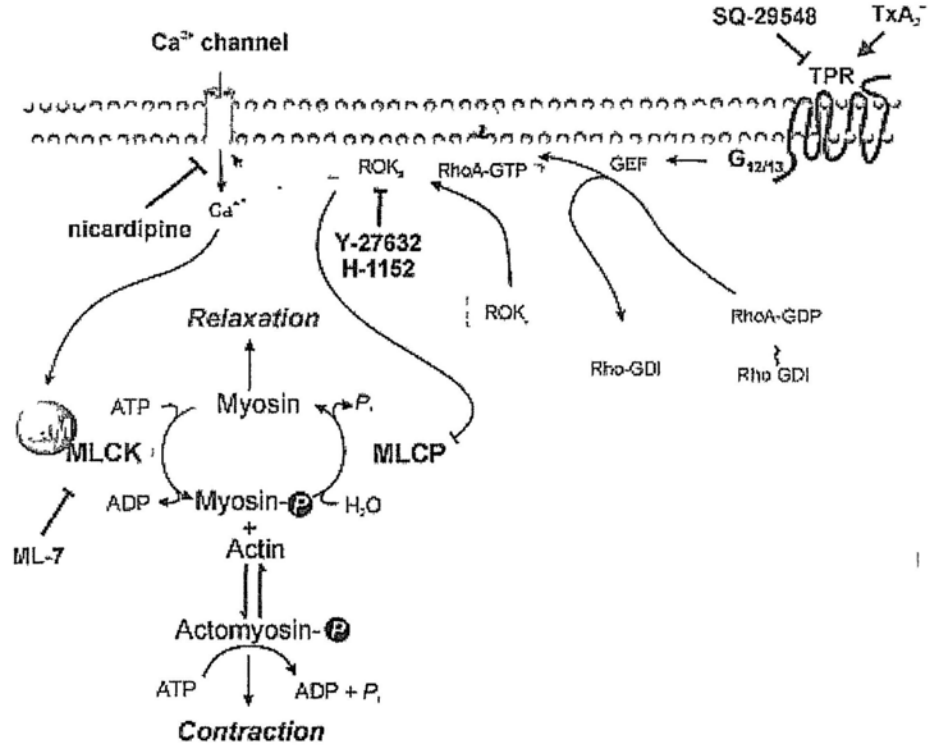

Figure 1-4 Signaling mechanism of TP receptor activation in SMC of rat caudal artery proposed by Wilson et al. 2005

Although Ca^{2+} sensitization is thought to be the dominating pathway in TP receptor activation, Sakurada et al. showed that activation of Rho which inhibits myosin phosphatase giving rise to Ca^{2+} sensitization, is partly dependent on an increase in Ca^{2+} concentration (2003). Endothelium may also play a role in the TxA2 induced contraction. McKenzie et al. (2009) showed that, in endothelium-intact pulmonary arteries, Ca^{2+} sensitization through Rho-kinase, NPPB-sensitive chloride channels and SOCC are involved in the U46619 (9,11-dideoxy-11α,9α-epoxymethanoprostaglandin F2α)-induced vasoconstriction, but the involvement of IP_3 and VOCC are not apparent. The extent of membrane depolarization caused by the opening of Cl^- channels may be limited by the activity of K_V and BK_{Ca} channels and hence unable to activate VOCC. On the other hand, the same contraction in endothelium-denuded arteries involves a nifedipine-sensitive VOCC but not SOCC, Ca^{2+} sensitization via Rho-kinase and possibly Ca^{2+} release via IP_3 receptor-linked channels. The VOCC may be activated by the simultaneous opening of Ca^{2+}-sensitive Cl^- channels and closing of K_V (Cogolludo et al., 2003) on plasma membrane. Inhibition of PLC reverts the transduction pathway to that of the endothelium-intact vessels, which is sensitive to SOCC blockers (McKenzie et al., 2009). In general, stimulation of TP receptor preferentially activates Ca^{2+} sensitization pathways but Ca^{2+} plays a role in the contraction.

1.1.5 Cyclic nucleotides

1.1.5.1 Cyclic adenosine monophosphate (cAMP)

cAMP is generated by adenylyl cyclase (AC) from ATP and degraded by phosphodiesterase (PDE) to AMP. All the nine AC isoforms currently known are

membrane-bound, but are subject to different regulatory mechanisms. Ca^{2+}-sensitive AC are located to lipid rafts on plasma membrane (Willoughby et al., 2006). There are over 90 isoforms of PDEs, differ by their tissue distribution, subcellular localization and interaction with other signaling cascades (Zaccolo et al., 2007). The activities of PDE, AC, GC, cAMP, cGMP, PKA, PKG and Ca^{2+} are interconnected. For example, PDE1 is activated by Ca^{2+} and calmodulin but inhibited by PKA-mediated phosphorylation. PDE3 is inhibited by cGMP but activated by PKA-mediated phosphorylation.

Different isoforms of ACs and PDEs existing in different subcellular locations allow localized elevation of cAMP and prompt degradation and hence compartmentalization of cAMP, cGMP signaling. The dynamic spatial and temporal regulation of cAMP level regulate complex signaling cascades through immediate downstream effectors, including protein kinase A, Epac, Eag-like K^+ channels, HCN and CNG channels.

1.1.5.2 Cyclic guanosine monophosphate (cGMP)

cGMP may be synthesized by the soluble (sGC) or particulate (pGC) form of guanylyl cyclase. sGCs are expressed in the cytosol while pGCs are localized to cell membranes. Membrane bound guanylyl cyclases has been shown to be activated by the binding of natriuretic peptides in vascular endothelial cells (Chen et al., 2008).

1.1.6 Cyclic-nucleotide gated (CNG) channels

Up to now, six genes encoding CNG channel subunits, four A subunits (A1-A4) and two B subunits (B1 and B3) had been identified. CNG A subunits, except CNG A4 can assemble into functional channels on their own, while CNG B subunits serve

regulatory roles by modifying ion permeability, ligand sensitivity and the gating mechanisms. Homomeric expression of one type of the CNG A channels has different channel properties to heterotetrameric assembly of A and B subunits. Native channels are heterotetrameric channels.

CNG channel subunits consist of 6 transmembrane segments (S1-S6) with the ion-conducting pore located between the S5 and S6 region. The interactive N- and C-terminus are located intracellularly with the cyclic-nucleotide binding region on the C-terminus. Four ligands, each binding to the C-terminus of a subunit, are required for the full opening of the channel. Partial opening of the channels is possible with lower concentration of the ligand. Opening of CNG channels leads to membrane depolarization and increase in intracellular Ca^{2+} level. Membrane depolarization may lead to the opening of other ion channels while the increase in Ca^{2+} concentration may activate some Ca^{2+}-dependent enzymes or ion channels, followed by a signal cascade.

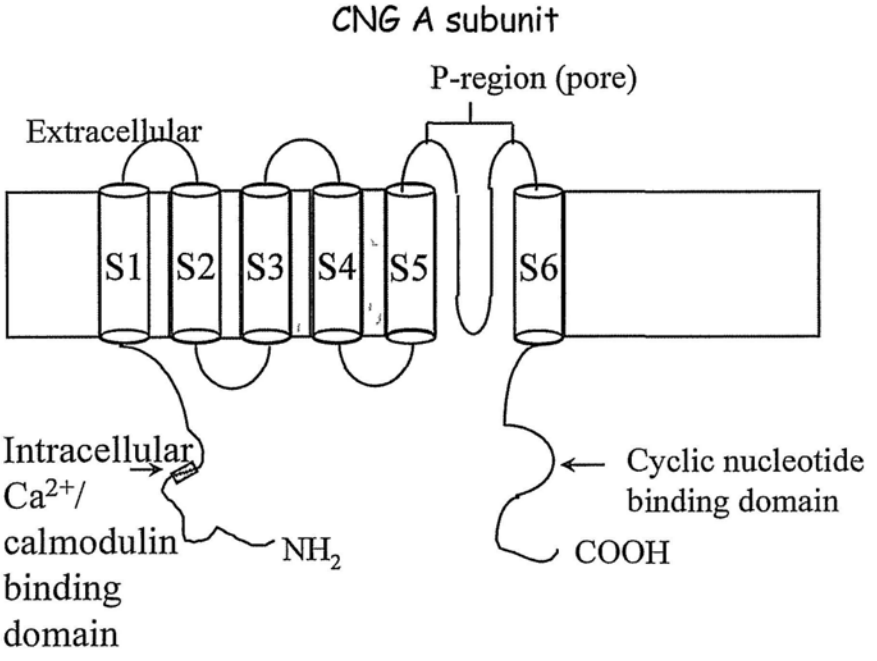

Figure 1-5 Schematic diagram of a CNG channel A subunit

CNG channels were first established in rod (3 CNGA1: 1 CNGB1a) and cone photoreceptors (2 CNGA3: 2 CNGB3), and then later in olfactory neurons (2 CNGA2: 1 CNGA4: 1 CNGB1b) (Zheng et al., 2004) and other tissues of the body including brain, kidney, endocrine tissues and sperm cells (Kaupp & Seifert, 2002). Different assembly of the CNG channels confer different relative Ca^{2+} permeability, voltage dependence of the blockage by extracellular Ca^{2+} and Mg^{2+}, and the fraction of current carried by Ca^{2+} (Frings et al.,1995). They are non-selective cation channels with similar permeability to Na^{+} and K^{+}. The passage of Ca^{2+} and Mg^{2+} acts as a voltage-dependent blocker of monovalent cation permeability (Frings et al.,1995).

In dark, basal level of cGMP cause the opening of CNG channels on the outer segment of the photoreceptors, rod and cone cells, allowing a steady cation current consisting of Na^{+} and Ca^{2+} which depolarizes the membrane and promotes synaptic transmission. Light absorption by opsin triggers a G-protein-mediated signaling cascade that activates a cGMP phosphodiesterase, leading to the hydrolysis of cGMP and hence closure of CNG channels, and finally hyperpolarization of the membrane and halting of the synaptic transmission.

In the majority of olfactory neurons, the binding of an odorant to its receptor activates adenylyl cyclase. Elevated cAMP opens the CNGA2 channels which conduct mainly Ca^{2+} and little Na^{+} under physiological conditions (Frings et al.,1995; Nakamura et al., 1987) resulting in depolarization of the plasma membrane. The Ca^{2+} influx activates a Cl^{-} channel and Cl^{-} efflux, leading to further membrane depolarization (Kleene et al., 1991).

The stoichiometry of CNG channels affect their ligand affinity, blockage by external divalent cations, ion selectivity and hence the fraction of current carried by Ca^{2+}, and the regulatory mechanism. These differences in properties affect the

function of CNG channels in different cells.

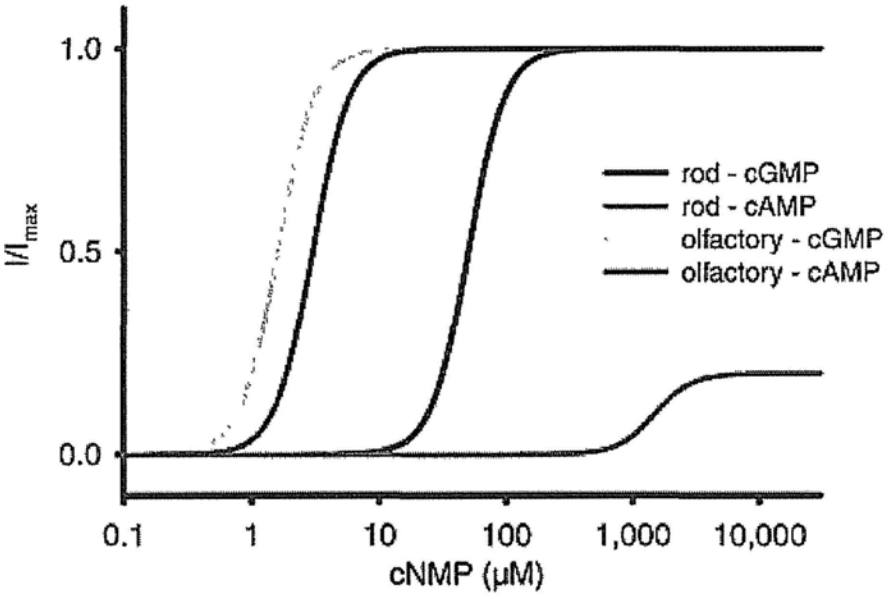

Figure 1-6 Ligand sensitivity of the native rod photoreceptor CNG channel and the native olfactory neuron CNG channel. Shown are normalized currents versus cNMP concentration. Adapted from Kaupp et al., 2002.

1.1.6.1 CNG channel regulation

CNGA2, CNGA4 and CNGB1 possess a binding site for Ca^{2+}/calmodulin on the N-terminus (Gordon et al., 1995; Song et al., 2008). Influx of Ca^{2+} through CNG channels may bind to calmodulin and then the regulatory site on the channel and decrease the ligand sensitivity of the CNG channel. Hence channels with any of these three subunits may be more susceptible to modulations by Ca^{2+}/calmodulin. For instance, only the CaM binding sites of CNGA4 and CNGB1b in the native CNG channel in OSN play a part in the Ca^{2+}-CaM modulation of the heteromeric channel and a Ca^{2+} free calmodulin is permanently associated on the two binding site. The presence and integrity of the CaM binding site on CNGA2 subunit does not affect the Ca^{2+}-CaM modulation in the native channel. Heteromeric channel expression of

CNGA4, CNGB1b and a mutant form of CNGA2 with an altered CaM binding site that is unable to bind CaM in HEK cells, and wild-type CNGA2-A4-B1b channels exhibit no significant difference in their current kinetics in patch clamp studies (Bradley et al., 2004). Increase in Ca^{2+} concentration may also desensitize CNG channels by inhibition of adenylyl cyclase by a CaM kinase II (Wei et al., 1998) or activation of a Ca^{2+}-sensitive PDE (Song et al., 2008).

CNGA4 (Bradley et al., 1994, Liman & Buck,1994) and CNGB1b increased the affinity for cAMP and changed the gating properties of native olfactory CNGA2 channels. Phosphorylation of channel subunits also represents an important regulatory mechanism for CNG channel activities. Phosphorylation of CNGA2 channels by protein kinase C can increase the ligand sensitivity (Bonigk et al. 1999).

Intracellular pH also severely affects ion permeability through CNG channels. Experiments in frog knob inside-out patch showed that cytosolic acidification inhibits cAMP-induced current (Zaccolo et al., 2007).

1.1.6.2 Expression of CNG channels in vasculature

Both CNGA1 and CNGA2 were found to be expressed in the vascular endothelium and smooth muscle cells in various vascular beds and across species (Yao X et al., 1999; Cheng KT et al., 2003).

1.1.6.3 Property of a CNG channel blocker, L-*cis*-diltiazem

In rod photoreceptors, L-diltiazem blocks the CNG channel by binding to the CNGB1a subunit and the absence of the B subunit decrease the potency of L-diltiazem by 100-fold (Chen TY et al., 1993). It has also been shown to block native cone (Haynes et al., 1992) and olfactory CNG channels (Frings et al., 1992)

but with less potency.

1.1.6.4 Possible role of CNGA2 channels in cultured endothelial cells in cAMP-elevating agent induced $[Ca^{2+}]_i$ rise

Previous studies performed by colleagues in our laboratory showed that L-*cis*-diltiazem or siRNA against CNGA2 channel was able to abolish the Ca^{2+} influx induced by adenosine in mouse microvessel endothelial (H5V) cells in Mg^{2+}-free NPSS, suggesting that CNGA2 channels may have mediated the Ca^{2+} influx. Similarly, patch-clamp experiments on bovine aortic endothelial cells and H5V cells showed a cAMP- and an adrenaline-induced current that were significantly inhibited by L-*cis*-diltiazem.

1.1.7 Ca^{2+} waves in vascular endothelial and smooth muscle cells

Due to the heterogeneity of endothelial cell and hence their responsiveness to various agents, the spreading of Ca^{2+} signaling among cells may represent an important mechanism to ensure amplified and coordinated action of the underlying smooth muscle cells to stimulus.

Intracellular and intercellular Ca^{2+} waves have been observed in a variety of cell types (Berridge, 1993), including vascular smooth muscle cells and endothelial cells. They may be triggered by stimulus-mediated mechanisms or spontaneously occurring mechanisms. For intracellular waves, calcium induced calcium release involving RyRs and IP_3Rs on Ca^{2+} stores are suggested to play a key role in wave propagation. Spreading of the wave across cells, may be accomplished by diffusion of signal molecules such as Ca^{2+} or IP_3 through gap junctions or secretion of intermediates (Berridge, 1993).

1.1.8 Spontaneous Ca^{2+} activity in endothelial cells and smooth muscle cells

Ca^{2+} waves originating from pacemaker endothelial cells were observed in lung venular capillary endothelium and these waves may be inhibited by the gap junction uncoupler, heptanol (Ying et al., 1996). Ca^{2+} signal was also found to be spreading between smooth muscle cells and endothelial cells. A $[Ca^{2+}]_i$ rise induced by phenylephrine or KCl in SMC was found to produce a secondary rise in endothelial $[Ca^{2+}]_i$ which might be inhibited by BAPTA (Yashiro & Duling, 2000). Kansui et al. (2008) found spontaneous Ca^{2+} activity in about 34% of the endothelial cells in the pressurized small mesenteric artery examined. By using U73122, cyclopiazonic acid, ryanodine and nicotinamide, Kansui suggested that the Ca^{2+} activity originate from endoplasmic reticulum IP_3 receptors. The activity was inhibited by nifedipine and chelating extracellular Ca^{2+} ions, and regulated by endothelial ion channels and surrounding smooth muscle cell through myoendothelial gap junctions. These spontaneous Ca^{2+} events were found to align with endothelial cell projections which protrude through the internal elastic lamina and make contact with smooth muscle cells. Myoendothelial gap junctions are also found to be concentrated in these contact points.

1.1.9 Influence of magnesium ion on intracellular Ca^{2+} concentration regulation

Magnesium is the most abundant intracellular divalent cation, with a concentration estimated at ~10 mmol/L, among which only <5% exist in its free ion form. Normal serum magnesium concentration ranges between 0.75-0.95mmol/l (Musso, 2009). Magnesium is required in virtually every biological process. It is a cofactor in many enzymatic reactions, essential in maintaining the active conformation of

macromolecules, regulates lipid- and phosphoinositide-derived second messengers and modulates the activities of transporters and ion channels. Specifically, it is suggested to be a competitive inhibitor of many types of calcium channels (Ginsberg, 2008). Extracellular Mg^{2+} ion concentration influences $[Ca^{2+}]_i$ of both vascular smooth muscle cells and endothelial cells by blocking Ca^{2+} influx and release from intracellular stores. Basal $[Ca^{2+}]_i$ of cultured vascular smooth muscle cell was dose-dependently reduced by extracellular Mg^{2+} concentration but that of culture human umbilical vein endothelial cell was not affected (Satake et al., 2004).

1.2 Regulation of Ca^{2+} mobilization by cGMP in T-lymphocytes

1.2.1 T-lymphocytes

80% of the circulating lymphocytes are T lymphocytes, which are central to the cell-mediated immunity. T lymphocytes are characterized by the presence of T cell receptors (TCR) on cell surface which, like the heavy and light chains of antibodies, can recognize and bind to antigens presented by antigen presenting cells. A crucial early step in the signaling pathway of TCR engagement is an increase in intracellular Ca^{2+} concentration which determines the strength and type of immune response (Luik & Lewis, 2007). This $[Ca^{2+}]_i$ rise consists of transient phase with relatively large amplitude and a sustained phase with low amplitude. The transient phase is believed to be initiated by a Ca^{2+} release from ER through the activation of phospholipase C-γ and an elevation in IP_3 level (Luik & Lewis, 2007). The sustained phase is due to store-operated Ca^{2+} entry (SOCE) through Ca^{2+} release-activated Ca^{2+} (CRAC) channels. Ca^{2+} influx may regulate diverse responses, some of which are fast in the time range of minutes including the motility of the cell and granule

exocytosis, and some of which are slow in the time range of hours and days including cell proliferation, regulation of activation-associated genes, production of cytokines and chemokines, development of T-cells in thymus and T-cell differentiation (Oh-hora, 2009). Thus understanding the regulation of SOCC in T lymphocytes is crucial to appreciate the regulation of immune response. STIM1 and Orai1 protein are suggested to be two key players in SOCE in T-lymphocytes with STIM1 being the ER Ca^{2+} sensor and Orai forming the channel pore on plasma membrane for Ca^{2+} influx (Luik & Lewis, 2007).

1.2.2 Effect of cGMP on intracellular Ca^{2+} mobilization

cGMP was suggested to reduce $[Ca^{2+}]_i$ in several ways. In vascular endothelial cells, cGMP has been shown to inhibit a store-operated Ca^{2+}-permeable channel through its action on PKG (Kwan et al., 2000). cGMP was also shown to stimulate SERCA (Lau et al., 2003) and plasma membrane Ca^{2+} pumps (Chen et al., 2000) in both endothelial and smooth muscle cells (Cohen et al., 1999). In addition, cGMP may decrease $[Ca^{2+}]_i$ by speeding up Ca^{2+} extrusion and/or enhancing Ca^{2+} sequestration into internal Ca^{2+} stores and/or decreasing Ca^{2+} influx through SOCC. Furthermore, cGMP can inhibit inwardly-rectifying K channels (K_{ir}) in endothelial cells, causing membrane depolarization, thus reducing the driving force for Ca^{2+} influx (Yao & Huang, 2003). However, there is also a report suggesting that NO, the initiator in the NO-cGMP-PKG pathway, potentiates Ca^{2+} influx in cultured bovine endothelial cells and has no effect on SERCA (Chen et al., 2000). Zolle et al. (2000) suggested that activation of particulate GC leads to inhibition of Ca^{2+} extrusion. Studies on Jurkat cells by Bian et al. (1996) showed that treatment with LY83583, a GC inhibitor, decreased SOCC slightly. Hence, the role of cGMP on intracellular Ca^{2+} mobilization

varies depending on cell type and stimulation, and it is interesting to investigate if cGMP plays a role in regulating intracellular Ca^{2+} level in T lymphocytes.

1.2.3 TRP channels in T-lymphocytes

Mammalian TRP channels are grouped into six subfamilies (TRPC1-7, TRPV1-6, TRPM1-8, TRPA, TRPML1-3, AND TRPP2,3,5) based on their amino acid sequence homology. They are non-selective cation channels involved in the regulation of intracellular concentrations of Na^{+}, Ca^{2+}, and Mg^{2+}. TRPC1, TRPC3, TRPC4, TRPC6 and TRPV6 are found to be expressed in Jurkat T-cell lines and circulating T-lymphocytes by RT-PCR analysis of the respective mRNA transcripts (Philipp et al., 2003; Gamberucci et al., 2002). Gamberucci A et al. found that the expression level of TRPC1, TRPC3 and TRPC4 may be quite low as western blot analysis did not reveal any immunoreactive band corresponding to their sizes, even in a purified plasma membrane fraction of Jurkat cells and T-lymphocytes. Philipp et al., however, were able to detect TRPC3 proteins in Western blot analysis of Jurkat cells.

TRPC channels (Huang 2006; Yuan 2007; Liao 2008; Liao 2007; Alicia 2008; Pani 2008) and Orai channels (Feske 2006; Vig 2006; Zhang 2006) have been demonstrated to be involved in store-operated Ca^{2+} entry and both channels may be regulated by STIM1. Kim went further to show that all TRPC channels, except TRPC7, are gated by STIM1 (Yuan 2007). Gene knockdown experiments on salivary gland cell line HSG and overexpression studies with TRPC1/ Orai /STIM1 suggest an interaction of Orai1-TRPC1-STIM1 in mediating SOC entry (Ong et al., 2007; Cheng et al.,2008). Co-expression of Orai1 and TRPC3 or TRPC6 may turn the TRP channels from store-independent to store-dependent channels (Liao et al., 2007).

Work by Kim MS showed that knocking-down of TRPC1 and TRPC3 by siRNA did not affect SOC in Jurkat cells (Kim et al., 2009). On the other hand, work by Philipp S showed that Jurkat cells carrying mutant TRPC3 gene displayed impaired SOC when stimulated with a TCR agonist, phytohemagglutinin. They also suggested that much of Ca through TRPC3 eventually enter the mitochondria (Philipp, 2003). In another study, TRPC6 is shown to be activated by diacylglycerol and cause cation influx in T-lymphocytes which is independent of intracellular calcium-store depletion (Gamberucci et al, 2002).

1.2.4 STIM and Orai protein in SOCC

STIM and Orai are found to be two key players in mediating SOCC in various cell types. There are three STIM subtypes, STIM1, STIM2 and STIM3. STIM1 are transmembrane proteins localized on the endoplasmic reticulum (ER) membrane with a Ca^{2+}-binding motif at the N-terminus functioning as a sensor in the lumen of the ER. A portion of the C-terminus located on the cytosolic side serves to gate the Orai channel protein (Yuan 2009; Park 2009; Kawasaki 2009; Muik 2009; Zhou 2010). Depletion of Ca^{2+} in ER dissociates the Ca^{2+} from STIM and causes a conformational change to the proteins, leading to oligomerization. STIM oligomers then move into discrete "puncta" in the apposition of ER and plasma membrane and recruit Orai proteins to the site. STIM2 and STIM3 have similar topology as STIM1, but their function is not well characterized. Orai form the pore region of the SOC channel in T cells.

Kwan et al showed that PKG phosphorylation of TRPC3 channels inhibits the SOCC mediated by the channel (Kwan et al., 2004). But there is little study on the relationship, if any, of cGMP/PKG with STIM1 or Orai.

1.2.5 Histamine

Histamine is a biogenic amine mainly produced and stored in mast cells or basophils, and released during inflammation. Histamine act directly on T lymphocytes affecting the level of cytokine production and release. It inhibits the production of interleukin-2 (IL-2) and interferon-gamma (IFN-gamma) in human T lymphocytes (Dohlsten et al., 1987)

Four plasma membrane bound extracellular histamine receptors subtypes have been cloned so far, namely H1R (De Backer 1993), H2R (Gantz et al., 1991), H3R (Lovenberg et al., 1999) and H4R (Oda et al., 2000). A putative intracellular histamine receptor "Hic" is also suggested by Brandes et al. in 1985. The receptor subtypes are differentially expressed in different cell types and coupled to different G proteins. Certain cells express more than one subtype and the net outcome of histamine binding may in part be determined by the expression ratio of different receptors. H1R and H2R are found to be expressed in T lymphocytes (Jutel et al., 2001).

1.3 Objective of study

As both Ca^{2+} and cyclic nucleotides are important second messengers in smooth muscle cells, endothelial cells and T-lymphocytes, and various reports implied a possible relationship between them, we proceed to examine their roles in relation to specific physiological functions. The study is divided into five parts:

1) Given that a non-selective Ca^{2+} channel was involved in the Ca^{2+} influx induced by TP receptor activation in smooth muscle cell, isometric tension measurement and Ca^{2+}-imaging experiments were designed to determine if cyclic

nucleotide-gated (CNG) channels play a role in the vasoconstriction induced by TP receptor activation.

2) As CNGA2 channels mediates Ca^{2+} influx in cultured endothelial cells in response to adenosine and adrenaline, experiments were designed to investigate its role at the tissue and functional level.
3) Identify the patterns of Ca^{2+} activities on aortic endothelial and smooth muscle cells in spontaneous and agonist-induced mechanisms.
4) Investigate the role of cGMP in store-operated Ba^{2+} influx in T-lymphocyte cell line Jurkat cells.
5) Investigate the role of cGMP in histamine-induced Ca^{2+} rise in Jurkat cells.

Chapter 2
Involvement of cyclic nucleotide channels in U46619-induced smooth muscle contraction

2.1 INTRODUCTION

Thromboxane A_2 (TxA_2) is an unstable prostanoid produced predominantly in platelets from prostaglandin H2 by thromboxane-A synthase. Functionally, TxA_2 acts on the TP receptor to promote platelet aggregation (Arita et al., 1989) and to induce smooth-muscle contraction (Wilson et al., 2005; Tosun et al., 1998). Two main mechanisms underlie the TxA_2-induced contraction of vascular smooth muscle. The first mechanism involves Ca^{2+} sensitization, which refers to a sensitized contractile response to a small rise in $[Ca^{2+}]_i$ (Somlyo & Somlyo, 2003). This mechanism has been extensively studied in recent years. It is clear that the Ca^{2+} sensitization can be attributed to a reduced activity of myosin light-chain phosphatase, followed by a greater degree of phosphorylation of myosin light chain 20, leading to the sensitized contractile response to Ca^{2+} (Hartshorne et al., 2004). The second mechanism is related to TxA_2-elicited increase in $[Ca^{2+}]_i$, which enhances the smooth muscle cell contraction via Ca^{2+}-calmodulin-myosin light-chain kinase pathway. Relatively little is known about the detailed mechanism of how TxA_2 elicits a $[Ca^{2+}]_i$ rise. Tosun et al. found that both L-type and non-L-type Ca^{2+} influx channels could account for thromboxane A2 receptor-mediated contraction in rat aorta, but the identity of the non-L-type calcium channel is unclear (1998). Evidence also showed that the Ca^{2+} sensitization process also requires Ca^{2+} influx, because removal of extracellular Ca^{2+} abolished the Ca^{2+} sensitization (Wilson et al., 2005, Sakurada et al., 2003).

Cyclic nucleotide-gated (CNG) channels are Ca^{2+}-permeable nonselective cation channels. Six CNG isoforms have been identified, these include four A

subunits and two B subunits. CNGA1-A3 subunits may form functional channels on their own, while B and A4 subunits serve modulatory functions. In native cells, CNG channels usually form heterotetrameric complexes consisting of A and B subunits (Kaupp & Seifert, 2002). CNG channels are widely expressed in vascular tissues across species and vascular beds (Cheng et al., 2003, Yao et al., 1999). Specifically, CNGA1 was found to be abundantly expressed in the endothelium layer of guinea pig arteries, but expressed at a much lower level in vascular smooth muscle layers (Yao et al., 1999). In contrast, strong expression of CNGA2 channel was detected in both the endothelium and smooth muscle layers of human arteries (Cheng et al., 2003). Functionally, endothelial cell CNG channels play an important role in endothelium-dependent vascular dilation to a number of cAMP-elevating agents including adenosine, adrenaline and ATP (Cheng et al., 2008, Shen et al., 2008, Kwan et al., 2009). However, up to the present, there is still no report on the functional role of CNG channels in smooth muscle cells.

In the present study, we tested the hypothesis that CNG channels may contribute to TxA_2-induced Ca^{2+} influx and contraction in vascular smooth muscle cells. A stable TxA_2 analogue U-46619 was used to induce contraction in the endothelium-denuded small mesenteric artery segments. This constriction was inhibited by L-*cis*-diltiazem and LY83583, two selective inhibitors for CNG channels, in a dose-dependent manner. Immunoblot experiments found the expression of CNGA2 proteins in the primary cultured vascular smooth muscle cells. These data suggest a functional role of CNG channels in U-46619-induced Ca^{2+} influx in smooth muscle contraction.

2.2 MATERIALS AND METHODS

2.2.1 Animal handling

The study was approved by the Animal Experimentation Ethics Committee of the Chinese University of Hong Kong (CUHK). Male Sprague-Dawley rats were supplied from Laboratory Animal Services Center and housed at room temperature (~25℃) with alternating 12-hour light/12-hour dark cycles and fed on standard rat chow and water.

2.2.2 Tissue preparation and vascular contractility studies

2.2.2.1 Preparation of small mesenteric arteries

Mesenteries with supplying blood vessels removed from adult Sprague Dawley rats (250g-300g) killed by carbon dioxide overdose were placed into Krebs solution. Second order small mesenteric artery ring segments of about 3 mm in length were isolated and cleared of adhering fatty tissues. Each segment was mounted in the tissue chamber of a Multi Myograph System (Danish Myo Technology, Aarbus, Denmark) (Figure 2-1) with two wires passing through the lumen. The tissue chambers contained Krebs solution that was constantly bubbled with 95% O_2 plus 5% CO_2 and maintained at 37℃ throughout the duration of the experiment. Endothelium was removed mechanically by gently rubbing the luminal surface with a piece of stainless steel wire. Each ring was stretched to an initial tension of 1 mN and the changes in tension were recorded in a myograph. The rings were precontracted twice in 60 mM K^+ Krebs solution. After washout of KCl, the rings were contracted with 2 μM phenylephrine, followed by 1 μM acetylcholine to ascertain the completeness of endothelium removal. Only those with less than 5% relaxation were considered as endothelium denuded. The rings were then washed three times in normal Krebs solution.

2.2.2.2 Arterial tension measurement

To study if Ca^{2+} influx is required for U46619-induced contraction, 100 nM U-46619 was added to initiate contraction in the rings. After that, the rings were washed three times with Ca-free Krebs solution and incubated in 1 mM BAPTA before the rings were recontracted with the same concentration of U-46619 (n = 4). In some experiments, EGTA (3 mM) was added (n = 4) or extracellular Ca^{2+} was removed after the U-46619-induced tension became stable (n = 4).

To assess the effect of L-*cis*-diltiazem on U-46619-induced contraction, the bathing solution was changed to 60 mM K^+ solution to open the voltage-gated Ca^{2+} channels, followed by an addition of 1 μM nifedipine to block L-type voltage-gated Ca^{2+} channels. After the tone returned to basal level, which is an indication that most, if not all, of the voltage-gated channels were blocked, the vessels were recontracted with 100 nM U-46619. Cumulative doses (from 20 μM to 200 μM) of L-*cis*-diltiazem, a specific CNG channel blocker, were added to assess the role of CNG channels in the contraction. The concentration-dependent relaxant effect of D-diltiazem was also examined for comparison. A control experiment running in parallel without the addition of diltiazem showed that the U-46619-induced contraction was sustained during the experimental time period.

2.2.3 Smooth muscle cell Ca^{2+} imaging

2.2.3.1 Primary smooth muscle cell culture

Aortic smooth muscle cells were isolated from SD rat aorta as described elsewhere (Ye et al., 2004). Briefly, the adherent adventitia layer was peeled off before the aorta was cut into small pieces and digested with 0.1% collagenase in Ca^{2+}-free PSS for 25 min at 37℃ under vigorous shaking. The tissues were then rinsed several times in

PSS to remove the collagenase. Smooth muscle cells were dissociated from the tissues by pipetting up and down using a Pasteur pipet. The cells were seeded on coverslips and grown in 80% DMEM and 20% fetal bovine serum with 1% antibiotic-antimicotic for a week before Ca^{2+}-imaging experiments.

2.2.3.2 Confocal Ca^{2+} measurement

Cultured cells were loaded with 10 μM Fluo-4/AM and 0.02% pluronic F-127 for 20 min in dark at 37°C in culture medium. Then the cells were briefly washed and bathed in NPSS. The experimental chambers were placed on the stage of an inverted microscope (Olympus IX81). Fluorescence was measured using the FV1000 laser scanning confocal imaging system. The excitation wavelength was at 488 nm and the fluorescence signals were collected using a 515 nm long pass emission filter. Data analysis was performed with FV1000 software. Changes in $[Ca^{2+}]_i$ were displayed as a ratio of fluorescence after the application of U-46619 relative to the fluorescence before.

2.2.4 Western blot analysis

2.2.4.1 Sample preparation

Thoracic aorta was isolated from Sprague Dawley rats (250-300g) and placed in ice cold PBS immediately. The surrounding connective tissue was carefully trimmed off and endothelial cells removed by rubbing with a piece of cotton. The aorta was then homogenized in protein extraction buffer, with addition of the protease inhibitor cocktail tablets (Roche) and centrifuged at 10,000*g* for 5 min at 4°C. The supernatant was collected, and the protein concentration was quantified using Bradford reagent (BioRad, Hercules, CA).

2.2.4.2 SDS-PAGE and protein transfer

SDS protein loading buffer containing 2.5% β-mercaptoethanol was added into the samples before the samples were boiled for 10 minutes. Samples (50 μg protein/lane) were subjected to sodium dodecyl sulfate polyacrylamide gel electrophoresis (SDS-PAGE). The resolved proteins were transferred to a nitrocellulose immobilon-P polyvinylidene difluoride (PVDF) membrane (Millipore, Billerica, MA, USA) using a Trans-Blot SD semi-dry electrophoretic transfer cell at 17V for 70 minutes at room temperature. The membranes were blocked with 5% non-fat milk in phosphate buffer saline 0.5% tween-20 (PBST) for 1 hr at room temperature. Primary antibodies against CNGA1 (1:200, Santa Cruz) or CNGA2 (1:1000, polyclonal, directed against residues 559-664 of CNGA2) or CNGA3 (1:200, Alamone lab) were incubated with the membrane overnight at 4°C. The anti-CNGA2 polyclonal antibody was self-raised following a previously published protocol (Bönigk et al., 1999). Immunolabeled membranes were subjected to probing with horseradish peroxidase-linked secondary antibodies, developed with enhanced chemiluminescence detection solutions (ECL kit; GE Healthcare, Little Chalfont, Buckinghamshire, UK) and exposed on X-ray films (Fuji).

2.2.5 Drugs, chemicals and other reagents

2.2.5.1 Drugs and chemicals for functional studies

Drugs and chemicals used in this study were listed in Table (2-1). They were commercially purchased from Sigma, Biomol International, RBI and Calbiochem. The chemical safety was approved by the Safety Office of the Chinese University of Hong Kong

Table 2-1 Drugs and chemical information.

Chemical	**Description**	**Solvent**	**Supplier**
Acetylcholine	Endogenous neurotransmitter at cholinergic synapses	H_2O	Sigma Aldrich
Nifedipine	L-type Ca^{2+} channel blocker	DMSO	Sigma Aldrich
ethylene glycol tetraacetic acid (EGTA)	Calcium ion chelating agent	H_2O	Sigma Aldrich
1,2-bis(o-aminophenoxy) ethane-N,N,N',N'-tetraacetic acid (BAPTA)	A calcium ion chelating agent	DMSO	Sigma Aldrich
D-diltiazem	Blocks slow, or L-type Ca^{2+} channels	H_2O	Sigma Aldrich
L-*cis*-diltiazem	A specific inhibitor of cyclic nucleotide-gated channels	H_2O	Biomol International
LY-83583	A potent inhibitor of cyclic nucleotide-gated channels	Ethanol	Calbiochem
U-46619	TP receptor agonist	DMSO	Calbiochem

2.2.5.2 Solution for measurement of isometric force

Krebs solution (pH value was maintained at 7.4 by continuously bubbling with 95% O_2 plus 5% CO_2 at 37℃)

	Final concentration
NaCl	118mM
$NaHCO_3$	25.2mM
$MgSO_4$.7H2O	1.2mM
KCl	4.7mM
KH_2PO_4	1.2mM
$CaCl_2$	2.5mM
D-glucose	11.1mM

60mM K^+ solution

	Final concentration
NaCl	63mM
$NaHCO_3$	25mM
$MgSO_4$.7H2O	1mM
KCl	60mM
KH_2PO_4	1.2mM
$CaCl_2$	2.5mM
D-glucose	11.1mM

2.2.5.3 Solution for smooth muscle cell isolation and cell culture medium

Ca^{2+}-free physiological saline solution (pH 7.4)

Final Concentration

NaCl	55mM
KCl	5.6mM
$C_5H_8NNaO_4$	80mM
HEPES	10mM
$MgCl_2$	2mM
Glucose	10mM

Cell culture medium

Trypsin (Type II), penicillin-streptomycin, antibiotic-antimycotic, Dulbecco's Modified Eagle Media (DMEM) and fetal bovine serum were purchased from Gibco Laboratories (Invitrogen Corporation). Collagenase (Type 1A) was purchased from Sigma.

2.2.5.4 Reagents for Western blot analysis

Solution for SDS-PAGE

Protein extraction buffer

	Final concentration
Tris–base	50 mM
NaCl	150 mM
NaF	50 mM
Nonidet P-40	1%
sodium deoxycholate	0.5%

Complete protease inhibitor cocktail tablets (Roche) (50ml/tablet) were added freshly before use.

3X SDS loading dye

	Final Concentration
1M Tris-HCl (pH 6.8)	50 mM
Bromophenol Blue	0.125%
SDS	2%
Glycerol	16.5%
β-mercaptoethanol	2.5%

Running buffer

	Final Concentration
Tris-base	25mM
Glycine	192mM
SDS	0.1%

Transfer buffer

	Final Concentration
Tris-base	25mM
Glycine	192mM
Methanol	20%

Phosphate-buffered saline (PBS, pH 7.4)

	Final Concentration
NaCl	140 mM
KCl	3 mM
Na_2HPO_4	10 mM
KH_2PO_4	2 mM

Rinsing buffer

PBS-T (pH 7.4)

0.1% Tween-20/PBS

Blocking solution

5% non-fat milk in PBS-T

SDS-PAGE gels

40% Acrylamide/Bis (Acry) Solution was purchased from Bio-Rad Laboratories, USA

7.5% resolving gel

H_2O	3.827 ml
40% acrylamide	1.339 ml
1.5M Tris base (pH 8.8)	1.834 ml
10% SDS	70 ul
10% ammonium persulfate (APS)	100 ul
Temed	5 ul

Stacking gel

H_2O	1.602 ml
40% acrylamide	256 ul
0.5M Tris-HCl (pH 6.8)	641 ul
10% SDS	40 ul
10% ammonium persulfate (APS)	25 ul

Temed	2.5 ul

2.2.5.5 Solution and reagents for Ca^{2+}-imaging

Normal Physiological Saline Solution (NPSS, pH7.4)

	Final Concentration
NaCl	140 mM
KCl	5 mM
$CaCl_2$	1 mM
HEPES	5 mM
D-glucose	10 mM

Fluorescence dye

Ca^{2+} indicators (Fluo-4/AM) and Pluronic F-127 were purchased from Molecular Probes Inc.

2.3 RESULTS

2.3.1 Ca^{2+} influx is required for U46619-induced vasoconstriction

Because TxA_2 is an unstable compound, we used a stable TxA_2 analogue U-46619 (100 nM) to induce contraction in isolated rat small mesenteric artery segments. To limit the study to vascular smooth muscle cells, the endothelial layer was rubbed off with a wire before all contraction studies. U-46619-induced vascular contraction depended upon Ca^{2+} influx, as removal of extracellular Ca^{2+} reversed the contraction (Figure inset of 2-2C). In addition, after the chelation of extracellular Ca^{2+} with BAPTA, U-46619 failed to induce contraction (Figure 2-2A).

2.3.2 Blocking L-type Ca^{2+} channels significantly reduced the U46619-induced contraction in rat small mesenteric arteries

We next explored the Ca^{2+} influx that mediates U-46619-induced vascular contraction. In the vessels that were pre-contracted with U-46619 (100 nM), an L-type Ca^{2+} channel inhibitor nifedipine relaxed the vessels (Figure 2-2B), suggesting an involvement of L-type Ca^{2+} channels in U-46619-induced smooth muscle contraction.

2.3.3 CNG channel blockers significantly reduced the contraction induced by U46619

Nifedipine reduced the U-46619-induced contraction significantly. In order to better resolve the component that was independent of L-type Ca^{2+} channels, arterial segments were first treated with nifedipine (500 nM) to inhibit L-type Ca^{2+} channels. In our preparation, the concentration of nifedipine (500 nM) was sufficient for the complete inhibition of L-type Ca^{2+} channels, because it could almost fully reverse the high K-induced contraction. High K^+ concentration in extracellular bath causes

membrane depolarization, which open voltage-gated L-type Ca^{2+} channels, resulting in vascular contraction (Sakariassen et al., 2009). After inhibition of L-type Ca^{2+} channels with nifedipine, subsequent addition of U-46619 can still induce contraction. This contraction also depends on Ca^{2+} influx, because chelation of extracellular Ca^{2+} abolished the contraction (Figure 2-2A,C). We next explored the possible involvement of CNG channels in U-46619-induced contraction. As shown in Figure 2-3, cumulative addition of (5-200μM) L-diltiazem caused a concentration-dependent inhibition of U-46619-induced contraction. Another CNG channel blocker LY-83583 also caused dose-dependent inhibition on U-46619-induced contraction (Figure 2-4). D-diltiazem (Figure 2-3B), which also inhibits olfactory type CNG channels, had similar effect. As expected for CNG channels, inhibitory potency of D-diltiazem was much smaller than that of L-*cis*-diltiazem (Figure 2-3B).

2.3.4 U-46619 elicits Ca^{2+} influx into primary cultured smooth muscle cells

U-46619-induced Ca^{2+} influx was studied in the primary cultured rat vascular smooth muscle cells. In these studies, L-type Ca^{2+} channels were inhibited by 300 nM nifedipine to better resolve the Ca^{2+} influx that is independent of L-type Ca^{2+} channels. As shown in Figure 2-5A,B, U-46619 still induced a $[Ca^{2+}]_i$ rise in these cells. L-*cis*-diltiazem (100 μM) inhibited this $[Ca^{2+}]_i$ rise, supporting a role of CNG channels in this $[Ca^{2+}]_i$ rise.

2.3.5 Presence of CNG channel proteins on smooth muscle cells

Immunoblots were used to examine the presence of CNG channel isoforms in vascular smooth muscle cells. Figure 2-6 shows that an anti-CNGA2 and an anti-CNGA3 antibody recognized respective proteins with expected molecular sizes,

while the anti-CNGA1 antibody failed to detect the expression of CNGA1 in protein lysates prepared from rat aortic smooth muscles. Note that for CNGA2, we followed the report from another group to prepare our antibody. Similar to the previous report (Ogletree, 1987), this antibody recognized a ~75KDa band, which represents unglycosylated CNGA2 protein, and also some other bands at ~82-100 KDa, which may represent glycosylated CNGA2 proteins.

2.4 DISCUSSION

TxA_2 is implicated in many cardiovascular, renal and respiratory diseases (Sakariassen et al., 2009). Many of these problems were associated with TxA_2-induced smooth muscle contraction, which led to vascular constriction, ischemia, pulmonary hypertension and broncho-constriction (Ogletree et al., 1987; Shore et al., 1989). In the present study, we explored the mechanism of TxA_2-induced vascular smooth muscle cell contraction. Our results showed that, in the absence of extracellular Ca^{2+}, U46619 failed to constrict the isolated small mesenteric artery segments. In addition, removal of extracellular Ca^{2+} relaxed the artery segments that were preconstricted with U-46619. Furthermore, inhibition of L-type Ca^{2+} channels by nifedipine reduced the contractile response to U-46619. These data agree with previous reports by others (Wilson et al., 2005; Tosun et al., 1998), and support the notion that Ca^{2+} influx is required for U46619-induced vascular constriction and that L-type Ca^{2+} channels play a role in this constriction.

Because the inhibition of L-type Ca^{2+} channels by nifedipine only caused a partial inhibition of U46619-induced constriction, we next explored the possible involvement of CNG channels in U46619-induced constriction. In these experiments, arterial segments were first treated with nifedipine to block L-type Ca^{2+} channels in order to better resolve the component that was independent of L-type Ca^{2+} channels.

Under this condition, U-46619-induced contraction was found to be inhibited by L-*cis*-diltiazem in a dose-dependent manner. L-*cis*-diltiazem also inhibited U-46619-induced cytosolic Ca^{2+} rise in the primary cultured vascular smooth muscle cells. L-*cis*-diltiazem is the enantiomer of D-*cis*-diltiazem. Both agents are membrane-permeable (Haynes et al., 1992; Frings et al., 1992). While D-*cis*-diltiazem is a therapeutically used blocker of the L-type Ca^{2+} channels. L-*cis*-Diltiazem is a highly selective inhibitor of CNG channels. It blocks all three functional types of CNG channels, including rod-type CNGA1, olfactory-type CNGA2 and cone-type CNGA3, at micromolar concentration (Haynes et al., 1992; Frings et al., 1992). The drug exerts its effect from the cytoplasmic face of the channel; extracellular application is less effective (Stern et al., 1986; Rispoli et al., 1988). The inhibitory action of L-*cis*-diltiazem suggests the involvement of CNG channels in U-46619-induced Ca^{2+} rise in smooth muscle cells and subsequent vascular constriction. This hypothesis was supported by the LY83583 experiments, in which LY83583 also caused a dose-dependent inhibition of U-46619-induced vascular constriction. LY-83583 is a less selective agent and it inhibits both CNG channels and soluble guanylate cyclase at similar concentrations (Leinders-Zufall et al., 1997). However, we reason that the inhibitory action of LY-83583 on U-46619-induced vascular constriction should be due to CNG channels but not to soluble guanylate cyclase, because an inhibition of soluble guanylate cyclase would result in contraction instead of the observed relaxation (Figure 2-4).

CNG channels are widely expressed in different vascular tissues including cerebral and coronary arteries (Cheng et al., 2003; Yao et al., 1999; Ding et al., 1997; Cassar et al., 2004). There are three functional subunits CNGA1-A3. All these three subunits were reported to be expressed both in vascular endothelial cells and vascular smooth muscle cells (Cheng et al., 2003; Yao et al., 1999; Ding et al., 1997; Cassar et

al., 2004, Kruse et al., 2006). Previous study also suggested that CNGA1 expression in vascular smooth muscle is very low, because RT-PCR could detect CNGA1 in cultured vascular smooth muscle cells but Western blot and in situ hybridization failed to detect CNGA1 in vascular tissues (Yao et al., 1999, Ding et al., 1997). In the present study, we found the expression of CNGA2 and A3, but not A1, in the protein lysates from rat vascular smooth muscle cell layers. These data are consistent with the previous reports, and suggest that CNGA2 or A3, but not CNGA1, are more likely to be involved in the U-46619-induced vascular constriction. Note that unlike other CNG isoforms (Stern et al., 1986) which are insensitive to D-*cis*-diltiazem even at mM concentration, olfactory-type CNGA2 is inhibited by D-*cis*-diltiazem though with much less potency compared to that of L-*cis*-diltiazem. In our experiments, high concentration of D-*cis*-diltiazem inhibited U-46619-induced vascular constriction with the dose-response curve mirrors that of olfactory-type CNGA2 reported by Frings et. al. (1992). These data suggest olfactory-type CNGA2 to be a more likely candidate that is involved in the U-46619-induced vascular constriction.

In conclusion, TxA_2-induced vascular contraction was inhibited by two CNG channel inhibitors L-*cis*-diltiazem and LY-83583. Our data suggest that CNG channels, olfactory-type CNGA2 in particular, contribute to TxA_2-induced Ca^{2+} influx in vascular smooth muscle cells.

Figure 2-1

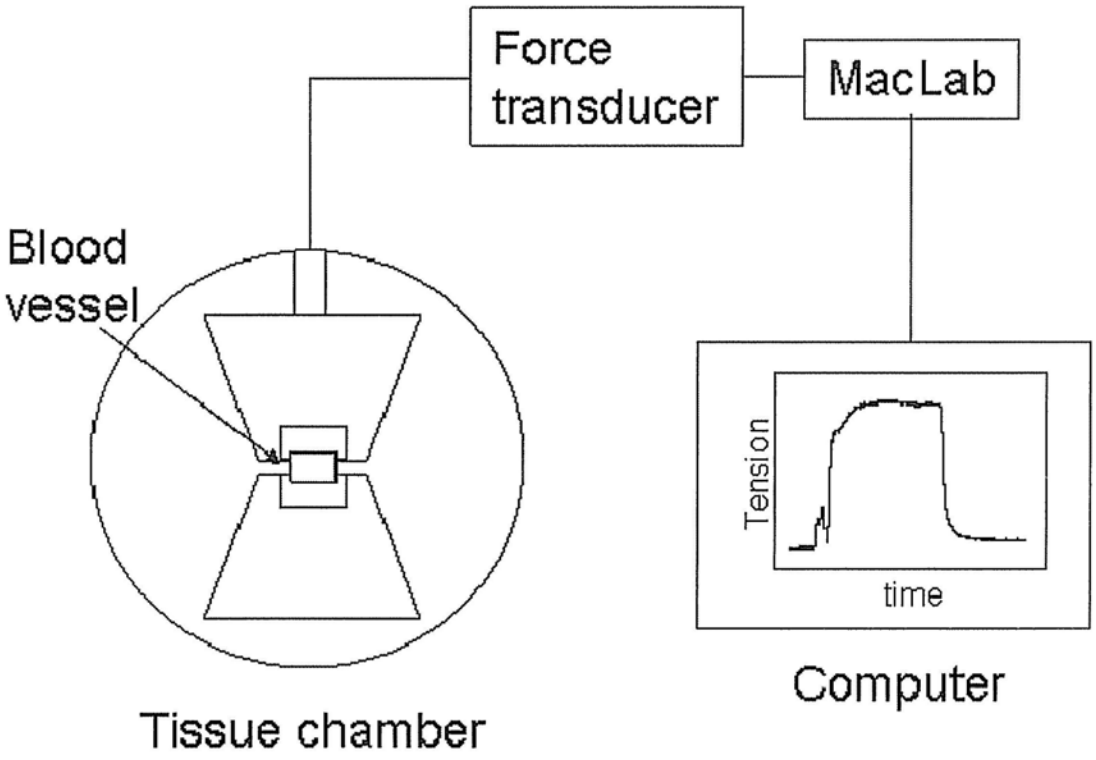

Figure 2-1 Schematic diagram of the myograph setup for isometric force measurement.

Figure 2-2

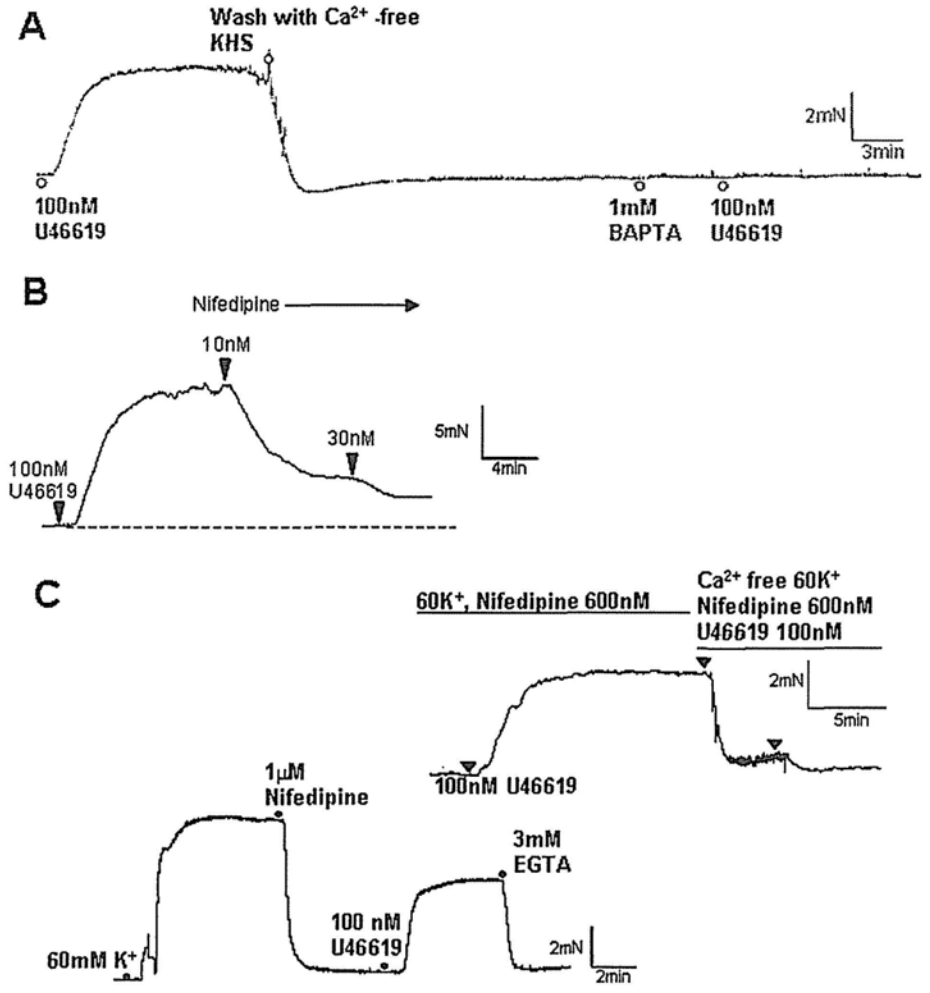

Figure 2-2. Representative traces of the tension developed in endothelium-denuded small mesenteric arteries.

A. Addition of 1 mM BAPTA in Ca^{2+}-free KHS prevented the U46619-induced contraction. **B**. Nifedipine significantly inhibited the U46619-induced contraction. **C**. 500 nM nifedipine was added to block the contraction induced by high K^+ solution. After stabilization, U46619 was added to recontract the vessel, followed by the addition of 3 mM EGTA. Inset of C. similar to C, except that the U46619-induced contraction was followed by replacing the bath solution by a Ca^{2+}-free Krebs solution. n = 5.

Figure 2-3

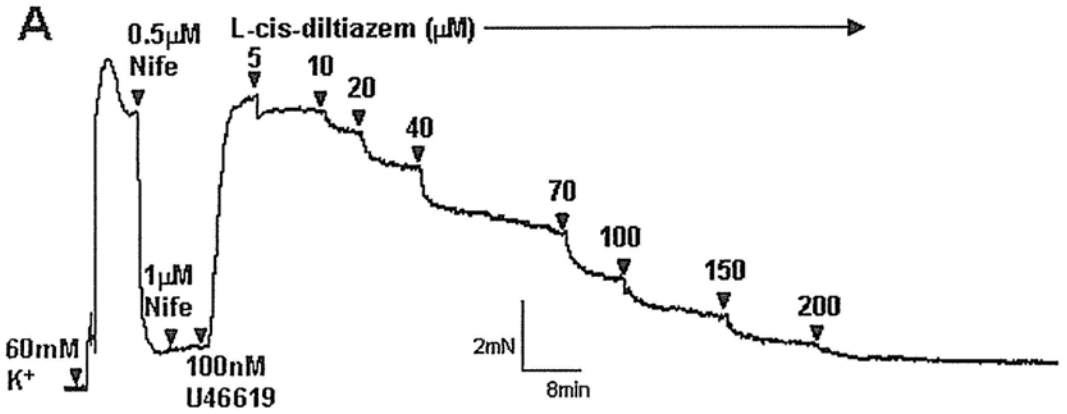

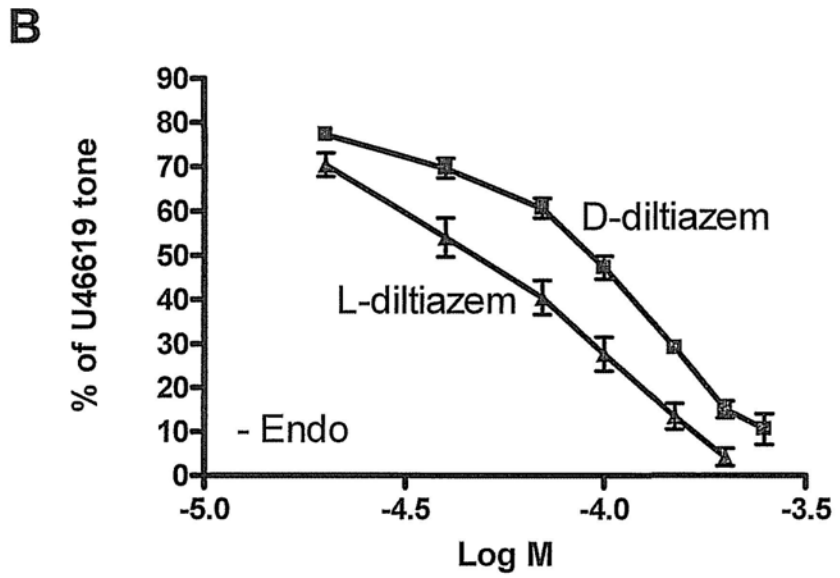

Figure 2-3. Effect of L-*cis*-diltiazem on the contraction induced by U46619.

A. A representative trace of the tension developed in an endothelium-denuded small mesenteric artery. 1 mM Nifedipine was added to inhibit L-type Ca^{2+} channels. U46619 (100 nM) was added to recontract the vessel, which is followed by cumulative doses of L-*cis*-diltiazem. N=5. **B.** A dose response curve showing the concentration dependent effect of L- and D-*cis*-diltiazem on contractions induced by U46619 after the blockage of L-type voltage-gated Ca^{2+} channels. Mean ± SE (n=5).

Figure 2-4

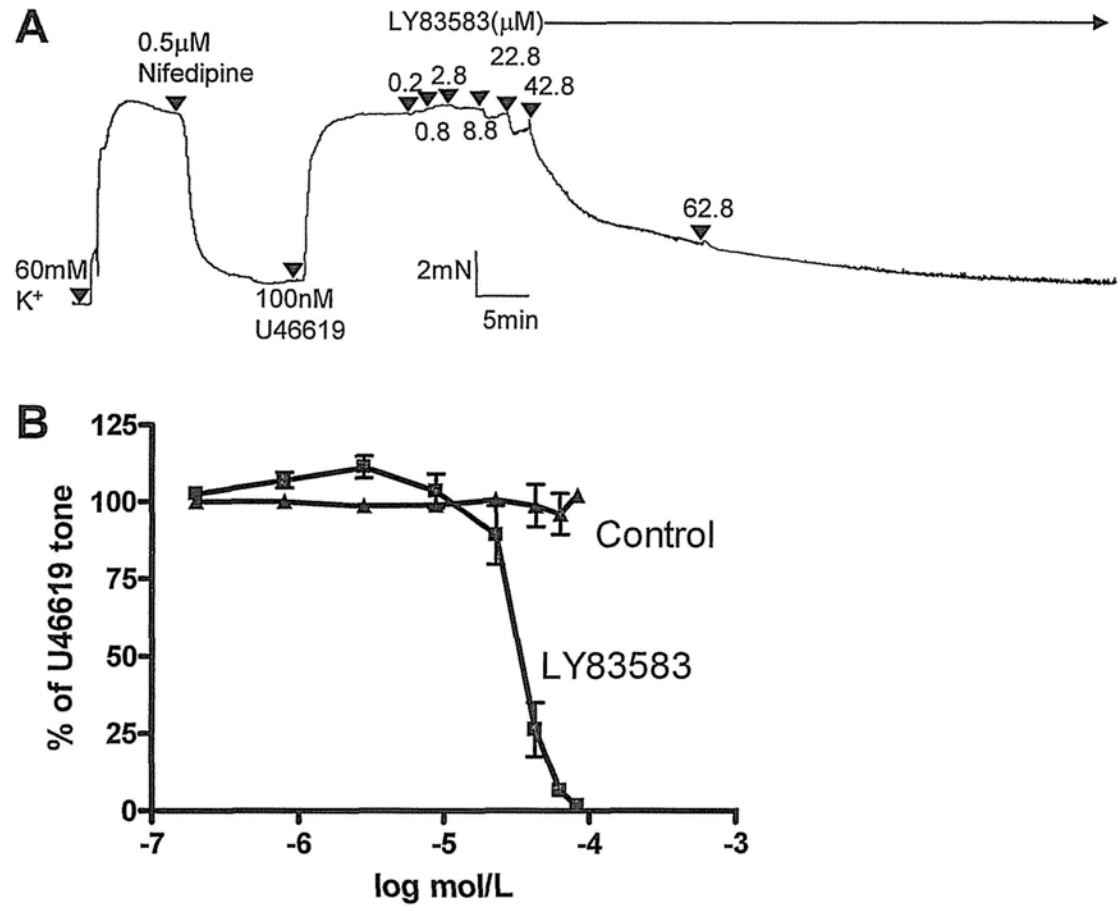

Figure 2-4. Effect of LY83583 on U-46619-induced vasoconstriction in an endothelium-denuded small mesenteric artery segment.
A. A representative trace of the tension developed in the ring upon various treatments. **B.** A dose response curve showing the concentration dependent effect of LY83583 on contractions induced by U-46619 in the presence of L-type voltage-gated Ca^{2+} channels blocker. Mean ± SE (n=4)

Figure 2-5

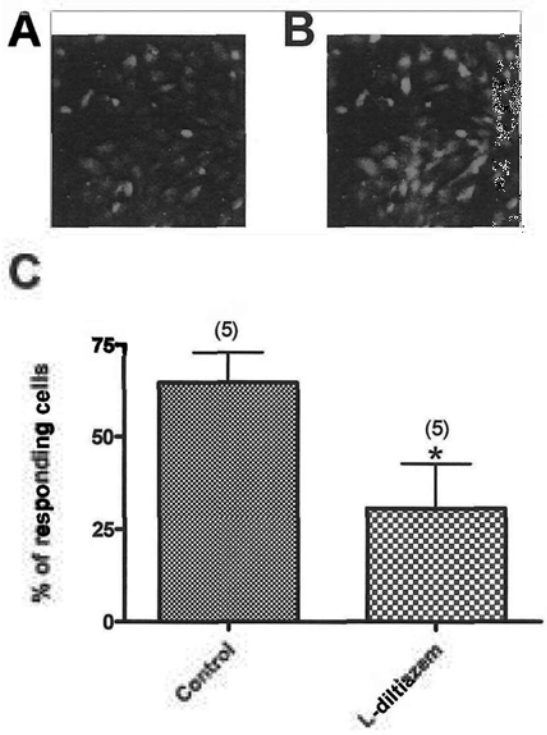

Figure 2-5. Effect of U46619 and L-*cis*-diltiazem on $[Ca^{2+}]i$ in the primary cultured aortic smooth muscle cells.

Cells were pretreated with 300 nM nifedipine to block L-type Ca^{2+} channels. **A**, **B**. Representative fluorescence images of cultured smooth muscle cells before (**A**) and after (**B**) 100 nM U46619. **C**. Summary of data showing the inhibitory effect of L-*cis*-diltiazem (100 μM) on U46619-induced $[Ca^{2+}]_i$ rises. Shown were the percentage of cells displaying U46619-induced $[Ca^{2+}]_i$ rises before and after U46619 challenge, Mean ± SE (n = 5). * $p < 0.05$ as compared with the control.

Figure 2-6

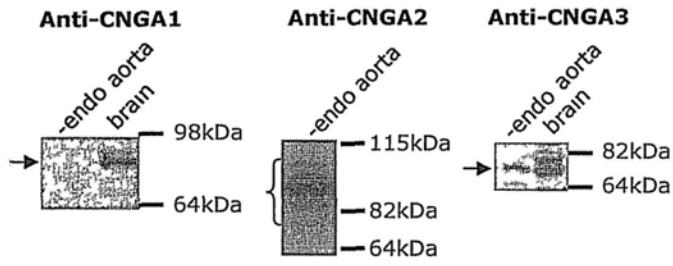

Figure 2-6. Western blotting showing the expression of CNGA2 and CNGA3 proteins in rat aortic smooth muscle cells.

Shown were representative images from 3 independent experiments.

Chapter 3

Effect of CNG channel inhibition in isoprenaline- and adenosine-induced vasorelaxation

3.1 INTRODUCTION

cAMP-elevating agents such as adenosine and epinephrine (after binding to β-adrenergic receptor) contribute to local vascular dilation.

Adenosine is a key metabolite involved in metabolic hyperemia in many vascular beds including coronary circulation, cerebral circulation, and skeletal muscle circulation. The roles of adenosine in vasculature are most prominent during hypoxia, ischemia, and reactive hyperemia (Tabrizchi et al., 2001). One important action of adenosine is to induce endothelium-dependent vasorelaxation (Wyatt et al., 2002; Duza et al., 2003; Ray et al., 2006). It is previously shown that, at least in some arteries, such as skeletal muscle arteries, a rise in $[Ca^{2+}]_i$ is required for the endothelium-dependent vasorelaxation in response to adenosine (Duza et al., 2003; Ray et al., 2006; Duza et al., 2004). Four adenosine receptors have been cloned, namely A1, A2A, A2B and A3. A2A and A2B are coupled to adenylyl cyclase, the activity of which generates cAMP.

Epinephrine is the primary catecholamine released from the adrenal medulla in response to low blood glucose, exercise and stress. It exerts a profound effect on vascular system. Depending on vascular beds and chemical concentration, epinephrine may either induce vascular dilation or contraction (Guimaraes & Moura, 2001; Mark et al., 1972). The currently known adrenergic receptors may be classified into two main groups, alpha (α1, α2) and beta (β1, β2, β3) group. Alpha

adrenoceptors exist on vascular smooth muscle cells and activation of them causes contraction. Beta adrenoceptors are located on both the vascular endothelial and smooth muscle cells and their activation causes relaxation. All adrenoceptors are coupled to G protein. β-adrenoceptors are more sensitive to epinephrine than the alpha type, so at low concentration of epinephrine, the vessel will relax. Isoprenaline is a selective agonist of β-adrenoceptors. In many vascular beds, the dilation to β-adrenoceptor agonists is, at least partly, endothelium-dependent and can be attributed to an increased production of nitric oxide (NO) in endothelial cells (Brawley et al., 2000; Priest et al., 1997; Gray & Marshall, 1992; Xu et al., 2000; Ferro et al., 1999).

cAMP is an important second messenger that participates in the endothelium-dependent vascular dilation. Adenosine receptor A2A, A2B and β-adrenoceptors are coupled to adenylyl cyclases, the activity of which generate cAMP. Elevated cAMP then activates endothelial nitric oxide synthase (eNOS) either via a Ca^{2+}-independent pathway that involves protein kinase A (Boo et al., 2002) or via a Ca^{2+}-dependent pathway that involves Ca^{2+}-calmodulin (Brock et al.,1988; Graier et al.,1992, Buchan et al.,1991). However, it is not clear how cAMP can elevate $[Ca^{2+}]_i$ level in vascular endothelial cells.

Vascular endothelial cells express multiple Ca^{2+}-permeable channels, which include transient receptor potential (TRP) and cyclic nucleotide-gated (CNG) channels (Nilius et al., 2001; Cheng et al., 2003; Yao et al., 1999). CNG channels are activated by cAMP and cGMP (Kaupp and Seifert, 2002), the levels of which are elevated when endothelial cells are exposed to adenosine and β-adrenoceptor agonists (Priest et al., 1997; Graier et al., 1992; Graier et al., 1993; Trochy et al., 1999).

Therefore, CNG channels could be a potential candidate that mediates adenosine and β-adrenoceptor agonist-induced Ca^{2+} influx in endothelial cells.

Recent studies in our laboratory showed that adenosine and isoprenaline (a β-adrenoceptor agonist) elicit a rise in $[Ca^{2+}]_i$ in cultured bovine aortic endothelial cells and H5V cell line, the effect of which was blocked by L-*cis*-diltiazem, LY83583 and siRNA against CNGA2, suggesting that adenosine and isoprenaline activate CNGA2 channels to induce Ca^{2+} influx (Cheng et al., 2008; Shen et al., 2008). However, there is a concern that the experimental results generated from cultured cells may not fully represent the cells in vivo, because cell isolation and culture procedures could cause phenotypic drift. Hence the present study moves on to study the $[Ca^{2+}]_i$ changes in endothelial cells within isolated mouse aortic strips to verify the above findings. Furthermore, myograph studies were employed to explore the possible role of CNG channels in adenosine- and isoprenaline-induced vascular relaxation. The data demonstrated that CNG channels, especially CNGA2, mediate the endothelial Ca^{2+} influx in response to adenosine, epinephrine and β- adrenoceptor agonists in endothelial cells in mouse aortic strips. Furthermore, inhibition of CNG channels greatly reduced NECA and isoprenaline-induced vascular dilation in mouse aortic segments.

3.2 MATERIALS AND METHODS

3.2.1 Animal handling

The study was approved by the Animal Experimentation Ethics Committee of the Chinese University of Hong Kong (CUHK). Male C57 mice were supplied from Laboratory Animal Services Center and housed at room temperature (~25℃) with

alternating 12-hour light/12-hour dark cycles and fed on standard rat chow and water.

3.2.2 Tissue preparation and vascular contractility studies

3.2.2.1 Mice aorta preparation

Adult C57 mice (6-8 weeks) were killed by carbon dioxide overdose. Aortae removed were placed into Krebs solution. After carefully trimming off surrounding fat and connective tissue, aortae were cut into segments of about 3mm.

3.2.2.2 Arterial tension measurement

Each segment was mounted in the tissue chamber of a Multi Myograph System (model 610M, DMT, Denmark) under a normalized tension as previously described (Dora et al., 2001). The tissue chambers contained Krebs solution that was constantly bubbled with 95% O_2 plus 5% CO_2 and maintained at 37℃ throughout the duration of the experiment. For some of the rings, endothelium was removed mechanically by gently rubbing the luminal surface with a piece of stainless steel wire. Changes in tension were recorded in a myograph. The rings were precontracted twice in 60 mM K^+ Krebs solution. After washout of KCl, endothelium integrity or functional removal was verified by the presence or absence, respectively, of the relaxant response (over 80% relaxation) to 1 μmol/L acetylcholine at the start of each experiment. The rings were then washed three times in normal Krebs solution.

The aortic rings were preconstricted with 20 to 300 nmol/L 11-deoxy prostaglandin $F_{2\alpha}$ (Cayman Chemical) to achieve similar degree of constriction in different arteries. Cumulative doses of isoprenaline or NECA were then added to the bath to obtain the concentration–response curves. In some experiments, L-*cis*-diltiazem (100 μmol/L), L-NAME (100 μmol/L), or charybdotoxin (50nmol/L)

plus apamin (50nmol/L) was added 10 min before 11-deoxy prostaglandin $F_{2\alpha}$ treatment. L-*cis*-diltiazem did not cause a significant change in contraction of aortic rings to 11-deoxy prostaglandin $F_{2\alpha}$. The relaxation response to isoprenaline or NECA was expressed as % of 11-deoxy prostaglandin $F_{2\alpha}$-induced tone.

3.2.2.3 Endothelial cell Ca^{2+}-imaging

Isolated aortic strip, cut open and pinned down on a gel block with the endothelial layer facing upwards, was loaded with 10 μM Fluo-4 and 0.02% pluronic F-127 in NPSS solution, and placed in dark at 37℃ for 45minutes. After washing three times with Krebs solution, the experimental chambers containing the aortic strip was placed on the stage of an inverted microscope (Olympus IX81). Average $[Ca^{2+}]_i$ fluorescence from 20–30 adjacent endothelial cells was measured at 37 °C in Krebs solution bubbled with 95% O_2–5% CO_2. $[Ca^{2+}]_i$ fluorescence was measured using the FV1000 laser scanning confocal imaging system. The excitation wavelength was at 488 nm and the fluorescence signals were collected using a 515 nm long pass emission filter. Data analysis was performed with FV1000 software. Changes in $[Ca^{2+}]_i$ were displayed as a ratio of fluorescence relative to the fluorescence before the application of epinephrine, isoprenaline or adenosine (F1/F0). The $[Ca^{2+}]_i$ response was continuously monitored. When appropriate, 100 μmol/L L-*cis*-diltiazem was added 10 min before epinephrine, isoprenaline or adenosine.

3.2.3 Materials

Fluo-4/AM and pluronic F-127 were obtained from Molecular Probes Inc. Epinephrine, isoprenaline, NECA, L-NAME, charybdotoxine were from Sigma. 11-deoxy prostaglandin $F_{2\alpha}$ was from Cayman Chemical. L-*cis*-diltiazem was from Biomol, USA. LY-83583 was from Calbiochem.

3.3 RESULTS

3.3.1 Role of CNG channels in epinephrine- and isoprenaline-induced endothelial Ca^{2+} responses in mouse aortic strips

Application of isoprenaline (10 μmol/L) or epinephrine (1 μmol/L) induced a transient $[Ca^{2+}]_i$ rise in more than 90% of endothelial cells in the aortic strips (Figures 3-1A and B). Importantly, epinephrine- and isoprenaline-induced endothelial $[Ca^{2+}]_i$ rises were almost completely abolished in aortic strips that were pretreated with CNG channel inhibitor L-*cis*-diltiazem (100 μmol/L, 10 min) or LY-83583 (10 μmol/L, 10 min) (Figures 3-1C and D). In contrast, L-*cis*-diltiazem or LY-83583 had no effect on acetylcholine-induced $[Ca^{2+}]_i$ rise (Figures. 3-1C and D), which is known to be mainly resulted from store Ca^{2+} release (Busse et al., 1989). These results suggest that CNG channels mediate epinephrine- and isoprenaline-induced $[Ca^{2+}]_i$ rise in vascular endothelial cells.

In the present study, more than 90% of the endothelial cells responded to isoprenaline (10 μmol/L) or epinephrine (1 μmol/L), whereas in the previous work using cultured cells, only ~10–20% of cells responded with a small rise in $[Ca^{2+}]_i$. This may be due to different microenvironment within isolated aortic tissues and cultured cells. Besides, extensive gap junctions among endothelial cells and myoendothelial gap junctions in aortic strips might have facilitated the spreading of the Ca^{2+} signal.

3.3.2 Isoprenaline-induced vasorelaxation in mouse aortic strips

Consistent with the results from other groups (Akimoto et al., 2002), isoprenaline induced concentration-dependent vascular relaxation in aortic segments

preconstricted with 11-deoxy prostaglandin $F_{2\alpha}$ (Figure 3-2). The relaxation was largely endothelium-dependent, removal of the endothelium almost completely abolished isoprenaline-induced relaxation (Figure 3-2). L-*cis*-diltiazem (100 μmol/L) significantly reduced the relaxation to isoprenaline in endothelium-intact aortic rings (Figure 3-2). When endothelium was denuded and acting on smooth muscle alone, L-*cis*-diltiazem had a slight effect on promoting relaxation instead of blocking it, although the effect is insignificant at this concentration. These data suggest that CNG channels play a key role in the endothelium-dependent relaxation induced by β-adrenoceptor agonists.

3.3.3 Adenosine elicited endothelial $[Ca^{2+}]_i$ rise in mouse aortic strips

Adenosine induced a global but transient rise in $[Ca^{2+}]_i$ in about 12±2% (n=8) of endothelial cells in freshly isolated mouse aortic strips (Figure 3-3B,C) and the response was significantly blocked by L-*cis*-diltiazem (100 μmol/L) (Figure 3-3D, n=6). Some cells displayed an oscillatory pattern of $[Ca^{2+}]_i$ rise, while other cells only gave a single $[Ca^{2+}]_i$ transient (Figure 3-3C). On the other hand, the Ca^{2+} rise induced by 1 μmol/L acetylcholine was not affected by the application of L-*cis*-diltiazem (100 μmol/L) (n=6).

3.3.4 Role of CNG Channels in A_2 Adenosine Receptor-Mediated Vasorelaxation

In agreement with the results from other groups (Fahim et al., 2001), NECA, a selective A_2 adenosine receptor agonist, induced concentration-dependent vasorelaxation in mouse aortic segments preconstricted with 11-deoxy PG $F_{2\alpha}$ (Figure 3-4A). The relaxation was mostly endothelium-dependent, because removal of the endothelium greatly reduced NECA-induced relaxation (Figure 3-4C).

Importantly, L-*cis*-diltiazem (100 μmol/L) markedly inhibited the vasorelaxation to NECA in normal (endothelium-intact) aortic rings (Figure 3-4B, C), but it had no effect on the residual small relaxation to NECA in endothelium-denuded aortic rings (Figure 3-4C). These data suggest that CNG channels play a key role in the endothelium-dependent relaxation induced by NECA.

We also explored the vasodilator(s) involved in NECA-induced relaxation. L-NAME (100 μmol/L) reduced the NECA-induced relaxation in endothelium-intact aortic rings to a level similar to that of endothelium-denuded rings (Figure 3-5). Furthermore, combined application of charybdotoxin (50 nmol/L) and apamin (50 nmol/L), a treatment considered to be a hallmark of EDHF response (Busse et al., 2002), had no effect on the NECA-induced relaxation (Figure 3-5). These results suggest that the NECA-induced vasorelaxation is mediated by NO but not EDHF.

Note that the adenosine-induced $[Ca^{2+}]_i$ rises were transient (Figures 3-3C), whereas the NECA-induced vasorelaxation lasted much longer (Figure 3-4A). This is reasonable, because the vasorelaxation involves the Ca^{2+}-NO-protein kinase G signaling pathway and the protein kinase G-mediated protein phosphorylation (Lincoln et al., 2001), which has a much long-lasting effect.

3.4 DISCUSSION

The current study on freshly isolated mice aortic strips confirmed the results on cultured cells that adenosine, epinephrine and isoprenaline could induce a $[Ca^{2+}]_i$ rise in endothelial cells through the opening of CNG channels because the $[Ca^{2+}]_i$ rise could be blocked by the selective CNG channel blockers, L-*cis*-diltiazem and

LY-83583. Myograph studies using L-*cis*-diltiazem suggested that Ca^{2+} influx through CNG channels mediated the isoprenaline-induced endothelium-dependent vasorelaxation in mice aorta. CNG channels exist on smooth muscle cells as well, but they do not significantly contribute to isoprenaline-induced vascular relaxation, because in the endothelium-denuded arteries, isoprenaline-induced relaxation was rather small and L-*cis*-diltiazem had no effect on this relaxation.

Various studies have shown that activation of A2A and A2B adenosine receptors and β-adrenoceptors on blood vessel leads to endothelium-dependent vasorelaxation through an elevation of intracellular cAMP level (Guimaraes & Moura 2001; Brawley et al., 2000; Gray & Marshall 1992; Xu et al., 2000; Ferro et al., 1999). But the involvement of $[Ca^{2+}]_i$ in the endothelium-dependent relaxation to agonists for adenosine receptors and β-adrenoceptors was controversial. cAMP can stimulate eNOS in a Ca^{2+}-independent manner through protein kinase A phosphorylation on Ser-1179 and Ser-635 (Boo et al., 2002). On the other hand, β-adrenoceptor agonists can stimulate a rise in $[Ca^{2+}]_i$ (Graier et al., 1992), which can activate eNOS directly via Ca^{2+}-calmodulin (Graier et al., 1992). The current study confirmed that Ca^{2+} influx through endothelial CNGA2 channels is necessary for β-adrenoceptor agonist-induced endothelial Ca^{2+} influx and vascular dilation in mouse aorta. However, note that agonists of adenosine receptors and β-adrenoceptors could also directly act on vascular smooth muscle cells to cause endothelium-independent relaxation depending on species and vascular beds. But, apparently this endothelium-independent vascular relaxation to adenosine and β-adrenoceptor agonist only plays a small role in mouse aorta.

It has been found that CNGA1, CNGA2 and CNGA4 are expressed in vascular endothelial cells (Cheng et al., 2003; Yao et al., 1999; Wu et al., 2002; Zhang et al.,

2002). In this study, we did not attempt to differentiate which CNG isoform is involved. However, the previous study from our lab has already identified that CNGA2 mediates endothelial Ca^{2+} influx in response to adenosine and β-adrenoceptor agonists (Cheng et al., 2008; Shen et al., 2008).

In the present study, more than 90% endothelial cells responded to isoprenaline (10 μmol/L) or epinephrine (1 μmol/L), whereas in the previous work using cultured cells, only ~10–20% of cells responded with a small rise in $[Ca^{2+}]_i$. However, in cultured endothelial cells, the percentage of cells respond to isoprenaline (10 μmol/L) or epinephrine (1 μmol/L) could be greatly increased if the bathing medium contained a Ca^{2+}-mobilizing agonist bradykinin (10 nmol/L). We speculate that this discrepancy in results between cultured endothelial cells and ex vivo vascular tissues may be related to the microenvironment within isolated vascular tissues. It is possible that microenvironment within isolated aortic tissues might already contain sufficient amount of Ca^{2+}-mobilizing agonists, so that exogenous addition of agonists was no longer needed. In contrast, another cAMP-elevating agent adenosine only stimulates $[Ca^{2+}]_i$ rise in a small percentage of endothelial cells even using isolated mouse aortic strips. This may due to heterogeneity of endothelial cells in situ with different population of cells responding to different agonists (Huang et al., 2000). For comparison, in our experiment, a well-recognized vasoactive agonist acetylcholine (1 μmol/L) elicited $[Ca^{2+}]_i$ transients in 21±5% (n=8) of the endothelial cells in aortic strips (Figure 3-3E), and furthermore this acetylcholine-induced $[Ca^{2+}]_i$ rise is insensitive to L-*cis*-diltiazem (100 μmol/L) (Figure 3-3E). Therefore, it is expected that only certain percentage of cells can respond to adenosine, but such a response is enough to generate the vasodilatation caused by adenosine as demonstrated in

experiments measuring the isometric tension developed in the aortic rings using NECA, an A_2 adenosine receptor agonist (Figure3-4C).

In conclusion, the results in this chapter showed that CNGA2 mediates adenosine- and isoprenaline-induced endothelial Ca^{2+} entry in endothelial cells in aortic strips and vasorelaxation. Note that vascular endothelial cells in vivo are also the targets of several other physiologically important cAMP-elevating agents including calcitonin gene-related peptide (Brain et al., 2003) and adrenomedullin (Brain et al., 2003). In future, it will be interesting to explore whether CNG channels also participate in the vasorelaxation in response to other cAMP-elevating agents.

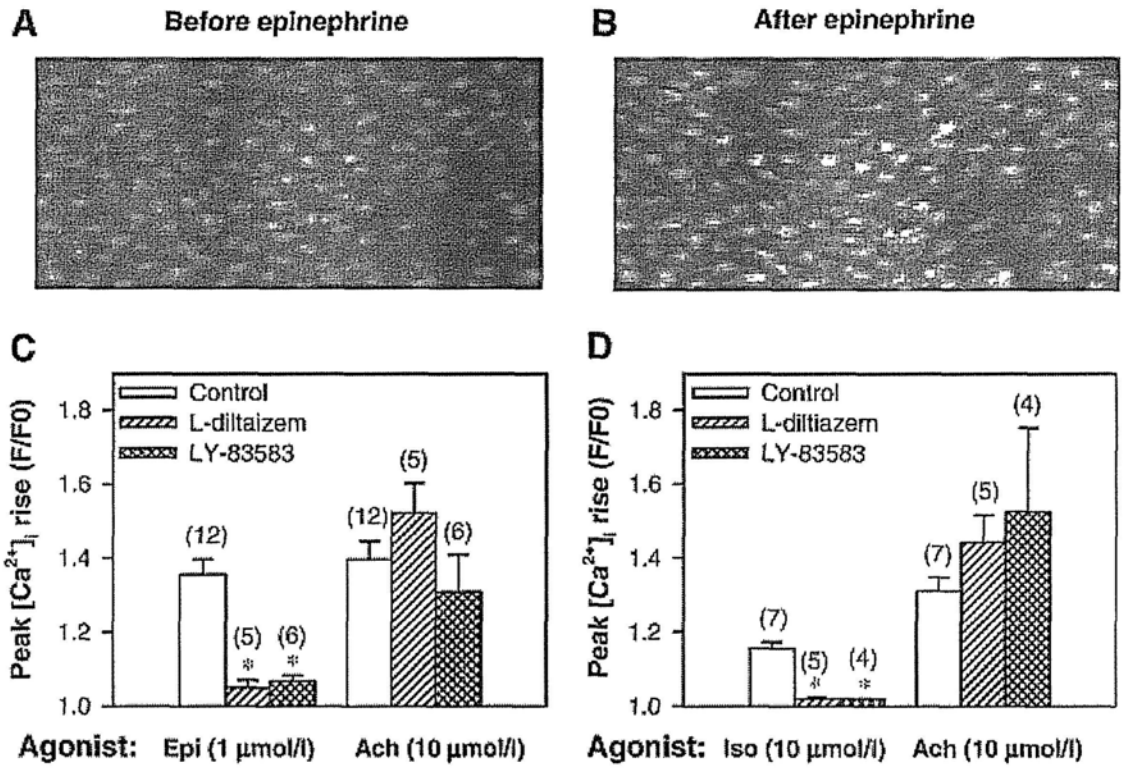

Figure 3-1 Effect of CNG channel inhibitors on epinephrine- and isoprenaline-induced endothelial $[Ca^{2+}]i$ rises within mouse aortic strips.

(**A** and **B**), representative endothelium fluorescence images before (**A**) and after (**B**) 1 μmol/L epinephrine. (**C** and **D**), summary of data showing the effect of L-*cis*-diltiazem (100 μmol/L) and LY-83583 (10 μmol/L) on the magnitude of first $[Ca^{2+}]i$ transient in response to 1 μmol/L epinephrine (Epi, **C**), 10 μmol/L isoprenaline (Iso, **D**), and 10 μmol/L acetylcholine (Ach, C and D).

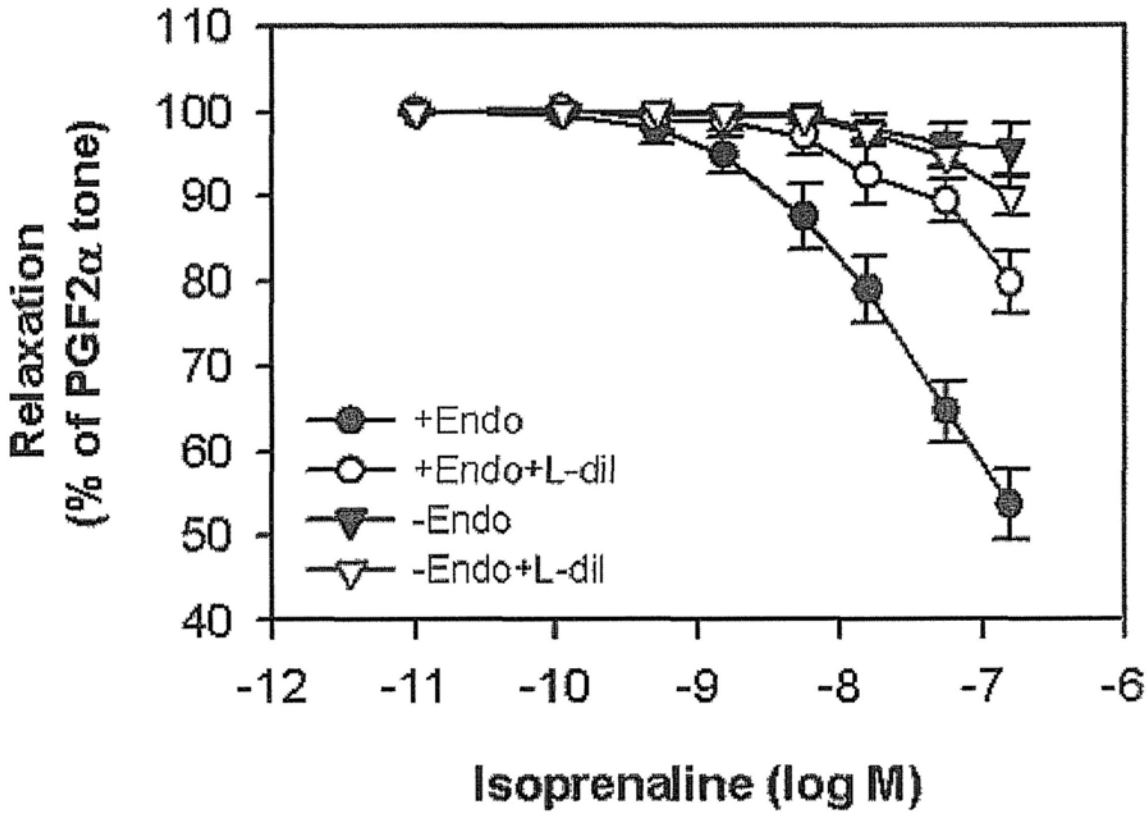

Figure 3-2 Effect of L-*cis*-diltiazem on isoprenaline-induced vascular relaxation in mouse aortic segments.

Mouse aortic segments, were preconstricted with 11-deoxy prostaglandin F2α in the absence or presence of 100 μmol/L L-*cis*-diltiazem. Isoprenaline was then added in a cumulative fashion to the bath to induce vascular relaxation. + Endo, endothelium-intact; − Endo, endothelium-denuded; L-dil, L-*cis*-diltiazem. Mean ± SEM (n = 5 independent experiments)

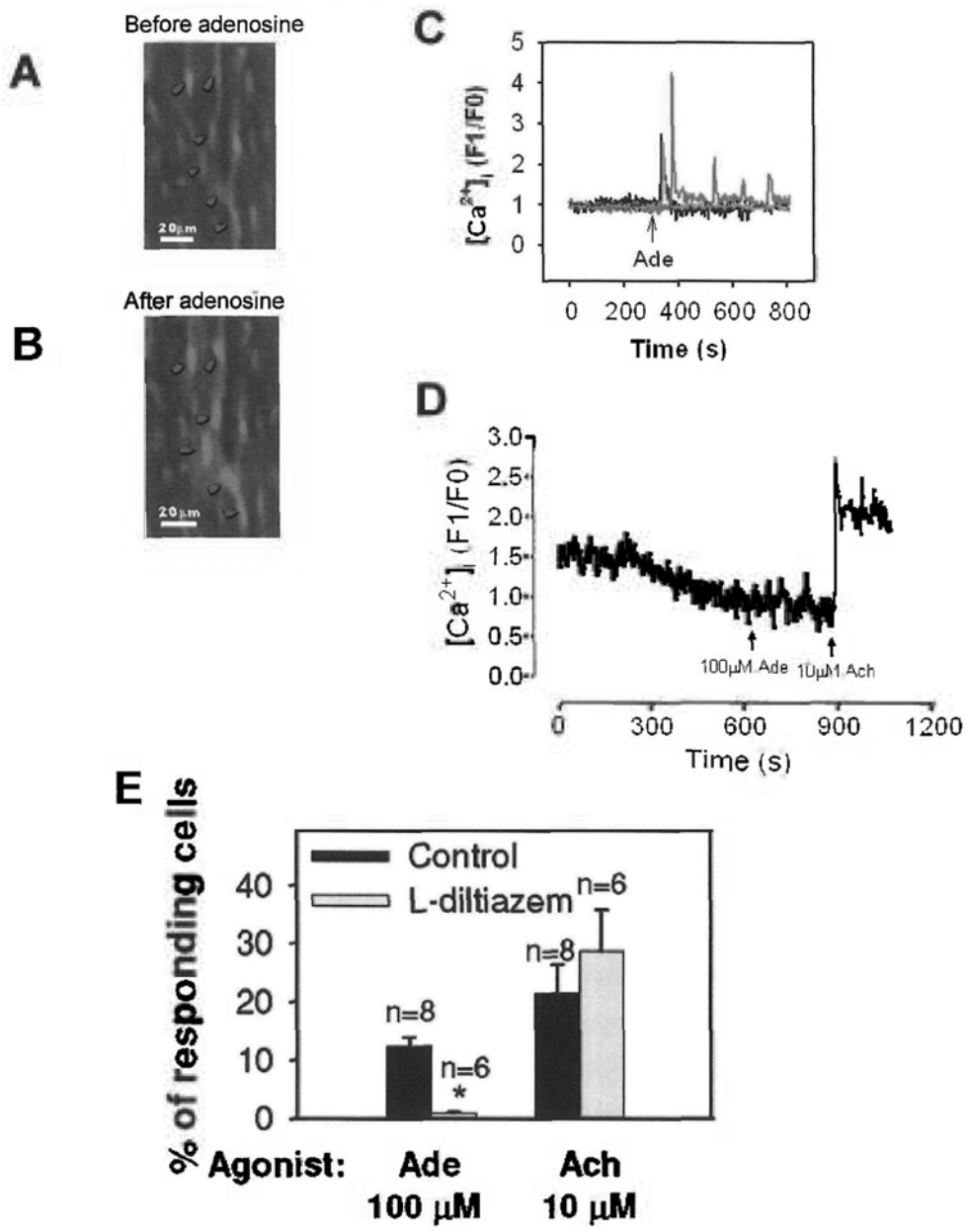

Figure 3-3 Effect of L-*cis*-diltiazem on adenosine-induced Ca^{2+} rise in endothelial cells lining mouse aortic segments.

(A and B), representative endothelium fluorescence images before (A) and after (B) 100 μmol/L adenosine. Red arrows point to the adenosine-responding cells. C. Respresentative trace of the fluoresence level of three cells responding to 100 μmol/L adenosine. D. Representative trace of the adenosine response of one cell after L-*cis*-diltiazem pretreatment. E. Summary of data showing the effect of L-*cis*-diltiazem (L-dil, 100 μmol/L) on the percentage of cells displaying adenosine (Ade, 100 μmol/L)- and acetylcholine (Ach, 1 μmol/L)-induced Ca^{2+} rise. Mean±SEM (n=6-8 experiments). *P<0.01 as compared to the control.

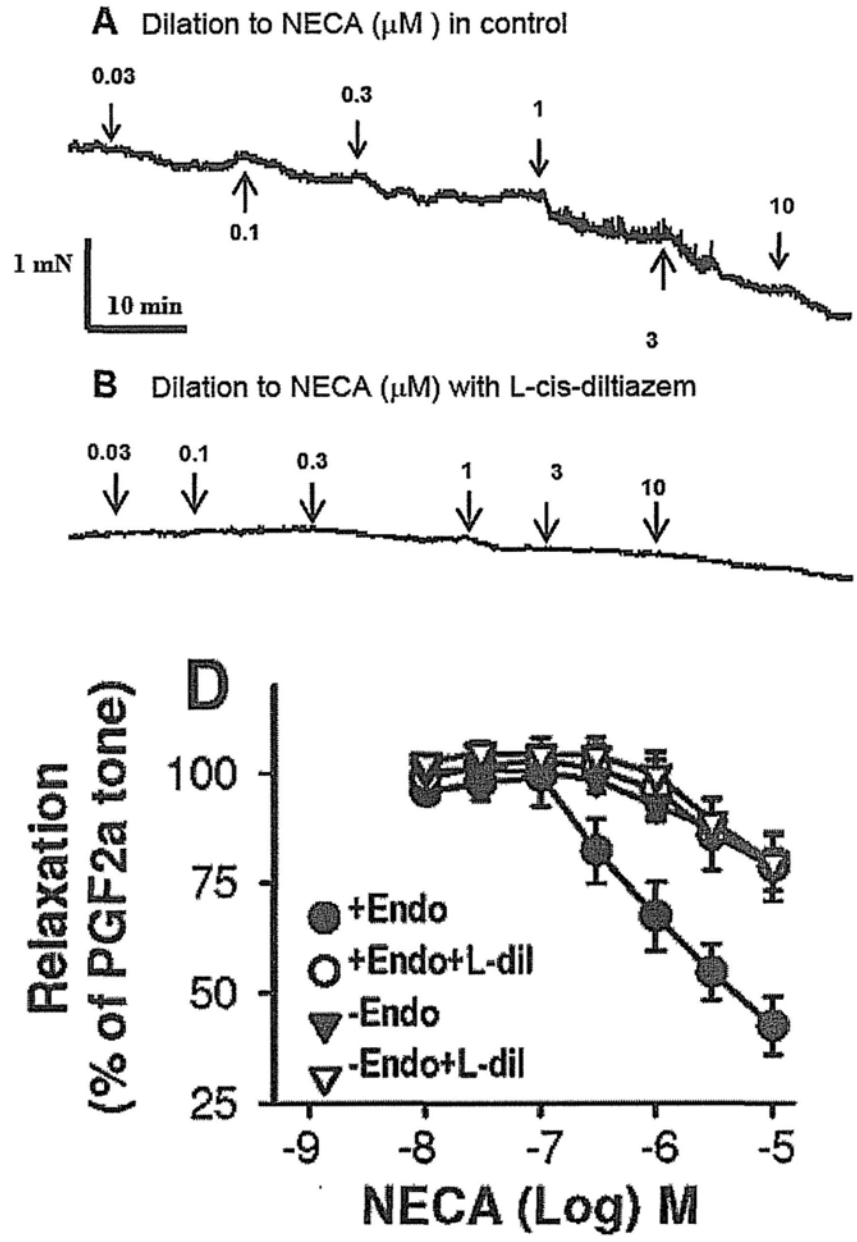

Figure 3-4 Effect of L-cis-diltiazem on NECA-induced vasorelaxation in mouse aortic segments.

A and B, representative traces showing the time course of NECA-induced relaxation in mouse aortic segments preconstricted with 11-deoxy prostaglandin F2a in the absence (A) or presence (B) of 100mmol/L L-cis-diltiazem. C, summary of data. +Endo indicates endothelium-intact; -Endo, endothelium-denuded. Mean±SEM (n=6 to 10 experiments).

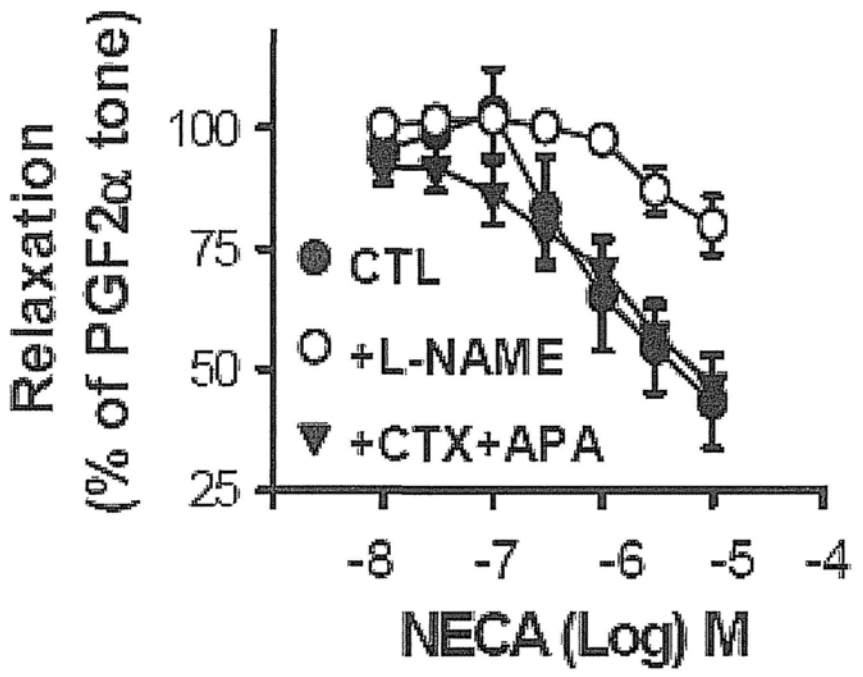

Figure 3-5 Summary of data showing the effect of L-NAME (100μmol/L) and charybdotoxin+apamin (50nmol/L each) on NECA-induced relaxation. CTX, charybdotoxin; APA, apamin. All rings were endothelium-intact. Mean±SEM (n=5-7). *P<0.01 as compared to the control.

Chapter 4

Various Ca^{2+} spreading patterns observed in vascular endothelial and smooth muscle cells

4.1 INTRODUCTION

Ca^{2+} signaling may be coded by the amplitude of $[Ca^{2+}]_i$ concentration change, frequency in $[Ca^{2+}]_i$ oscillation and spatial restriction to a subcellular domain. Ability of a endothelial or smooth muscle cell to communicate its Ca^{2+} signal to neighboring cells may be important for coordinating physiological activities such as vascular contractility. Little has been described about the patterns of Ca^{2+} wave in rat aortic endothelial cells. The current study demonstrated several patterns of Ca^{2+} signal spreading in aortic endothelial cells and spontaneous activity in smooth muscle cells in Mg-free KHS.

4.2 MATERIALS AND METHODS

4.2.1 Blood vessel preparation.

The animal study was conducted in conformity with the *Guide for Animal Care and Use of Laboratory Animals* published by the US National Institute of Health. C57 mice aged between 6-8 weeks were killed by carbon dioxide overdose. Aortas were isolated, with fatty tissue carefully trimmed off, and cut into segments of 3 mm each in Krebs solution (in mM): 118 NaCl, 4.7 KCl, 2.5 $CaCl_2$, 1.2 $MgSO_4$, 25.2 $NaHCO_3$, 1.2 KH_2PO_4, and 11.1 D-glucose. Each aorta ring was cut opened and mounted on a transparent gel block with lumen facing up before it was loaded with 10 μmol/L Fluo-4/AM for 30 min in dark at 37℃ in NPSS.

4.2.2 Intracellular Ca^{2+} imaging

The tissue was then taken out and washed twice in normal or Mg^{2+}-free KHS solution before placing into a normal or Mg^{2+}-free KHS bathing solution with lumen facing down. The cell layer was examined under a confocal microscope.

4.3 RESULTS

Data shown in this chapter are preliminary results obtained from a sample size of $n<3$.

4.3.1 Patterns observed in endothelial cells

Oscillatory calcium sparks were observed in about 20% of the rat aortic endothelial cells in Mg^{2+}-free KHS (Figure 4-1A-M), but these were absent in endothelial cell bathing in normal KHS solution. In some cells, each Ca^{2+} spark consists of two components, a fast Ca^{2+} transient with large amplitude followed by a relatively slow Ca^{2+} transient with much smaller amplitude (Figure 4-1N). For other cells, only first fast Ca^{2+} transient could be observed. Each Ca^{2+} spark typically lasted for 1-3 minutes. The frequency of oscillation for the measured cell in Figure 4-1N was ~1 cycle/3 min, but the frequency varied greatly in different cells. The Ca^{2+} wave spread in all directions with varying speeds. Often times, the speed along the longitudinal axis of the vessel is faster than along the transverse axis.

Application of 10 μM acetylcholine induced Ca^{2+} oscillations in endothelial cells bathing in Mg^{2+}-free-KHS (Figure 4-2Q). The Ca^{2+} rise spread like waves to neighboring endothelial cells. The speed of spread was different in different direction (Figure 4-2 A-P).

Damage of endothelial cells by mechanical stress imposed by air bubbles initiated a Ca^{2+} transient in the neighboring cells and the Ca^{2+} rise radiated out across several endothelial cells in all directions. These Ca^{2+} transients quickly vanished.

(Figure 4-3A-J)

In normal KHS solution, Ca^{2+} waves were observed spreading to neighboring endothelial cells about 10 minutes after the addition of 20 μM LY-83583. Within the area under observation (840 x 840 μm), there are multiple initiation foci of Ca^{2+} wave (Figure 4-4 A-L).

4.3.2 Patterns observed in smooth muscle cells

Besides endothelial cells, smooth muscle cells also displayed spontaneous repetitive Ca^{2+} spikes. In Mg-free KHS, smooth muscle cells exhibited Ca^{2+} oscillations even in the presence of 1 μM nifedipine. Again, the frequency of spikes in different cells varied considerably. The endothelial cells on top apparently were not influenced by the Ca^{2+} spikes of the underlying smooth muscle cell and had little activity in the presence of nifedipine.

After the addition of 100-200 μM adenosine, the number of smooth muscle cells displaying Ca^{2+} oscillations increased and the oscillation frequency of some smooth muscle cells also increased slightly, but the amplitude was unaffected (Figure 4-5A-M). A few endothelial cells also responded to adenosine (Please refer to Chapter 3 for analysis on endothelial cell response to adenosine). There were lots of Ca^{2+} activities in the smooth muscle cell underneath, but Ca^{2+} activity of endothelial cells remained limited (Figure 4-5A-M).

In Mg^{2+}-free KHS solution, 40 μM LY-83583 was found to significantly increase the number of smooth muscle cells displaying repetitive Ca^{2+} sparks (Figure 4-6A-I). In an area of 60 x 60 μm, the number of cells displaying Ca^{2+} sparks in a period of 276 seconds increased from 6 to 16.

4.4 DISCUSSION

4.4.1 Endothelial cells

Ca^{2+} waves were observed with the addition of LY83583. The speed of spreading of Ca^{2+} signal along the longitudinal axis of the blood vessels is faster than along the transverse axis. This may be due to the elongated shape of the cells. Different from the observations in pressurized mesenteric resistance arteries (Kansui et al., 2008), aortic endothelial cells in our experiments exhibited no spontaneous Ca^{2+} activity in normal KHS. This may be due to the absence of physiological pressure applied to the vessel in our experiment, or different vascular bed. Whether spontaneous Ca^{2+} activity in normal KHS is related to mechano-sensitive channels on endothelial cells or smooth muscle cells which in turn activate endothelial cells is unknown, but it is well accepted that endothelial cells from different vascular beds have different properties. Intravascular pressure induces depolarization in membrane potential of smooth muscle cells which in turn increases $[Ca^{2+}]i$ through activation of L-type Ca^{2+} channels (Jaggar et al., 1998), and $[Ca^{2+}]i$ of endothelial cells may be influenced by the Ca^{2+} activity of smooth muscle cells (Kansui et al., 2008). Removal of Mg^{2+} ion from the bathing solution promotes Ca^{2+} oscillation in some of the aortic endothelial cells and spreading of the Ca^{2+} rise to neighboring endothelial cells. This is consistent with the findings that Mg^{2+} ions can act as a physiological antagonist of Ca^{2+} ions (Teragawa et al., 2002), its removal can induce endothelium-dependent vasodilation (Sontia & Touyz, 2006). The often faster speed of propagation of the Ca^{2+} wave along the longitudinal axis of the vessel may be a result of the shape of endothelial cells. Endothelial cells are elongated along the longitudinal axis of the vessel and Ca^{2+} spread within a cell may be faster than across cells. This pattern of spreading may suggest the involvement of electrical/chemical signaling passing across gap junctions rather than diffusion of secretory intermediates as the latter is affected by the liquid

flow. Gap junction blockers such as 18-α-Glycyrrhetinic acid or carbenoxolone may be used to ascertain the contribution of gap junctions in the Ca^{2+} spread.

Agonist triggered Ca^{2+} rise may also propagate to surrounding cells. Ca^{2+} waves were observed in endothelial cells upon the addition of 10 μM acetylcholine.

4.4.2 Smooth muscle cells

Spontaneous calcium spikes in smooth muscle cells were observed in rat aortic smooth muscle cell in Mg-free KHS in the presence of 1 μM nifedipine suggesting that either L-type Ca channel was not involved in this spontaneous activity of smooth muscle cell or L-type channel was not the only source of Ca^{2+} in such activity. Due to the short duration of the spikes and limited resolution of individual smooth muscle cells and time constraints, it is not clear if the spikes in one smooth muscle cell could affect the $[Ca^{2+}]_i$ of neighboring smooth muscle cells. The spiking frequency and amplitude of some of the cells increased after the addition of adenosine.

A_{2B}, one of the receptor subtype of adenosine, is coupled to adenylyl cyclase and stimulation of it causes a rise in $[Ca^{2+}]_i$. A_{2B} is ubiquitously expressed and its presence on vascular smooth muscle cell was linked to the regulation of growth (Baraldi et al., 2006). However, the influence of adenosine on the frequency of Ca^{2+} oscillation in vascular smooth muscle cell was not documented. Difference in frequency of Ca^{2+} oscillation may regulate distinctive sets of physiological activities or gene expression (Lewis, 2003). Ca^{2+} sparks may also activate K_{Ca} channels, producing spontaneous outward currents which cause membrane hyperpolarization and hence muscle relaxation (Wray & Burdyga, 2010). This increased Ca^{2+} sparks in response to adenosine is consistent with a vasodilatation role of adenosine in smooth muscle cells (Phillis, 2004; Wang et al., 2009).

Figure 4-1

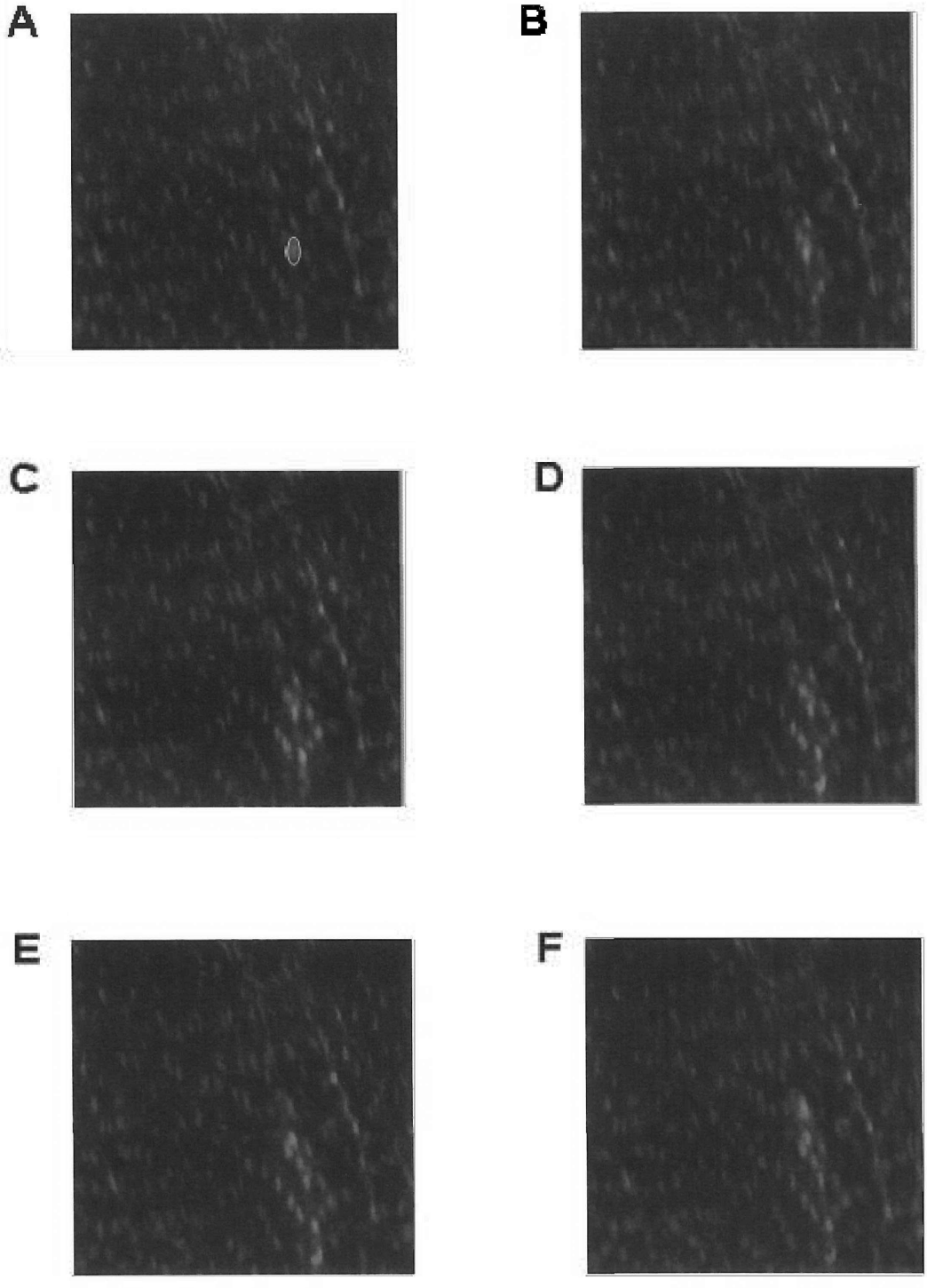

Figure 4-1

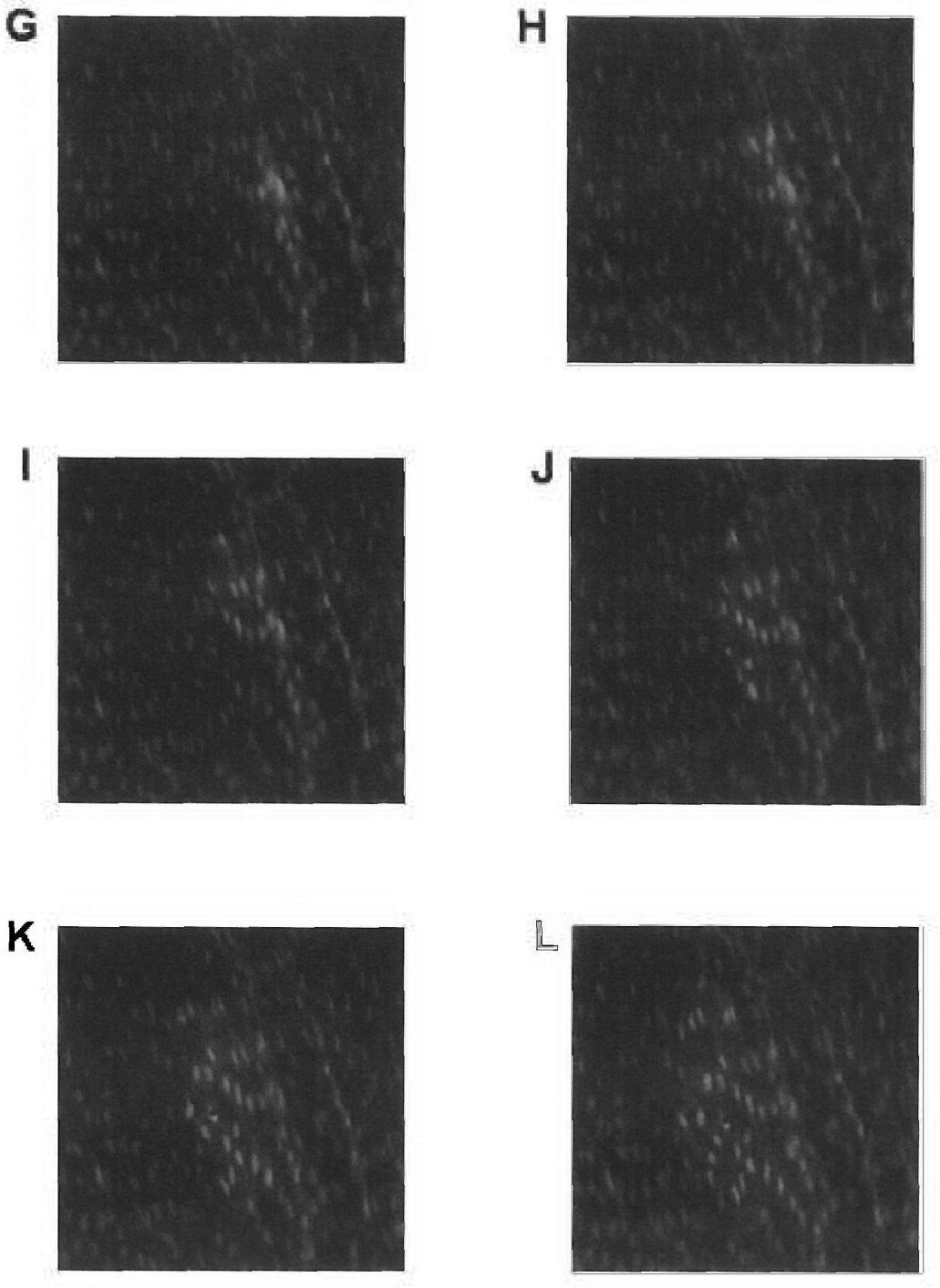

Figure 4-1

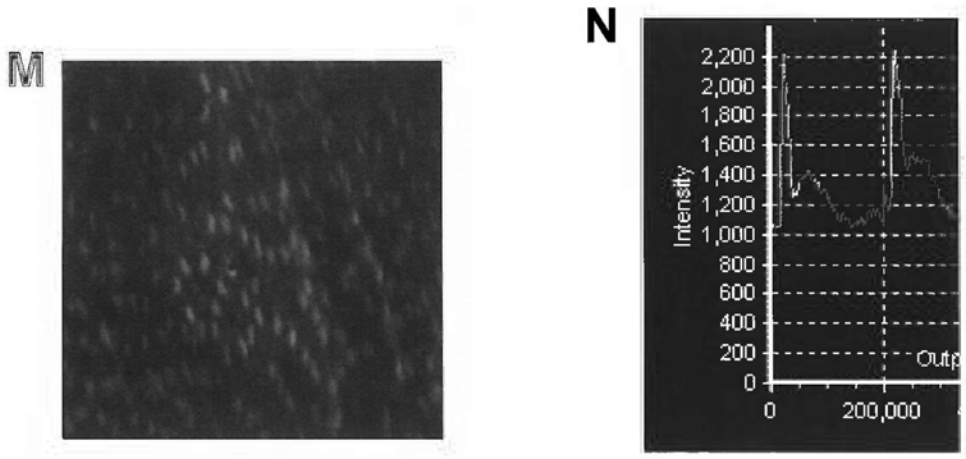

Figure 4-1. $[Ca^{2+}]_i$ activity in aortic endothelial cells in freshly isolated aortic ring in Mg-free KHS

A – M show the sequential fluorescence image of the luminal face of the aortic ring. Images were taken 2.3 seconds apart. The cell in yellow circle initiated the spontaneous Ca^{2+} wave.

Representative trace of the change in $[Ca^{2+}]_i$ in a single aortic endothelial cell (yellow circled cell).

Figure 4-2

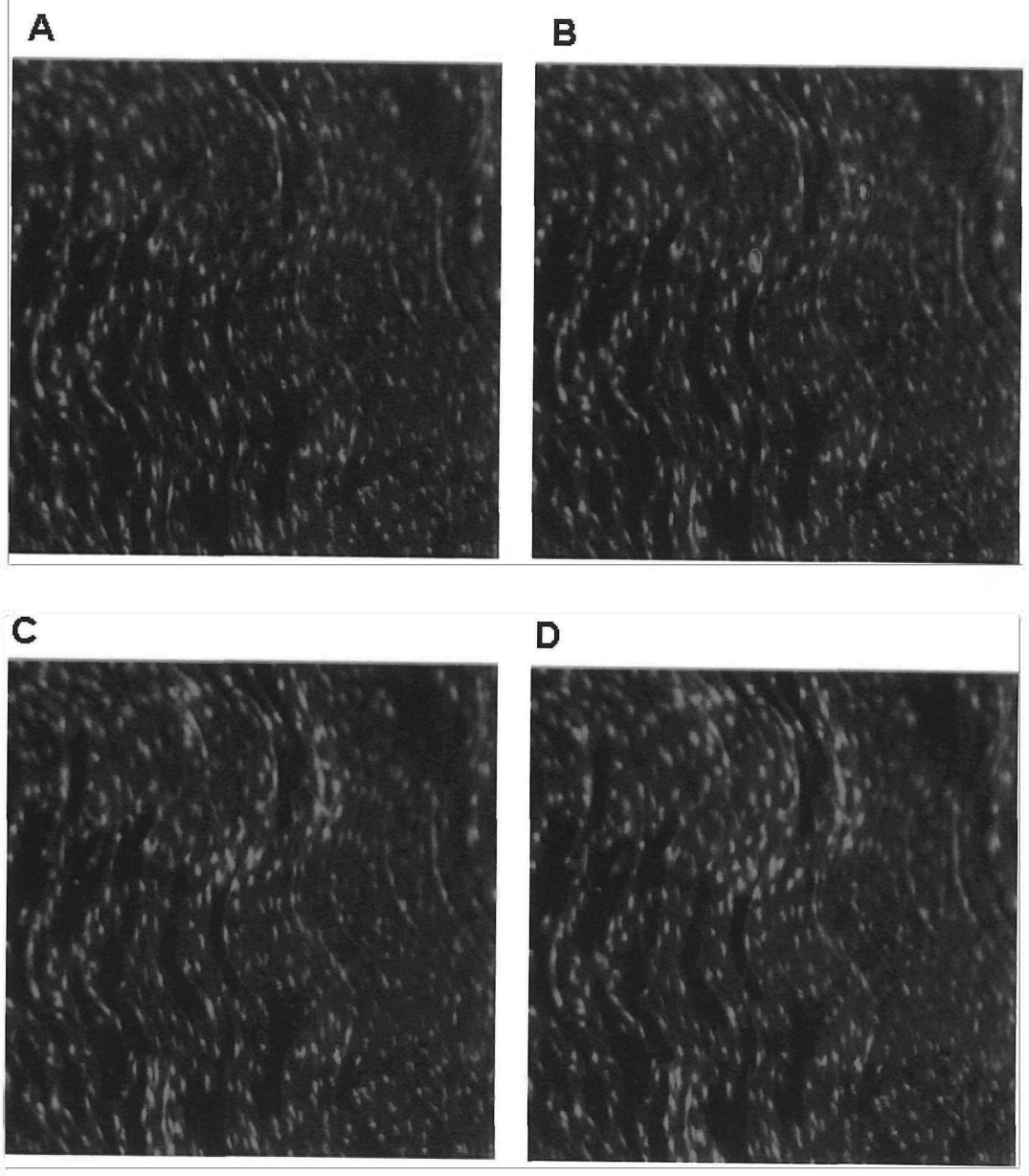

Figure 4-2

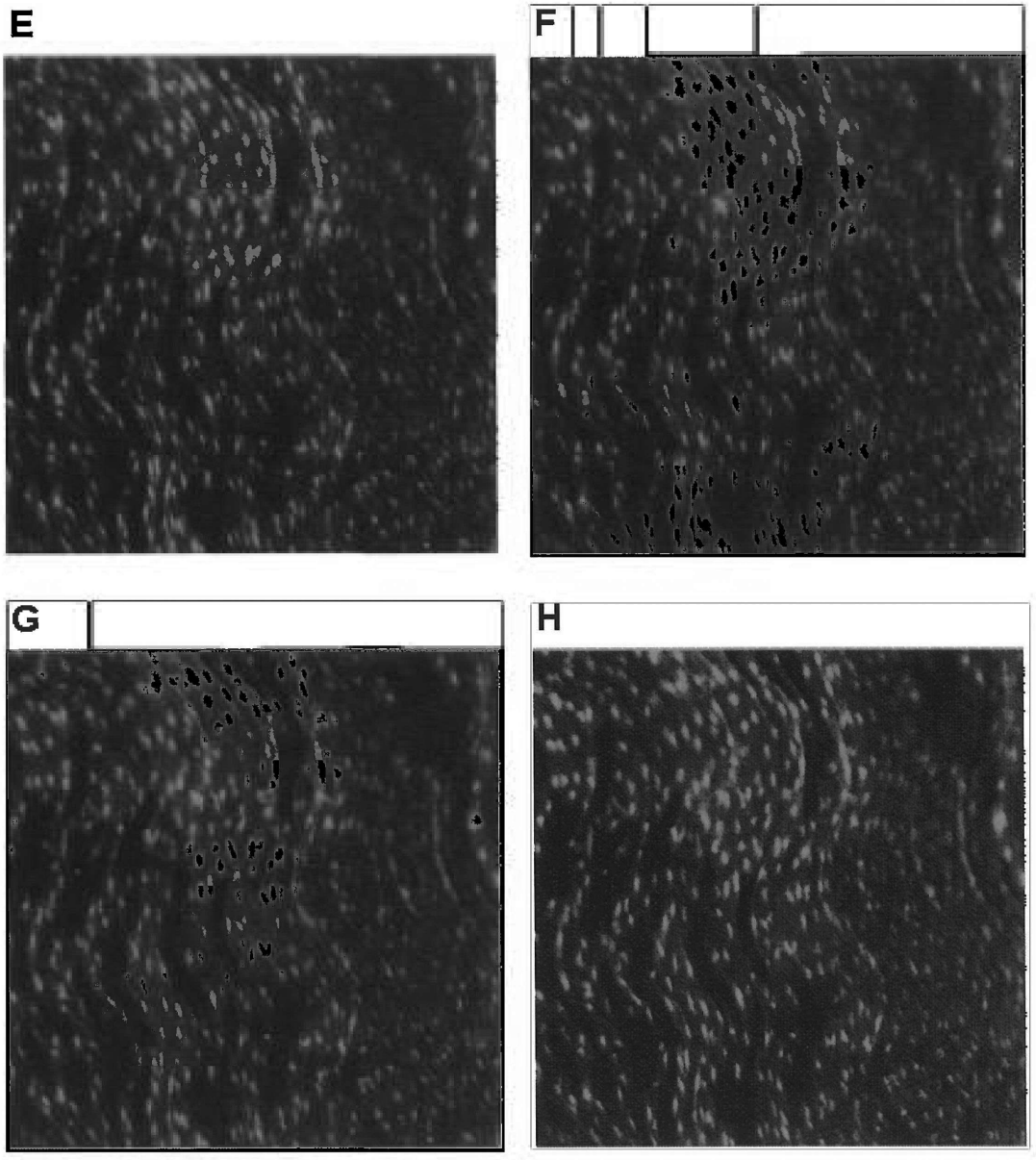

Figure 4-2

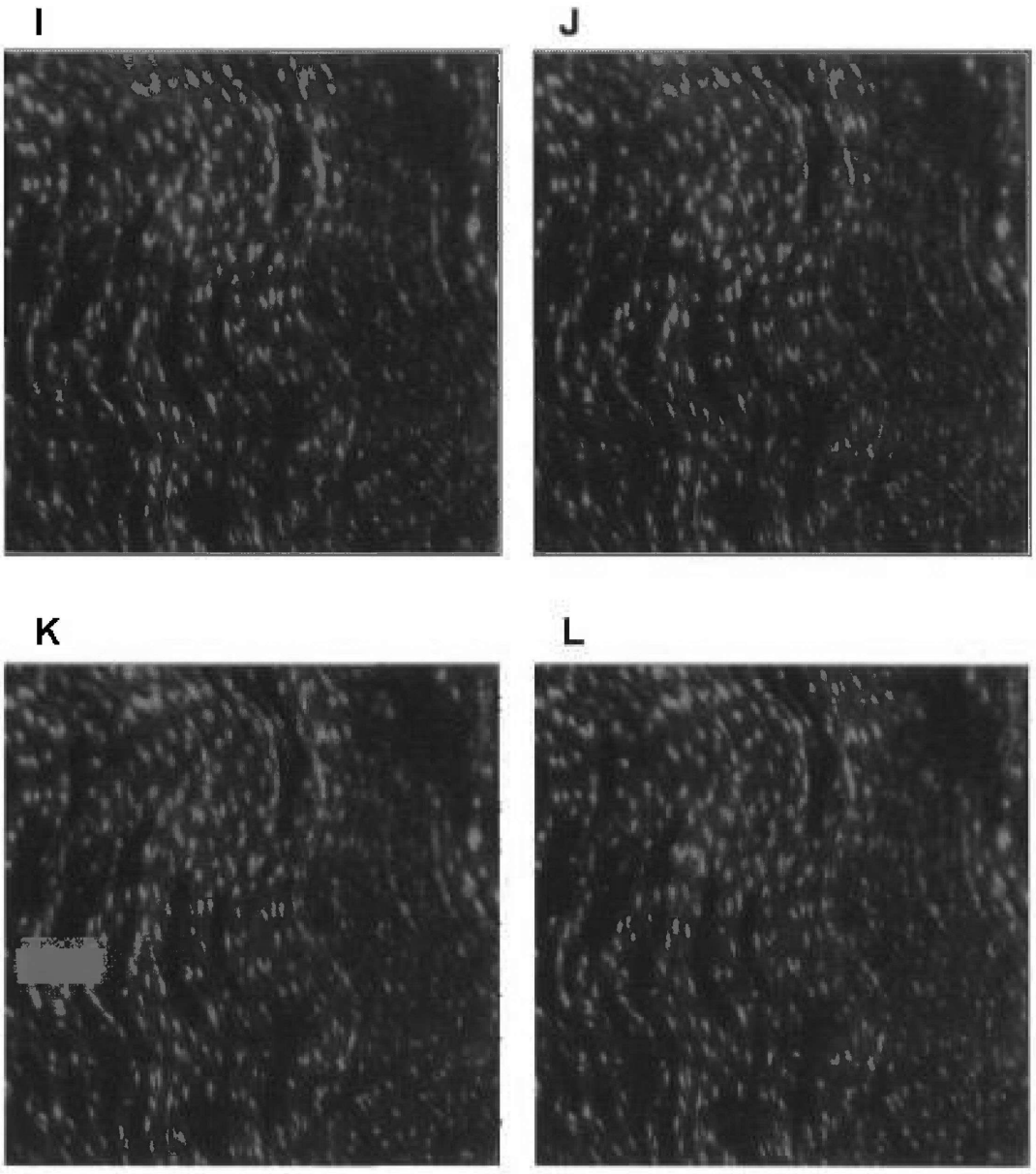

Figure 4-2

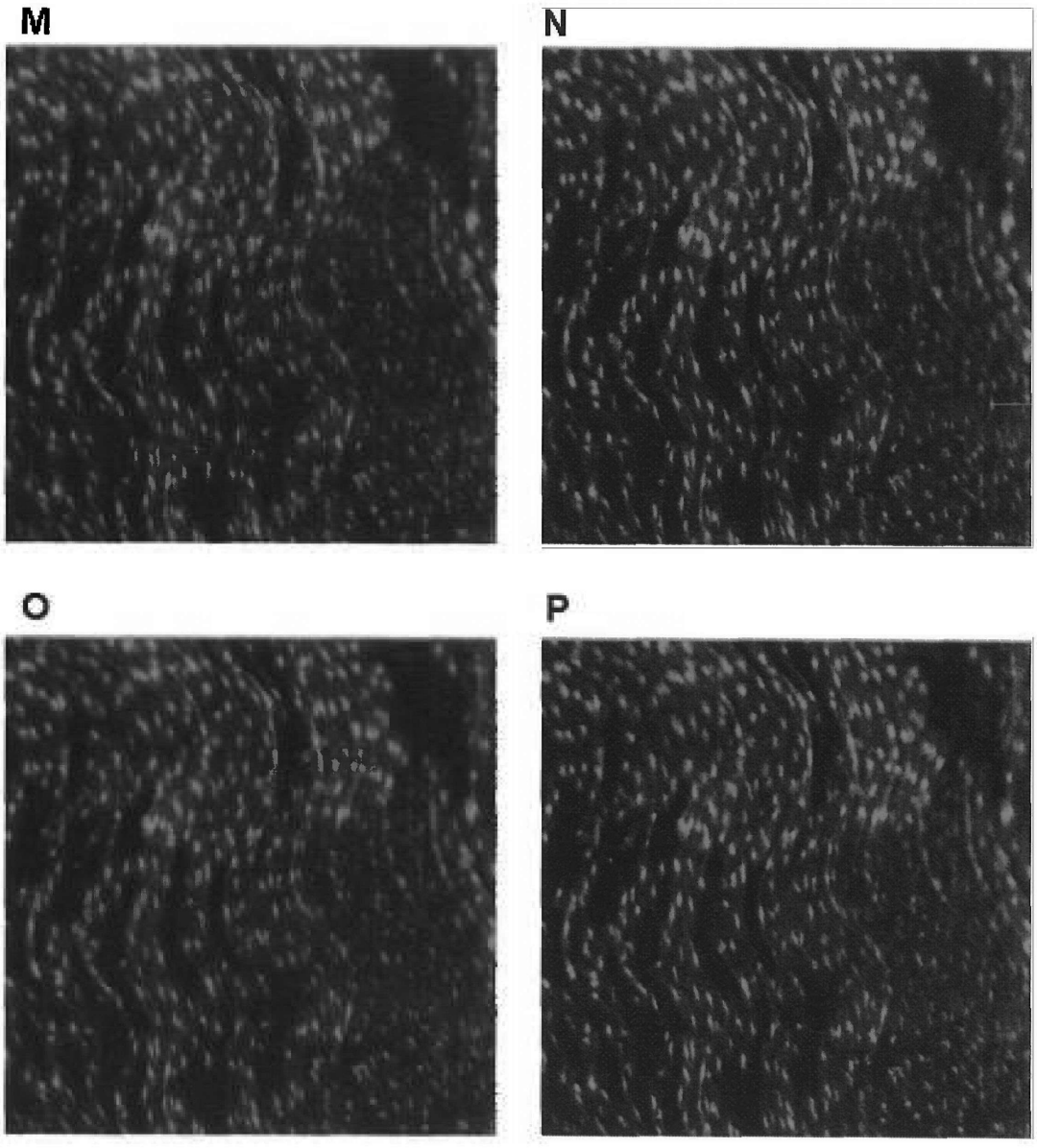

Figure 4-2

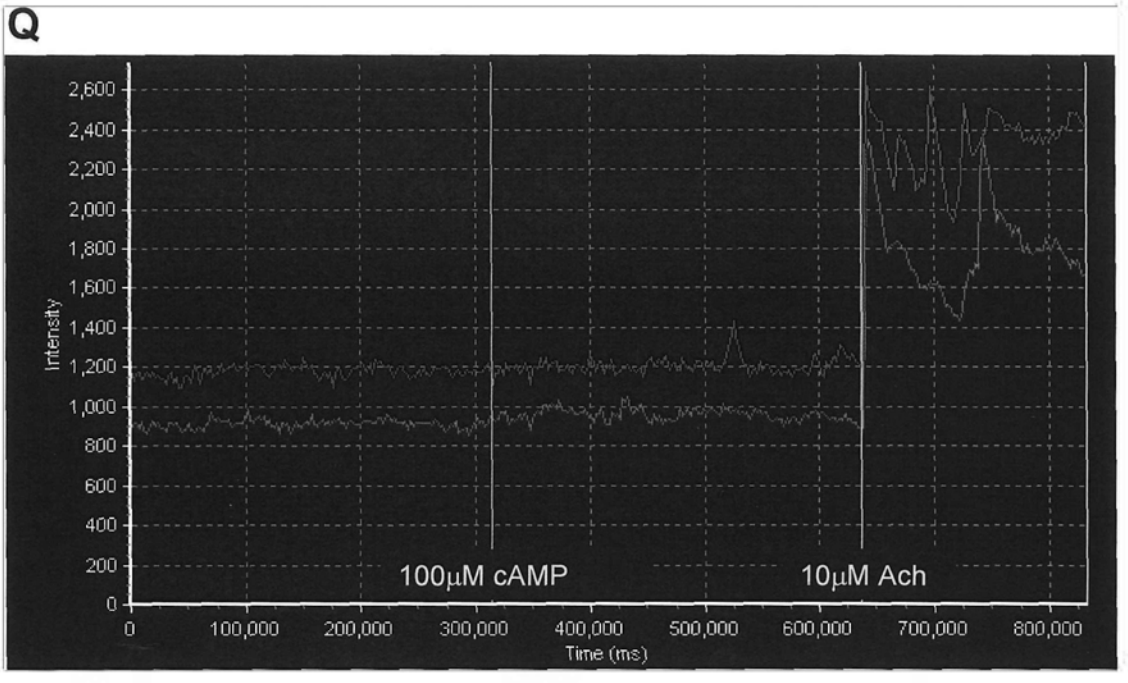

Figure 4-2. $[Ca^{2+}]_i$ activity in aortic endothelial cells in freshly isolated aortic ring in Mg-free KHS in response to 100μM cAMP and 10μM Ach.

A – O show the sequential fluorescence image of the luminal face of the aortic ring after the addition of Ach. Images were taken 2.3 seconds apart. **Q** Red and green lines correspond to the $[Ca^{2+}]_i$ fluctuation in the two endothelial cells circled red and green in **B**.

Figure 4-3

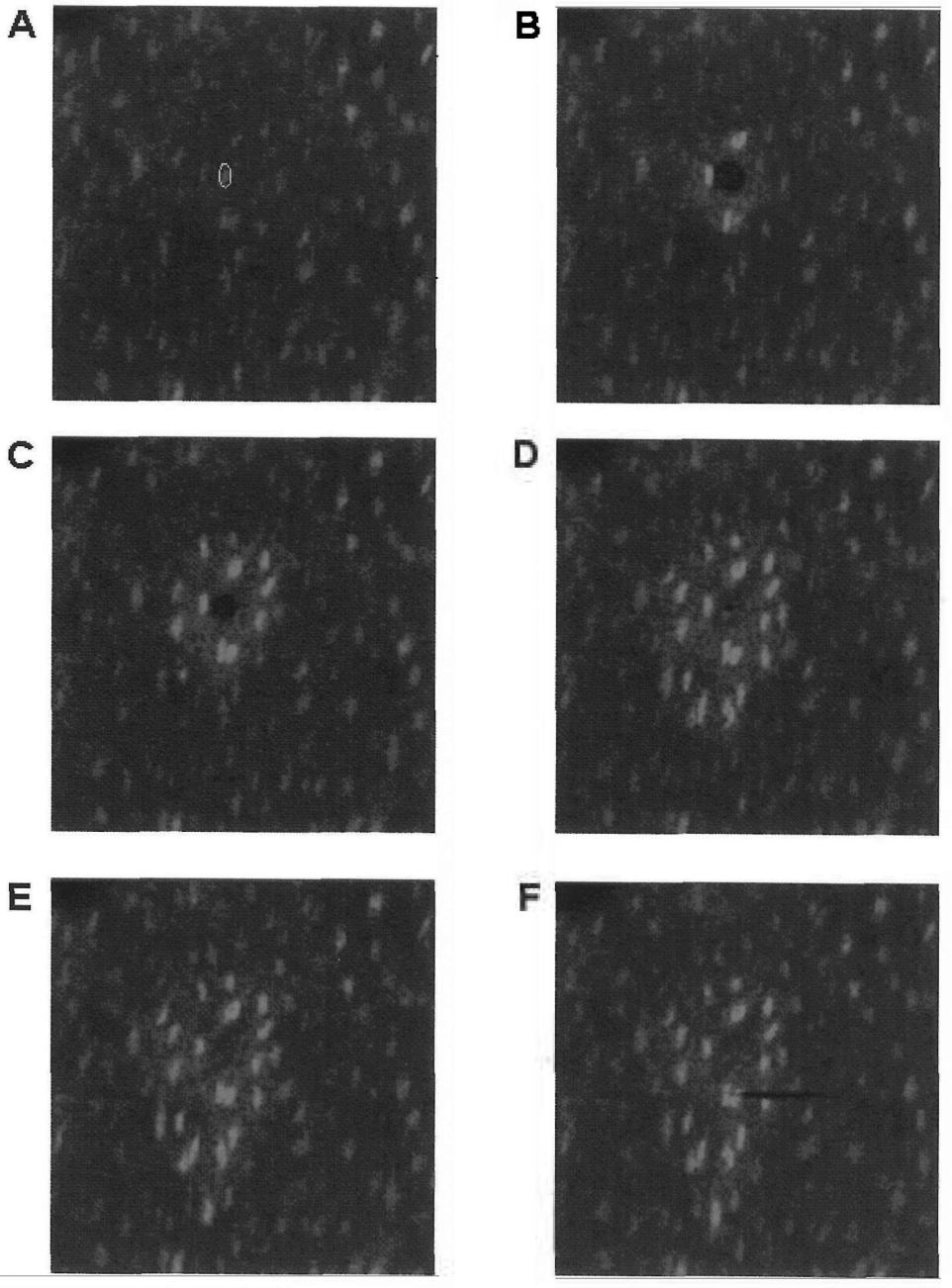

Figure 4-3

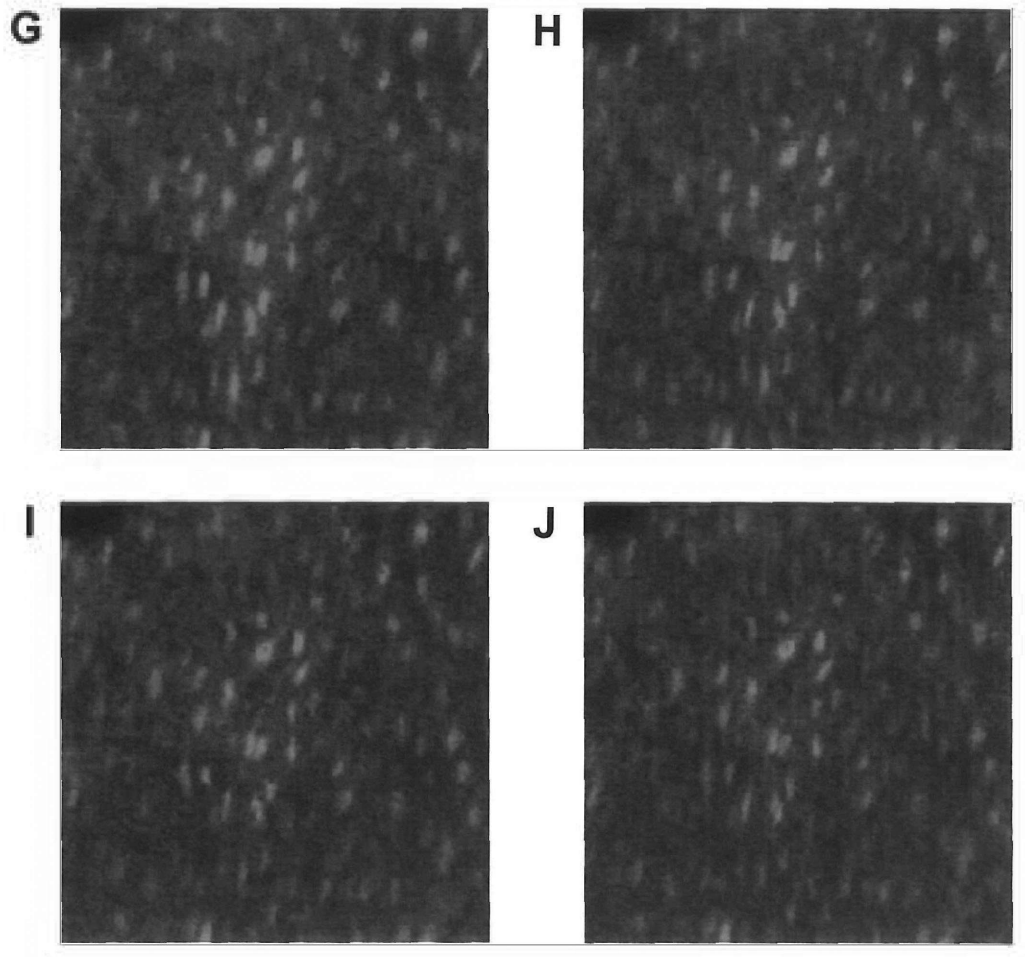

Figure 4-3. $[Ca^{2+}]_i$ activity in aortic endothelial cells in freshly isolated aortic ring in Mg-free KHS in response to mechanical injury by gas bubble. The cell circled in yellow was damaged and disappeared.

Figure 4-4

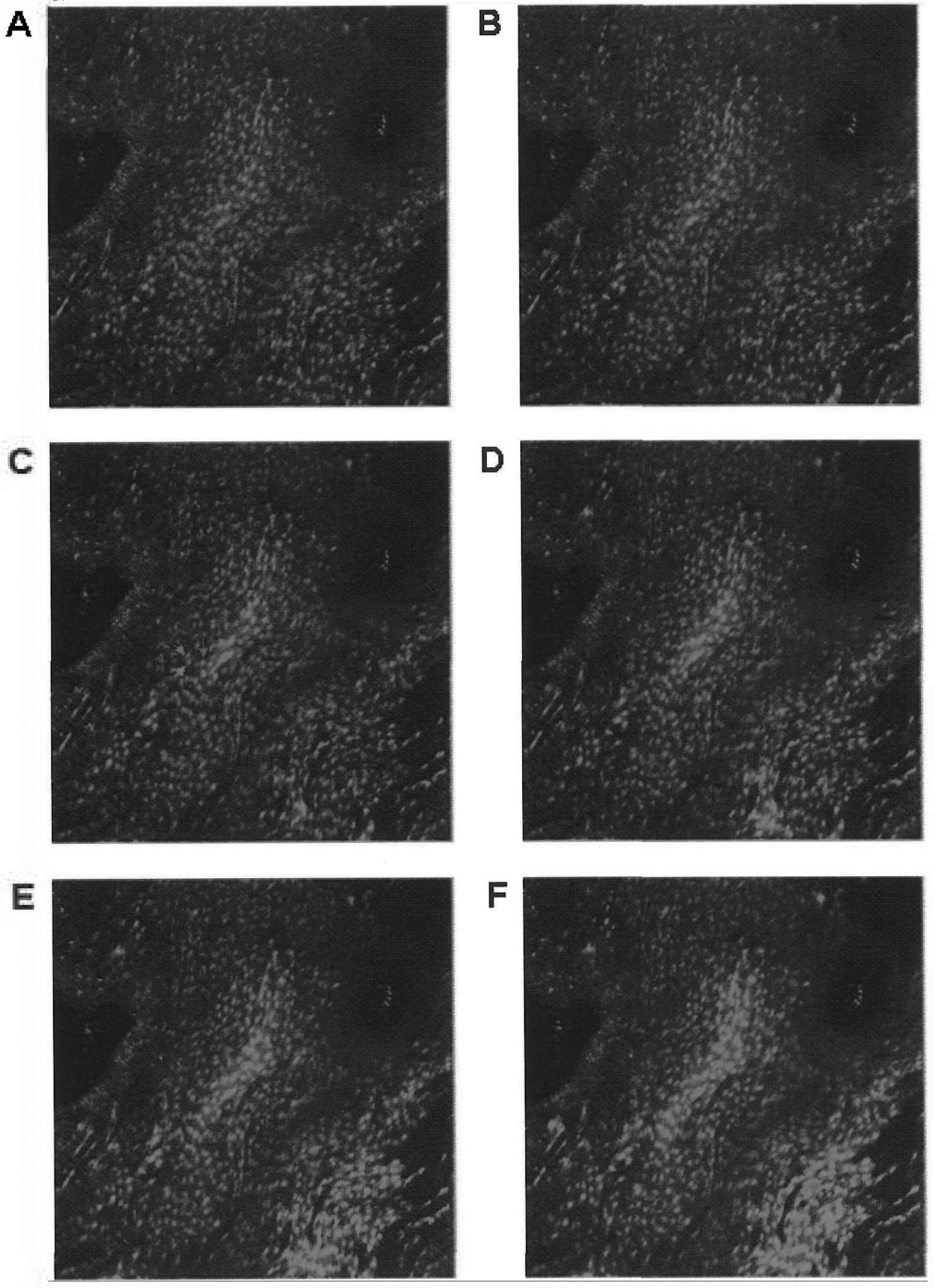

Figure 4-4

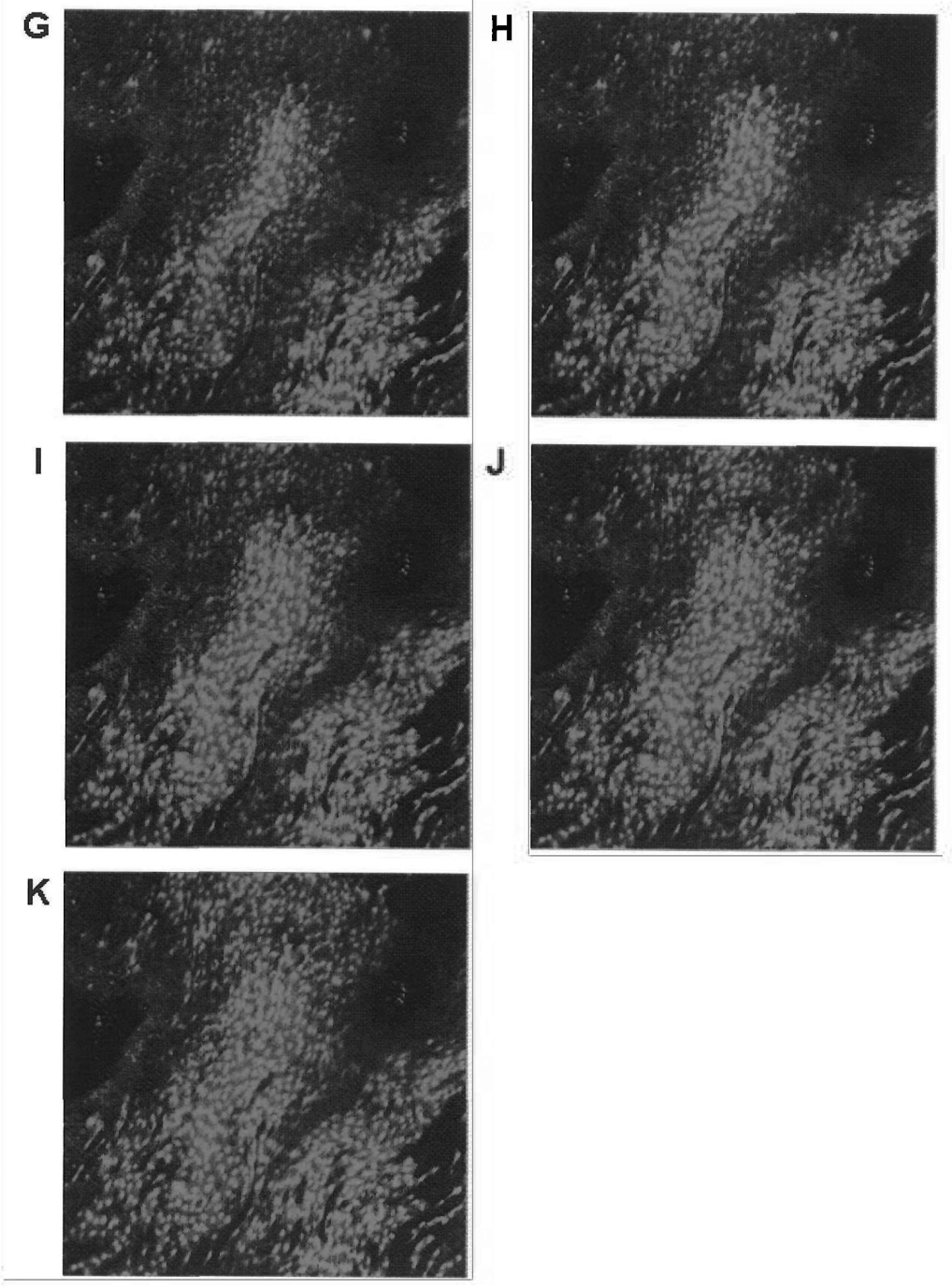

Figure 4-4

L

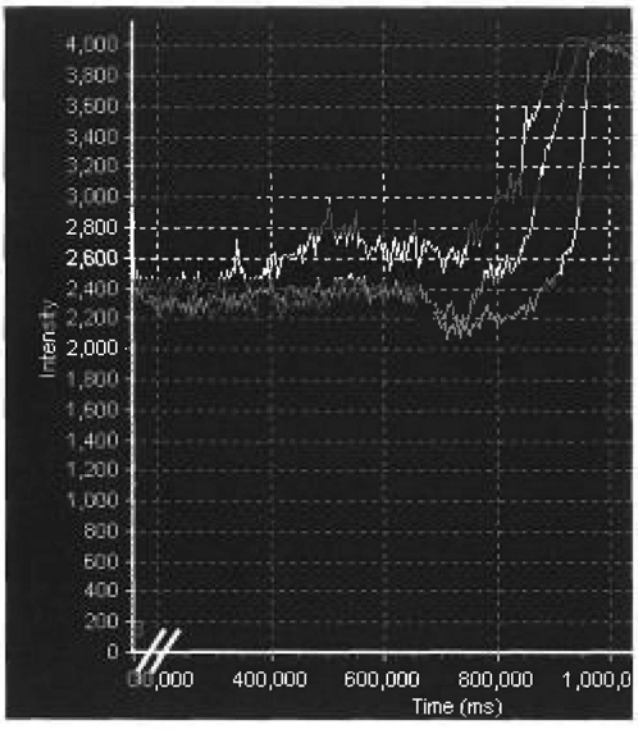

Figure 4-4. $[Ca^{2+}]_i$ activity in aortic endothelial cells in freshly isolated aortic ring in normal KHS in response to 20μM LY-83583.

A – K show the sequential fluorescence image of the luminal face of the aortic ring 600 seconds after the addition of LY-83583. Images were taken 35 seconds apart. **L** Red, blue and orange lines are representative traces of the $[Ca^{2+}]_i$ fluctuation in the three neighboring endothelial cells indicated with the corresponding color of arrows in **C**.

Figure 4-5

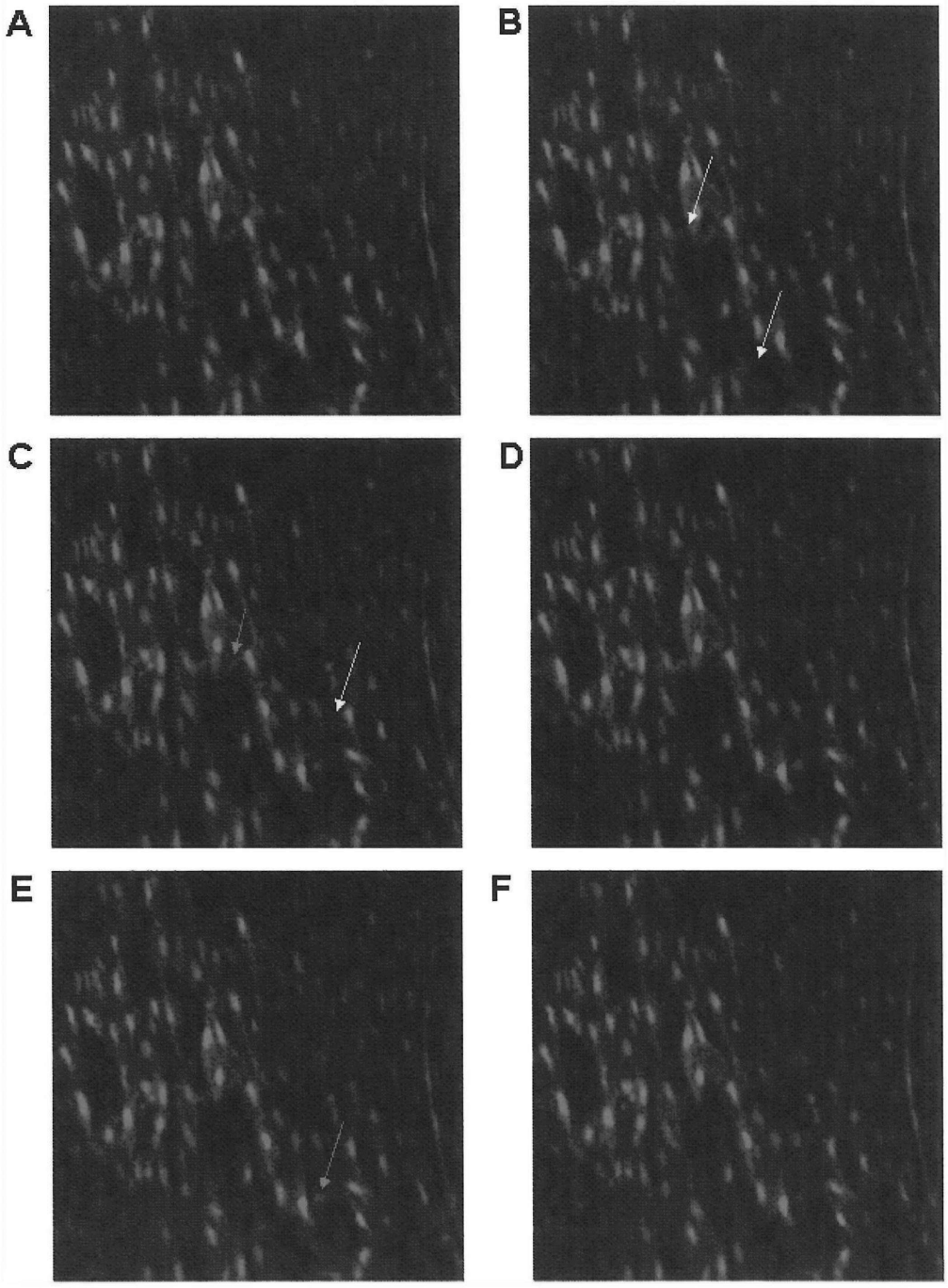

Figure 4-5

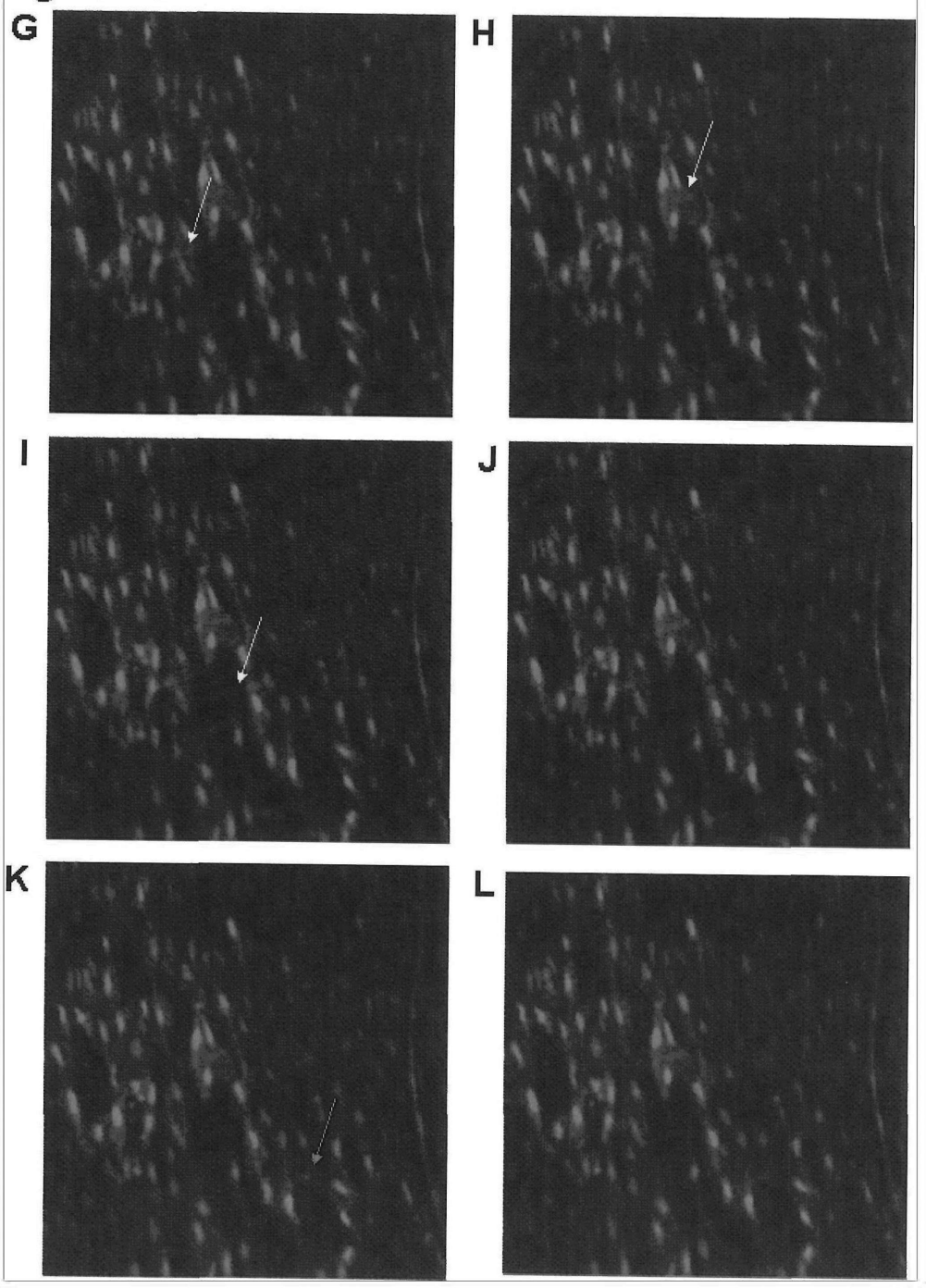

Figure 4-5

M

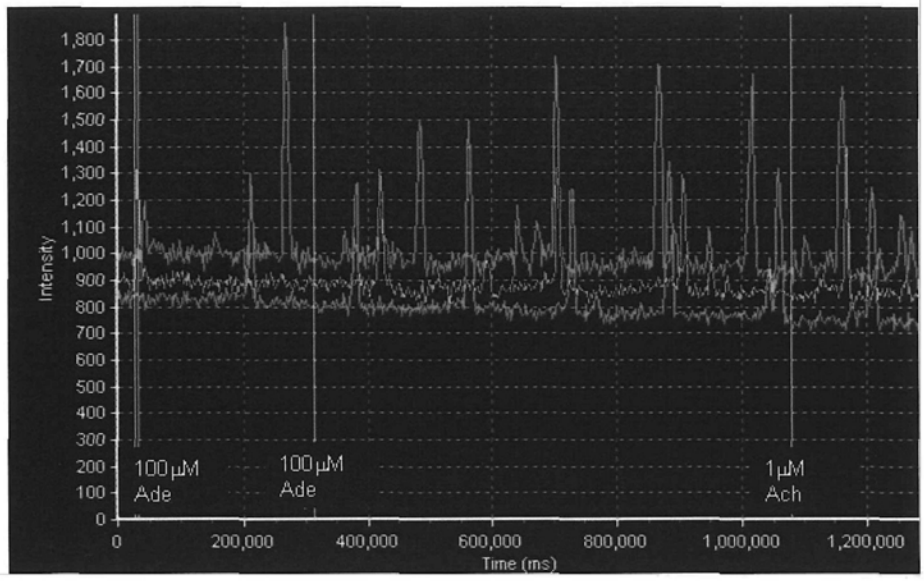

Figure 4-5. $[Ca^{2+}]_i$ activity in aortic smooth muscle cells in freshly isolated aortic ring in response to adenosine and acetylcholine in Mg-free KHS and the presence of 1μM nifedipine

A – L show the sequential fluorescence image of the luminal face of the aortic ring taken every 2.3 second. The fusiform shaped cells on the superficial layer are the endothelial cells while those running perpendicular to the endothelial cells are smooth muscle cells. Yellow arrows point to smooth muscle cells displaying a $[Ca^{2+}]$I rise in the presence of 1μM nifedipine and 100-200μM adenosine in the 27.6 second duration.
G shows representative traces of the change in $[Ca^{2+}]_i$ in three separate aortic smooth muscle cell as indicated by the colored arrows in **C** and **K** over the course of the experiment.

Figure 4-6

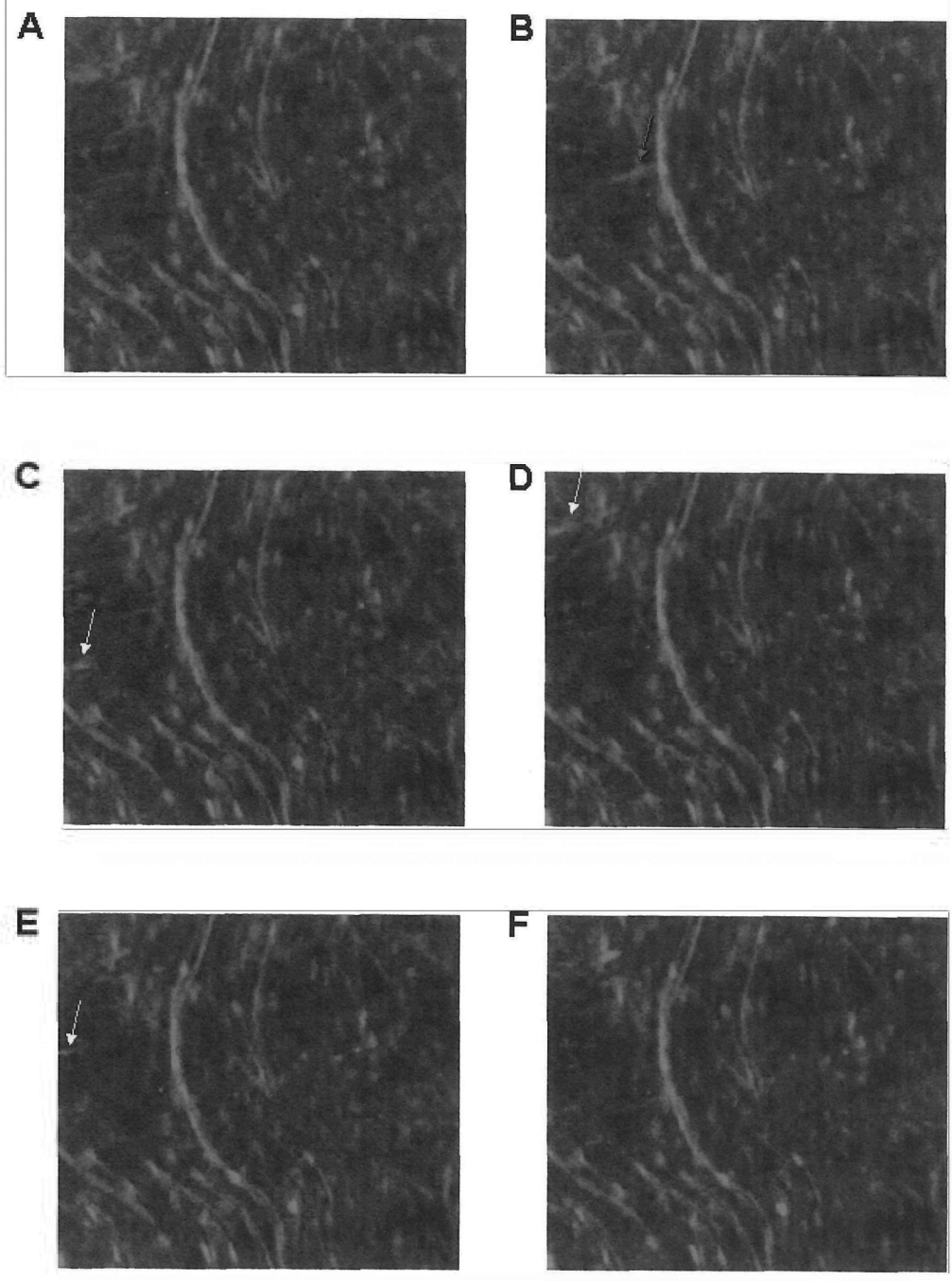

Figure 4-6

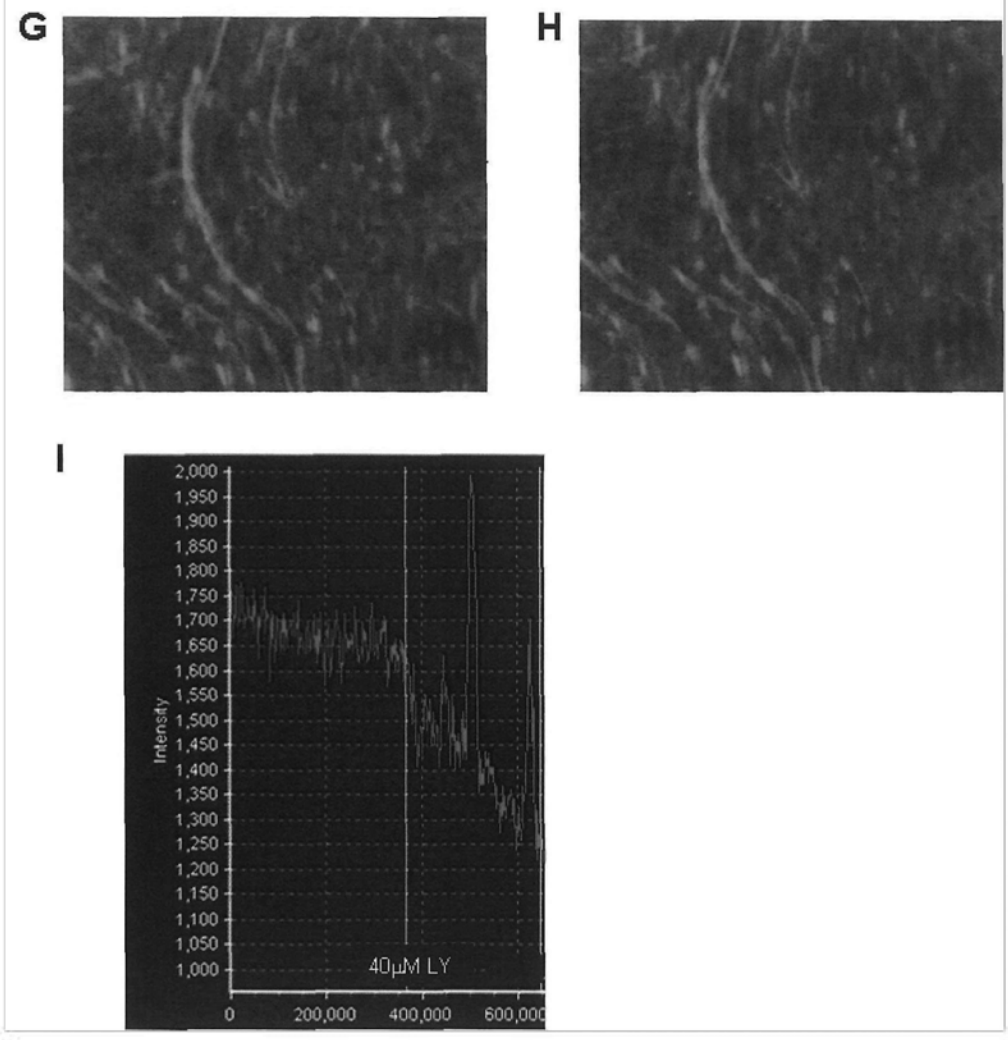

Figure 4-6. $[Ca^{2+}]_i$ activity in aortic smooth muscle cells in freshly isolated aortic ring in response to 40mM LY-83583 in Mg-free KHS.

A –H show the sequential fluorescence image of the luminal face of the aortic ring. Images were taken 2.3 seconds apart. Yellow arrows point to some of the smooth muscle cells displaying $[Ca^{2+}]_i$ sparks. **I** shows a representative trace of the change in $[Ca^{2+}]_i$ in the smooth muscle cell indicated by red arrow in **B**. The overall declining trend of $[Ca^{2+}]_i$ may because of the movement of the muscle due to a change in contractility making the cells a little bit out of focus.

Chapter 5

cGMP inhibits store-operated Ca^{2+} channels in Jurkat cells

5.1 INTRODUCTION

Stimulation of T cell receptors elevates IP_3 which induce the release of Ca^{2+} from intracellular Ca^{2+} stores (Imboden & Stobo, 1985). Subsequent Ca^{2+} depletion of the stores activates store-operated Ca^{2+} entry (SOCE), resulting in a sustained elevation in $[Ca^{2+}]_i$ level that is essential for diverse cellular responses including gene transcription and expression, production of cytokines and chemokines, differentiation of T cells and T cell clonal expansion. The gene expression profile is regulated by the magnitude and duration of Ca^{2+} signals as the signaling molecules and transcription factors, such as the nuclear factors of activated T cells (NFAT), JUN N-terminal kinase (JNK) and nuclear factor-κB (NF-κB), have different requirements for Ca^{2+} activation (Feske, 2007).

cGMP was demonstrated to regulate intracellular Ca^{2+} level in several ways. In endothelial cells, store-operated Ca^{2+} influx induced by depletion of intracellular Ca^{2+} stores by endoplasmic reticulum Ca^{2+} -ATPase inhibitors was inhibited by the application of cGMP through a PKG dependent mechanism (Kwan et al., 2007). Ca^{2+} entry through store-independent mechanism, such as DAG-stimulated Ca^{2+} entry, was also inhibited by cGMP through its action on PKG (Kwan et al., 2007). One of the ion channels activated by DAG, TRPC3, was shown to be inhibited by a direct phosphorylation by PKG (Kwan et al., 2004). Further studies identified the PKG phosphorylation sites on TRPC3 channels and found that two of them are conserved on TRPC6 and TRPC7 as well, suggesting similar regulation of them by PKG (Yao, 2007). Besides its action on Ca^{2+}-permeable channels, cGMP also stimulate SERCA

and Ca^{2+} pumps in endothelial and smooth muscle cells. Given the ubiquitous expression of cGMP and limited investigation on its effect on Ca^{2+} mobilization in T lymphocytes, the current study was designed to examine the role of cGMP on store-operated Ca^{2+} entry in Jurkat cells.

Specifically, thapsigargin pretreatment induced SOCC in Jurkat cells, which was associated with an elevation in intracellular cGMP in the presence of extracellular Ca^{2+} (Bian et al., 1996). In the current study, we examined the role of cGMP and PKG in regulating the store-operated Ca^{2+} entry in Jurkat cells.

5.2 MATERIALS AND METHODS

5.2.1 Materials

Calcium Green and pluronic F127 were purchase from Molecular Probes, Inc.

U73122

1-[6-[((17β)-3-Methoxyestra-1,3,5[10]-trien-17-yl)amino]hexyl]-1H-pyrrole-2,5-dione, KT5823, 8-Br-cGMP and thapsigargin were from Calbiochem.

S-nitroso-*N*-acetylpenicillamine (SNAP),

1H-[1,2,4]Oxadiazolo[4,3-a]quinoxalin-1-one (ODQ), DT-2, U73343

1-[6-[((17β)-3-Methoxyestra-1,3,5[10]-trien-17-yl)amino]hexyl]-2,5-pyrrolidinedione were from Sigma.

5.2.2 Cell culture

Human lymphoblastoid T cells (Jurkat cells) were routinely maintained in RPMI 1640 medium (Invitrogen), supplemented with 10% fetal bovine serum, 2 mM L-glutamine and 1% penicillin/streptomycin in a humidified atmosphere at 37 °C in 95% O_2 and 5% CO_2.

5.2.3 $[Ba^{2+}]_i$ measurement

Confocal microscopy was used to visualize the changes in cytosolic Ba^{2+} concentration revealed by the fluorescent indicator Calcium Green.

One day before experiment, the cells were trypsinized and seeded on 25mm glass cover slips in 6 wells plates. Jurkat cells were loaded with Calcium Green and 0.02% pluronic F-127 in NPSS for one hour in dark at 37℃ before the imaging experiment. After washing three times with $0Ca^{2+}$-PSS (OPSS), the cover slip with cells was fixed in a chamber filled with OPSS and the chamber placed on the stage of the microscope for fluorescence imaging.

Cells were treated with 4μM thapsigargin, a SERCA inhibitor, for 10 minutes to deplete the intracellular Ca^{2+} stores and initiate the opening of store-operated Ca^{2+} ion channels. 1mM $BaCl_2$ was then added into the bath to study the possible ion movement through SOCC channels.

To investigate the effect of cGMP, PKG on the SOCC, different concentrations of cell membrane permeable 8-Br-cGMP, ranging from 0.2-1mM; PKG antagonists, 1μM KT5823 or 500nM DT2; GC inhibitor, 10nM ODQ; or GC activator and NO donor, 100nM S-Nitroso-*N*-acetylpenicillamine (SNAP) were added respectively to pretreat the cells for 5 minutes before stimulation of SOCC by thapsigargin.

5.3 RESULTS

5.3.1 cGMP inhibits SOC induced by thapsigargin in Jurkat cell line

Pretreatment with 4μM Thapsigargin, a selective inhibitor of endoplasmic reticulum Ca^{2+}-ATPase, in OPSS for 10 minutes caused depletion of Ca^{2+} store and the opening of store-operated calcium channels, leading to Ba^{2+} influx into Jurkat

cells upon the addition of $BaCl_2$ (Fig. 5-1). This is consistent with the results obtained by Philipp et al. (2003). 8-Br-cGMP, a membrane permeable form of cGMP, caused a dose dependent inhibition of the Ba^{2+} current into Jurkat cells (Fig. 5-2).

5.3.2 PKG inhibitors reversed the inhibitory effect of cGMP

We then proceed to examine if the inhibition of Ca^{2+}-store operated Ba^{2+} influx by cGMP was mediated by protein kinase G. (PKG). 1mM KT5823, a PKG inhibitor, reversed the 8-Br-cGMP inhibition on store-operated Ba^{2+} influx (Fig. 5-3). Similarly, another PKG inhibitor, DT2 (500nM), also reversed the inhibitory effect of 8-Br-cGMP (Fig. 5-4). 100nM SNAP, a NO donor and sGC activator, reduced the Ba^{2+} influx caused by SOC in a similar way as the addition of 8-Br-cGMP, and its effect was reversed by the addition of 10nM ODQ, a selective inhibitor of NO sensitive GC (Fig. 5-5). The Ba^{2+} influx in the case with ODQ pretreatment was even higher than in the control case suggesting that basal level of cGMP might serve a negative feedback role in SOCE.

5.4 DISCUSSION

Previous studies in primary aortic endothelial cells showed that cGMP, by activating protein kinase G (PKG), may inhibit Ca^{2+} influx through SOCC (Kwan et al., 2000). Another study on pulmonary artery smooth muscle cells suggested that NFAT nuclear translocation is dependent on SOCC through TRPC1 and inhibited by cGMP (Wang et al., 2009). In the current study, the channels responsible for SOCC allow the passage of Ba^{2+} ion. Importantly, cGMP dose dependently decreased the Ca^{2+} store-operated Ba^{2+} influx in T lymphocytes. Nitric oxide donor SNAP, which could elevate cytosolic cGMP level, had similar effect on store-operated Ba^{2+} influx. The action of nitric oxide and cGMP was mediated through protein kinase G, because

the effect could be inhibited by KT5823 and DT2.

However, it is unclear which specific Ca-permeable channels mediates this store-operated Ba^{2+} influx that is sensitive to protein kinase G inhibition. Previous studies have shown that TRPC3 channels are present on the plasma membrane of Jurkat T-cell lines and were suggested to play a pivotal role in the T-cell receptor-dependent calcium entry (Philipp et al., 2003). Furthermore, Kwan et al showed that PKG can phosphorylate and thus inhibit TRPC3 channels (Kwan et al., 2004). Hence, TRPC3 is a possible candidate for mediating the SOCC in Jurkat cells pretreated with thapsigargin. However, caution may have to be taken for this statement, because another study by Kim et al. (2009) argued against the involvement of TRPC1 and TRPC3 in SOC of Jurkat cells. Orai1 was also suggested to be a pore-forming subunit in mediating SOCC in T cells (Luik & Lewis, 2007). However, there is no report on whether Orai1 can be modulated by protein kinase G. Nevertheless, it is reported that Orai1 may interact with TRPC3 or TRPC6, thus turn the TRP channels from store-independent to store-dependent channels (Liao et al., 2007). Therefore, we cannot exclude the involvement of Orai1.

Bian et al. showed that TG stimulates SOC entry and a sustained elevation of cGMP in Jurkat cells in the presence of extracellular Ca^{2+} (1996). An increase in cGMP level was not apparent in the absence of extracellular Ca^{2+}, suggesting that an elevated level of $[Ca^{2+}]i$ is required for the generation of cGMP. We reason that Ca influx through SOC would activate nitric oxide synthase to produce nitric oxide, which would elevate cGMP level in T lymphocytes. We have demonstrated that this indeed happened at least in vascular endothelial cells (Kwan et al., 2000; Yao & Huang, 2003).

cGMP was found to stimulate SERCA (Lau et al., 2003; Cohen et al., 1999) in endothelial and smooth muscle cells, which accelerate store refilling and decrease the

subsequent SOCC. But this may not apply to the current study as we are only studying the Ca influx in this study.

In conclusion, the current study suggests that cGMP and PKG may play a key role in the regulation of the store-operated Ca^{2+} entry in Jurkat cells.

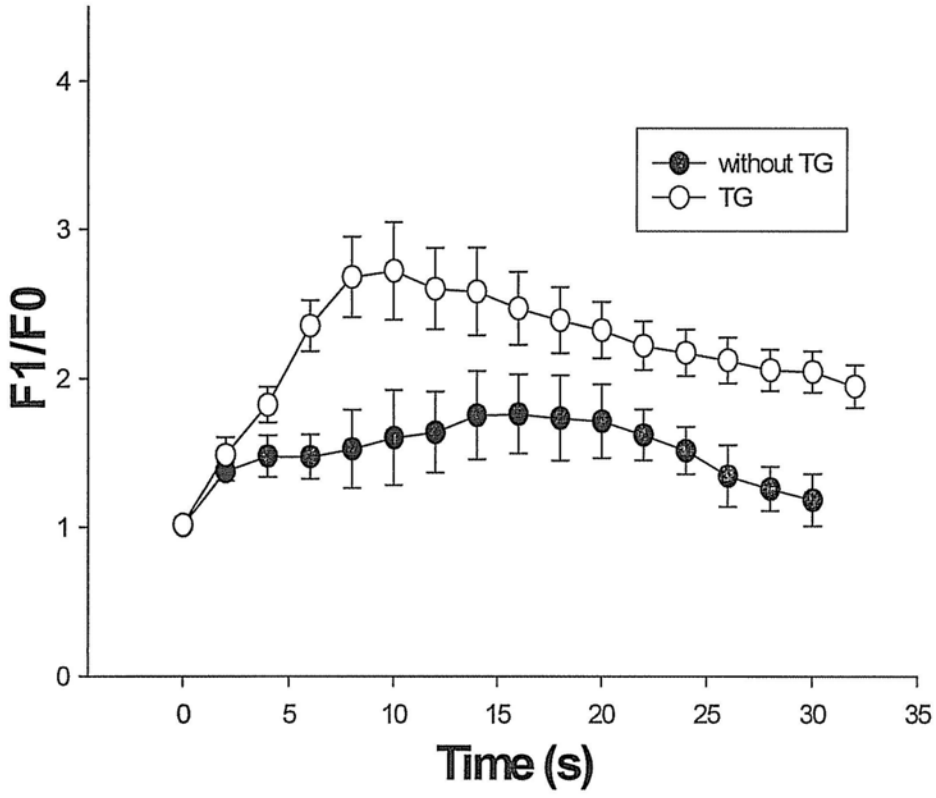

Figure 5-1 Traces showing changes in $[Ba^{2+}]_i$ in Jurkat cells upon the addition of $BaCl_2$ at time 0 in OPSS with or without 4 mM thapsigargin pretreatment.

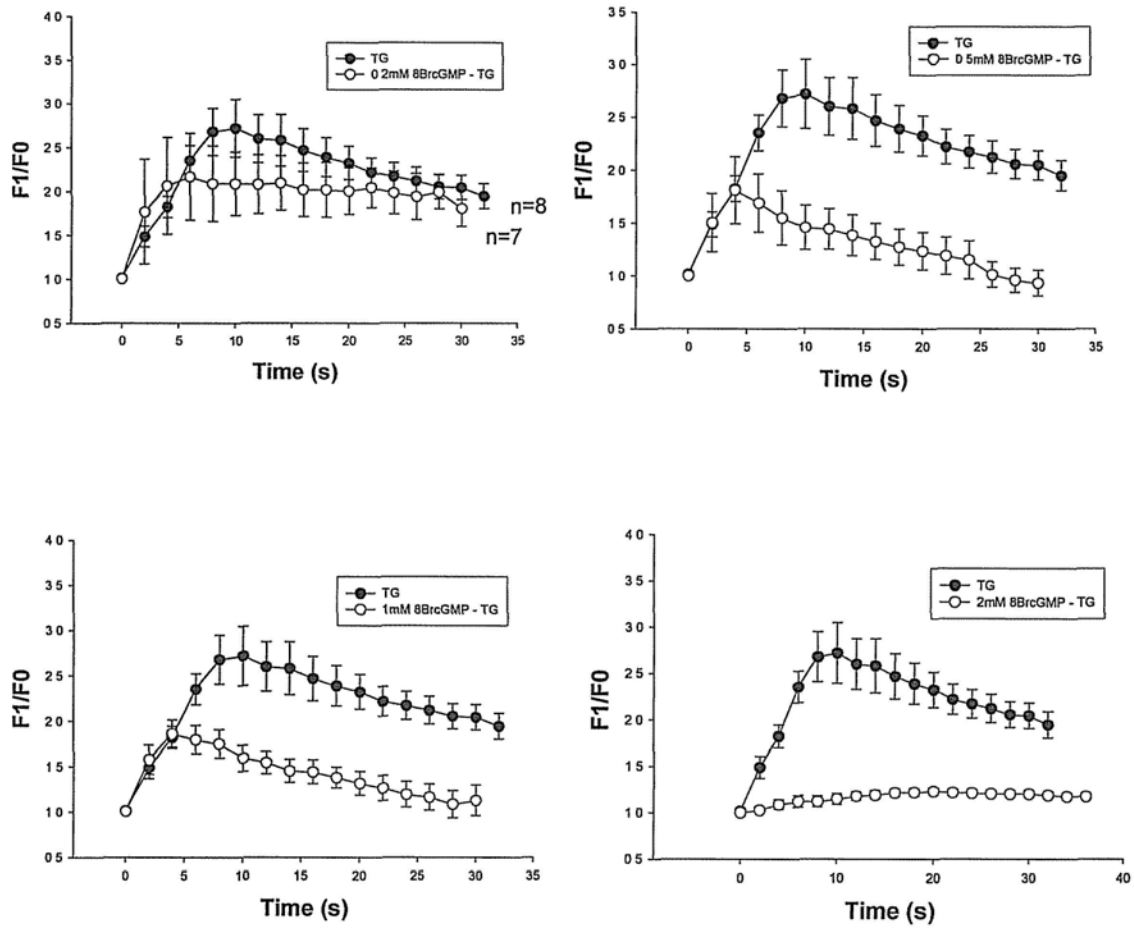

Figure 5-2 Traces showing the changes in $[Ba^{2+}]_i$ in Jurkat cells induced by pretreatment with 4mM thapsigargin in OPSS for 5 minutes in the presence of various concentrations of 8-Br-cGMP. (A) 0.2mM (n=7) (B) 0.5mM (n=8) (C) 1mM (n=8) and (D) 2mM (n=15). Ba^{2+} influx was initiated by addition of extracellular Ba2+ at time 0.

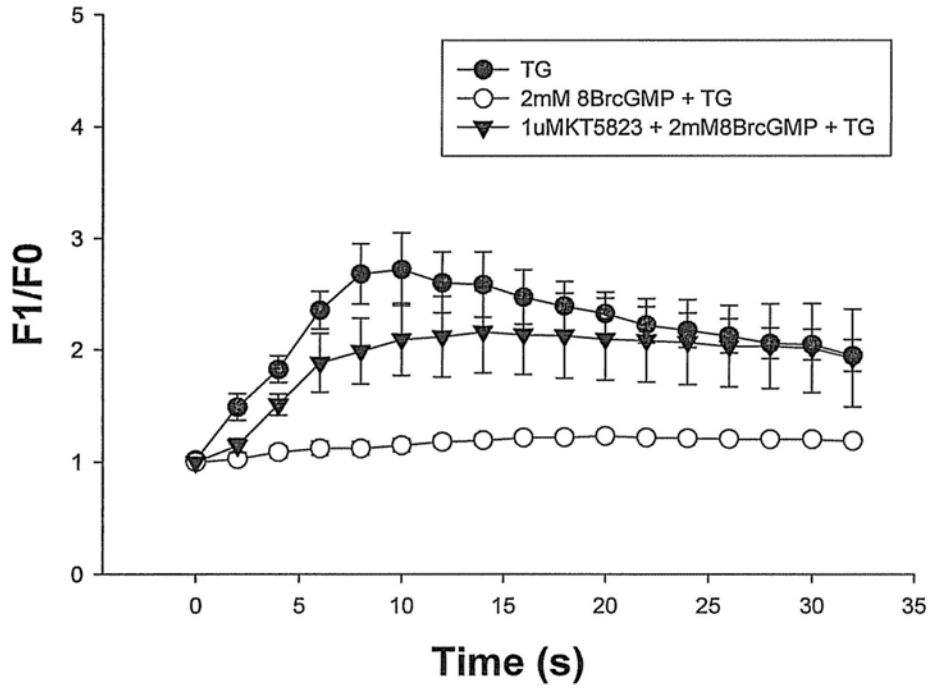

Figure 5-3 Traces showing that 1 μM KT5823 reversed the inhibitory action of 8-Br-cGMP on Ba^{2+} influx.

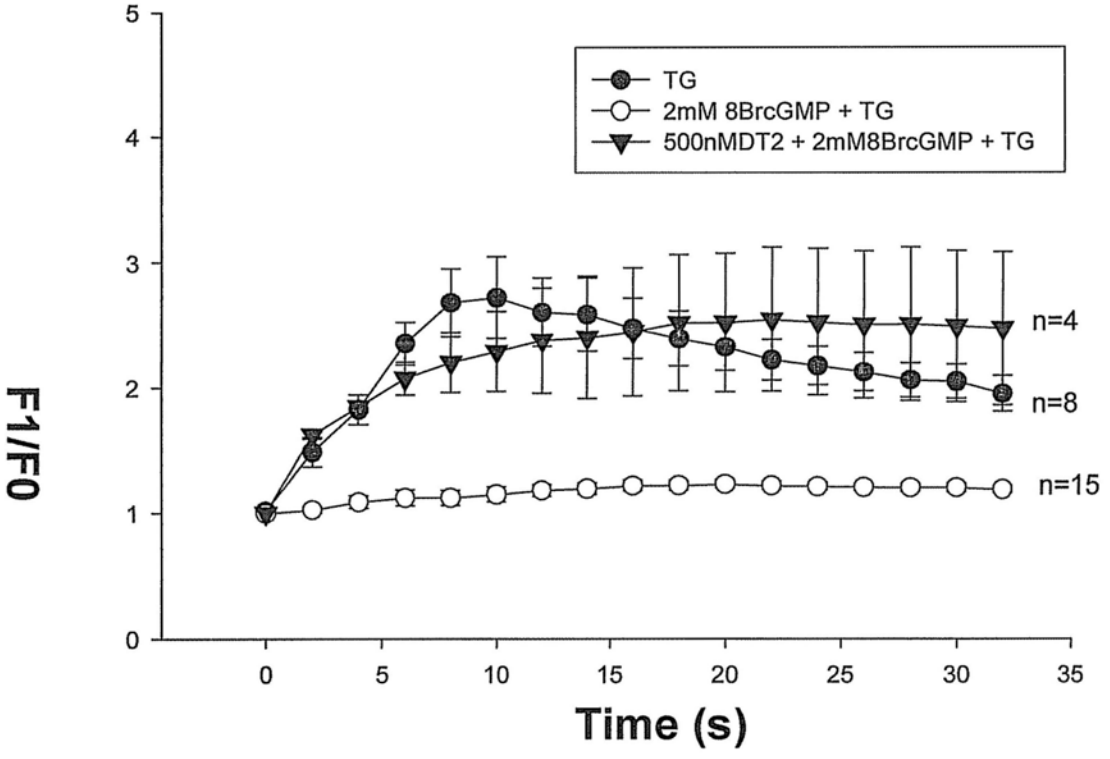

Figure 5-4 Traces showing that the effect of 500nM DT2 reversed the 8-Br-cGMP inhibition on Ba^{2+} influx.

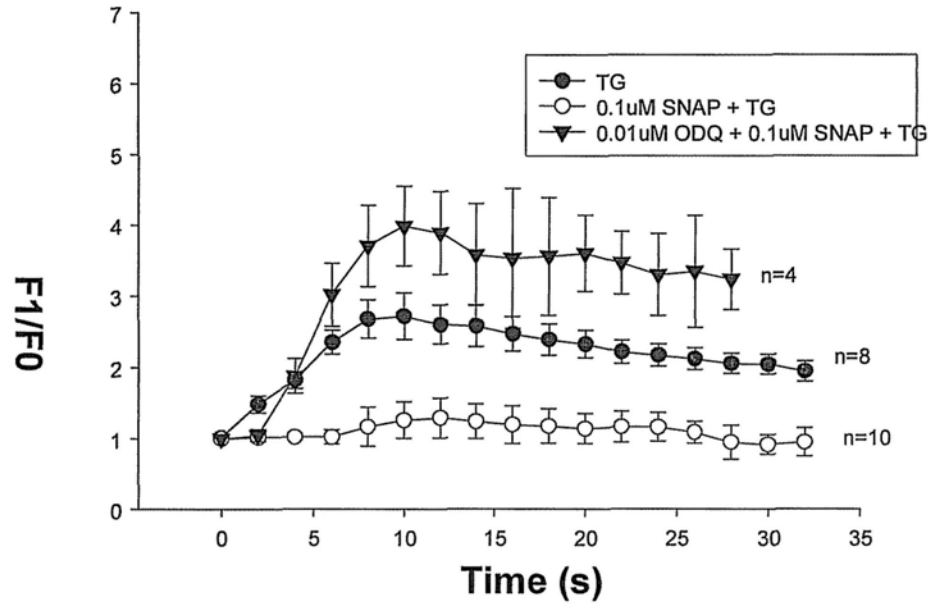

Figure 5-5 Trace showing the effect of 0.1 μM SNAP (○) and 10nM ODQ + 0.1 μM SNAP (▼) on thapsigargin-induced Ba^{2+} signal in Jurkat cells.

Chapter 6

cGMP inhibits histamine-induced Ca^{2+} rise in Jurkat cells

6.1 INTRODUCTION

Histamine (2,4-imidazolyl-ethylamine) is a biogenic amine. It is synthesized by decarboxylation of the amino acid histidine and the reaction is catalyzed by histidine decarboxylase. Histamine released from mast cells and basophils acts on T lymphocytes to affect their proliferation (Radvány et al., 2000) and the production and release of cytokines (Dohlsten et al., 1987). An elevation in $[Ca^{2+}]_i$ is an important early event in the signaling cascade triggered by histamine. Histamine-induced $[Ca^{2+}]_i$ rise in Jurkat T lymphocyte comprises of Ca^{2+} release from intracellular Ca^{2+} stores and Ca^{2+} influx from extracellular spaces. Chelation of extracellular Ca^{2+} by EGTA was found to reduce the magnitude of histamine-induced $[Ca^{2+}]_i$ rise by 50-80% (Kitamura et al.,1996). Up to the present, four different subtypes of histamine receptors have been cloned. They are H1 (De Backer, et al., 1993), H2 (Gantz et al., 1991), H3 (Lovenberg et al., 1999) and H4 (Oda et al., 2000). Activations of both histamine H1 and H2 receptors are known to stimulate phospholipase C activity, leading to the production of IP_3, which induces Ca^{2+} release from intracellular stores. In Jurkat T cells, it was found that H1 receptor antagonists pyrilamine and doxepin inhibited the histamine-induced $[Ca^{2+}]_i$ rise more potently than the H2 receptor antagonist cimetidine (Kitamura et al., 1996).

In the previous chapter, we found that cGMP inhibits store-operated Ca^{2+} influx in Jurkat cells through its activation of PKG. In this chapter, we explored whether cGMP and PKG affect histamine-induced $[Ca^{2+}]_i$ rise in Jurkat T cells.

6.2 MATERIALS AND METHODS

6.2.1 Materials

Fluo3-acetoxymethyl ester (AM) and pluronic F127 were purchased from Molecular Probes, Inc. U73122 1-[6-[((17β)-3-Methoxyestra-1,3,5[10]-trien-17-yl)amino]hexyl]-1H-pyrrole-2,5-dione, KT5823, 8-Br-cGMP and thapsigargin were from Calbiochem. Histamine, pyrilamine, cimetidine, DT-2, U73343 1-[6-[((17β)-3-Methoxyestra-1,3,5[10]-trien-17-yl)amino]hexyl]-2,5-pyrrolidinedione were from Sigma.

6.2.2 Cell culture

Jurkat cells were routinely maintained in RPMI (Invitrogen), supplemented with 10% FBS, 2 mM l-glutamine and 1% penicillin/streptomycin at 37°C in 95% O_2 and 5% CO_2.

6.2.3 $[Ca^{2+}]_i$ measurement

Confocal microscopy was used to visualize the change in $[Ca^{2+}]_i$ using fluorescent indicators, Fluo-3 actoxymethyl ester (Fluo-3/AM). One day before experiment, the Jurkat cells were trypsinized and seeded on 25 mm glass cover slips in 6 wells plates. The cells were loaded with 10 μM Fluo-3/AM ester and 0.02% pluronic F-127 in culture medium for one hour in dark at 37℃ before the imaging experiments. After washing three times, the cover slip with cells was fixed in a chamber filled with normal physiological saline solution and placed on the stage of the microscope for fluorescence imaging. An MRC-1000 laser scanning confocal

imaging system was used to monitor and record the fluorescent signal, and METAFLOUR software was used in data analysis.

Jurkat cells were pretreated with the respective reagents/antagonist (pyrilamine/ cimetidine/ U73122/ U73343/ 8-Br-cAMP/ KT5823+8-Br-cGMP/ DT-2 + 8-Br-cGMP) for 5 minutes in NPSS medium before 100 μM histamine was added. Changes in $[Ca^{2+}]_i$ were displayed as a ratio of fluorescence relative to the intensity before the application of histamine (F1/F0).

6.3 RESULTS

6.3.1 cGMP inhibited the $[Ca^{2+}]_i$ rise in response to histamine in Jurkat cells

100 μM histamine induced a significant increase in $[Ca^{2+}]_i$, which returned to basal level in less than 1 min (Figure. 6-1). This $[Ca^{2+}]_i$ increase was significantly inhibited by the addition of 1 mM or 2 mM 8-Br-cGMP (Figure. 6-2B,C), but minimally affected by 0.5 mM 8-Br-cGMP (Figure. 6-2A).

6.3.2 PKG inhibitors reversed the inhibitory effect of cGMP

Pretreatment of the cells with 1 μM KT5823 reversed the inhibitory effect of 8-Br-cGMP (Figure. 6-3A). Similarly, 500 nM of another PKG inhibitor DT2 also reversed the effect of 8-Br-cGMP (Figure. 6-3B). 0.1 μM SNAP, a nitric oxide donor, totally abolished the $[Ca^{2+}]_i$ rise (Figure. 6-4) and the effect of which was reversed by 10 nM ODQ, a selective inhibitor of guanylate cyclase (Figure. 6-5).

6.3.3 H1 receptor antagonist, pyrilamine, but not H2 receptor antagonist cimetidine, inhibited the histamine induced $[Ca^{2+}]_i$ rise.

0.1 μM pyrilamine, a histamine H1 receptor antagonist, was able to significantly

reduce the magnitude of histamine-induced $[Ca^{2+}]_i$ increase (Figure. 6-6A). The histamine H2 receptor antagonist, cimetidine (4 μM), had little effect on the histamine-induced $[Ca^{2+}]_i$ increase (Figure. 6-6B).

6.3.4 Phospholipase C inhibitor reduced the $[Ca^{2+}]_i$ rise induced by histamine

To determine if phospholipase C is involved in the signal transduction pathway in histamine-induced $[Ca^{2+}]_i$ increase , U73122, an inhibitor for phospholipase C, was used to pretreat the cells. The $[Ca^{2+}]_i$ increase by subsequent addition of histamine was significantly reduced by 10 μM U73122 (Figure. 6-7A). U73343, an inactive analog of U73122, had no effect on the peak $[Ca^{2+}]_i$ increase (Figure. 6-7B).

6.4 DISCUSSION

H1 and H2 histamine receptors are coupled to G proteins $G_{q/11}$ (Leopoldt et al., 1997; Wang et al., 1998). Stimulation of $G_{q/11}$ enhances the activity of phospholipase C, leading to the production of IP_3, which induces Ca^{2+} release from intracellular stores.

Our results showed that histamine induced a transient $[Ca^{2+}]_i$ rise in Jurkat T cells mainly through its action on histamine H1 receptors, but not H2 receptors. This is consistent with the previous findings by Kitamura et al. (1996).

8-Br-cGMP induced a dose-dependent inhibition of this $[Ca^{2+}]_i$ transient with almost total inhibition at 2 mM 8-Br-cGMP. The cGMP inhibition of $[Ca^{2+}]_i$ rise was partially reversed by inhibitors of PKG, suggesting that at least part of this cGMP inhibition is mediated by PKG. SNAP, a nitric oxide donor that stimulates the activity of guanylate cyclases to produce cGMP, also abolished this $[Ca^{2+}]_i$ rise (Figure. 6-4).

The inhibitory effect of SNAP could be reversed by ODQ, which inhibits guanylate cyclases. Taken together, these data indicate that cGMP and protein kinase G can inhibit histamine-induced $[Ca^{2+}]_i$ rise in Jurkat T cells. Previously, it has been shown that Ca^{2+} overloading may induce cell apoptosis in lymphocytes (Shen et al..2001). We speculate that the inhibitory effect of cGMP and protein kinase G on $[Ca^{2+}]_i$ rise protects T-lymphocytes from apoptotic cell death.

It is still not clear how much of this histamine-induced $[Ca^{2+}]_i$ rise is due to Ca^{2+} release from the intracellular Ca^{2+} stores and how much is due to Ca^{2+} influx. Previous studies suggested that both store Ca^{2+} release and extracellular Ca^{2+} influx contributes to this histamine-induced $[Ca^{2+}]_i$ rise, with Ca^{2+} influx being the major component (Kitamura et al.,1996). In the previous chapter, we found that store-operated Ca^{2+} influx is inhibited by cGMP and protein kinase G. Therefore, we speculate that histamine induces Ca^{2+} influx mainly through store-operated Ca^{2+} influx pathway. To our support, similar to store-operated Ca^{2+} influx in Jurkat T cells, this histamine-induced Ca influx could be inhibited by cGMP, protein kinase G and SNAP. The inhibition could be reversed by KT5823, DT2, and ODQ. Thus, the patterns of cGMP and PKG inhibition as well as the potency of inhibition are remarkably similar between store-operated Ca influx and histamine-induced Ca influx. We have shown that, in HEK cell studies, histamine activates TRPC3 channels (Kwan et al., 2009). TRPC3 channels are present on T lymphocytes (Philipp et al., 2003) and are negatively regulated by PKG (Kwan et al., 2004). Hence TRPC3 could be a possible downstream target in the cGMP signaling pathway.

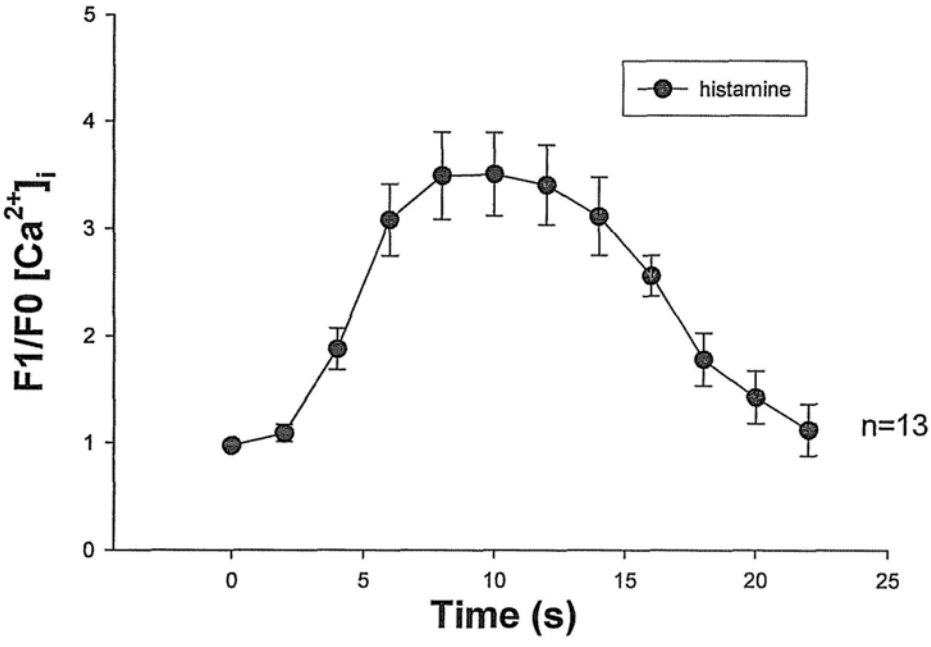

Figure 6-1. Trace showing the change in $[Ca^{2+}]_i$ induced by 100 μM histamine in Jurkat T cells bathing in normal physiological saline.

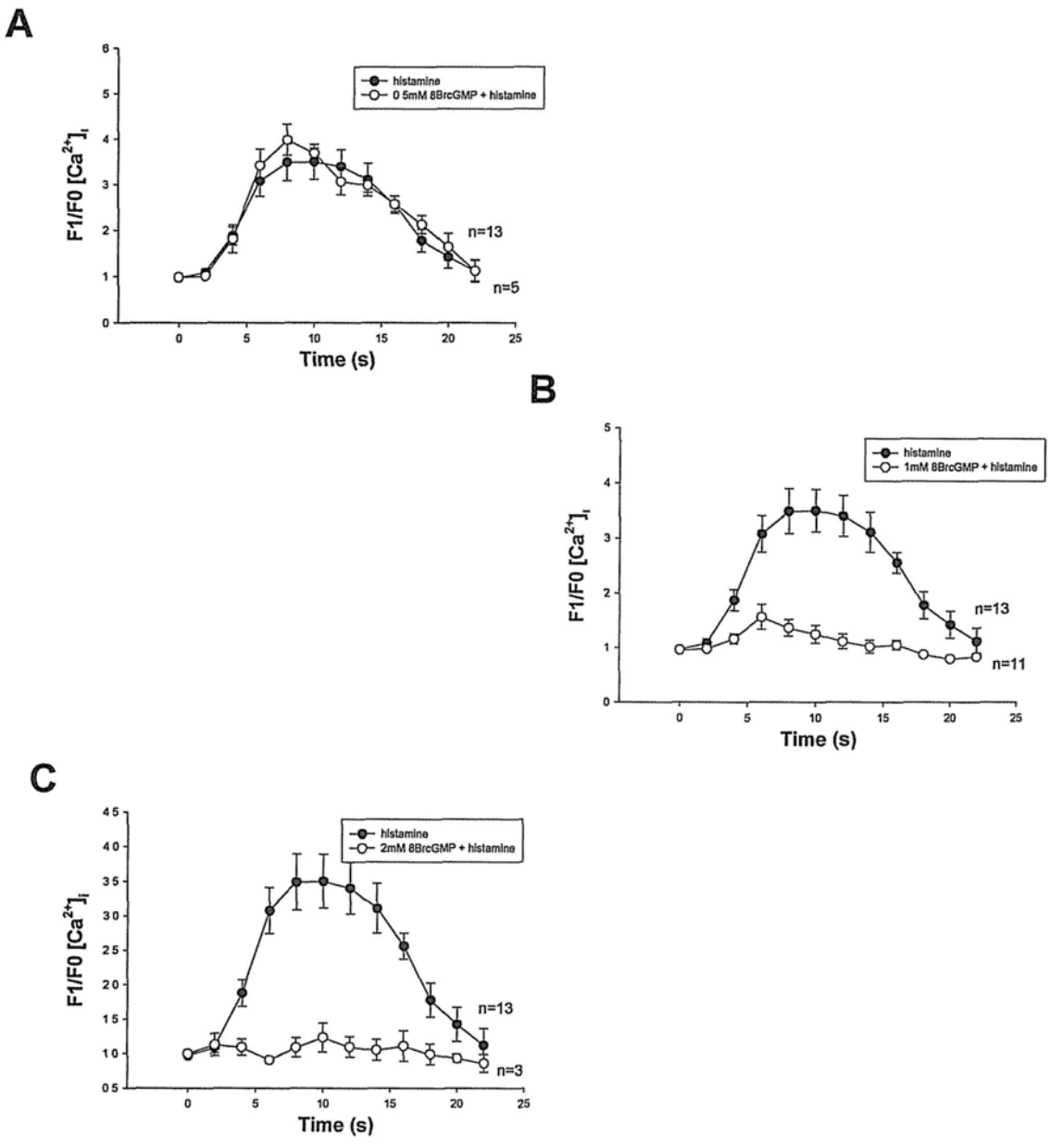

Figure 6-2. Traces showing the effect of different concentration of 8-Br-cGMP (0.5 mM to 2 mM) pretreatments on the histamine (100 μM)-induced $[Ca^{2+}]_i$ rise in Jurkat cells. A, 0.5 mM; B, 1 mM; C, 2 mM.

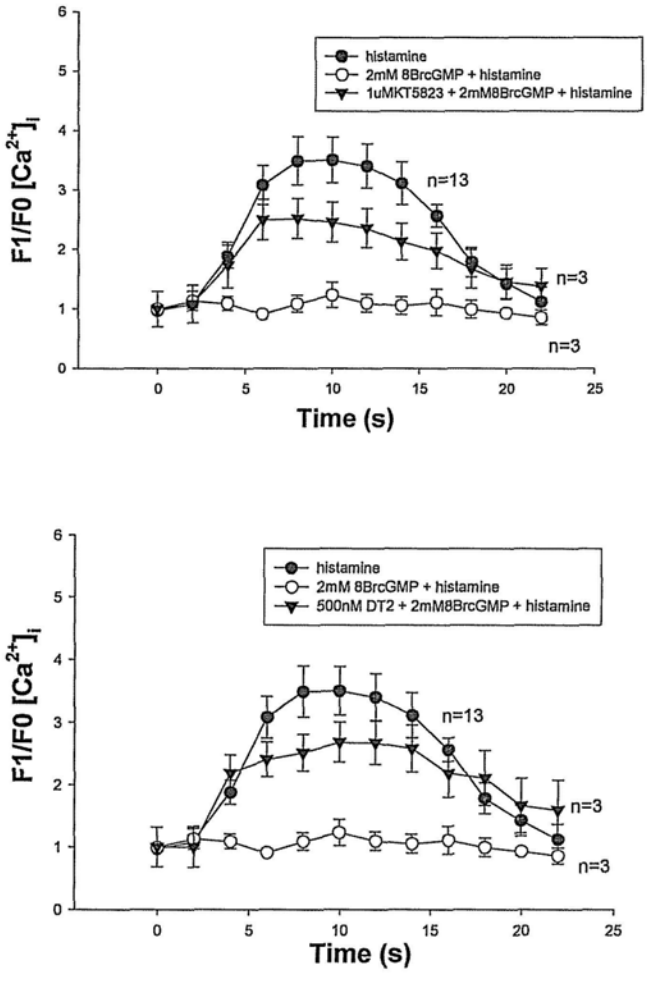

Figure 6-3. Effect of KT-5823 and DT-2 on the sensitivity of histamine-induced $[Ca^{2+}]_i$ increase to 8-Br-cGMP inhibition in Jurkat cells. **A**. 1 μM KT-5823 partially reversed the inhibition imposed by 2 mM cGMP on the histamine-induced $[Ca^{2+}]_i$ rise. **B**. 500 nM DT-2 partially reversed the cGMP inhibition.

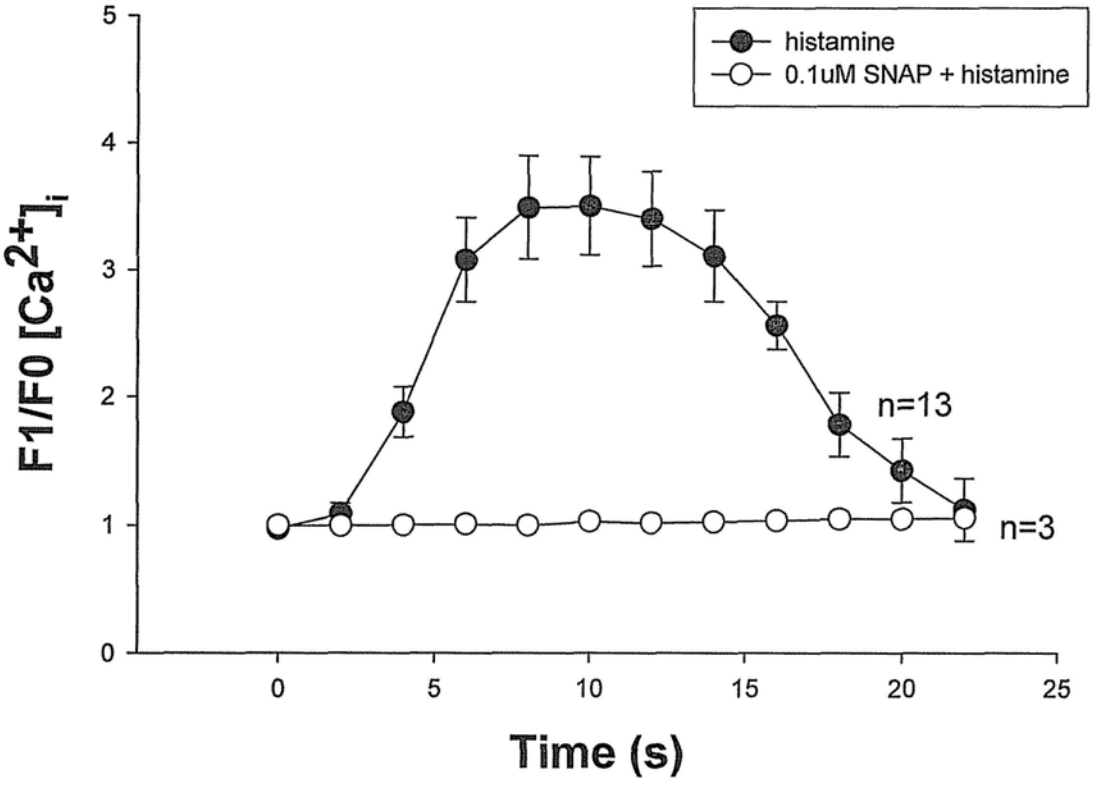

Figure 6-4. 0.1 μM SNAP pretreatment totally abolished the $[Ca^{2+}]_i$ rise induced by 100 μM histamine.

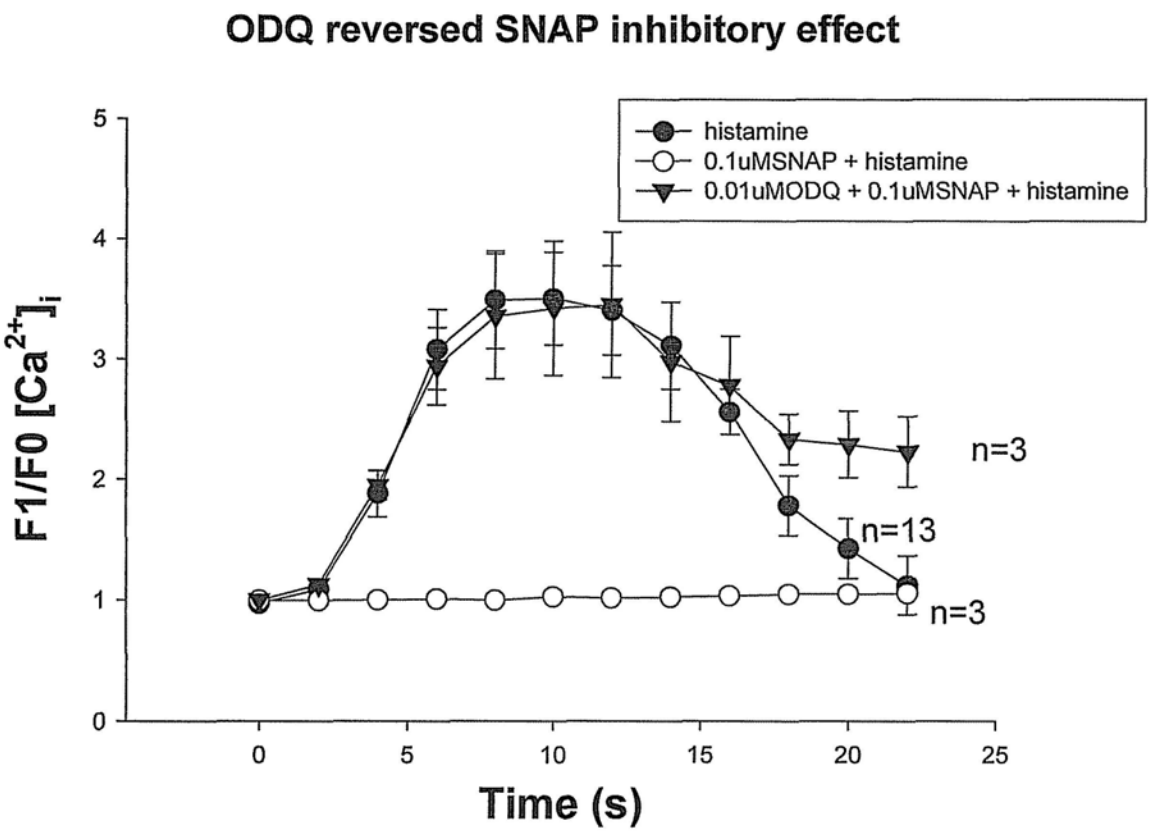

Figure 6-5. 10 nM ODQ, a guanylate cyclase inhibitor, was able to reverse the effect of 100 nM SNAP on the histamine-induced $[Ca^{2+}]_i$ rise.

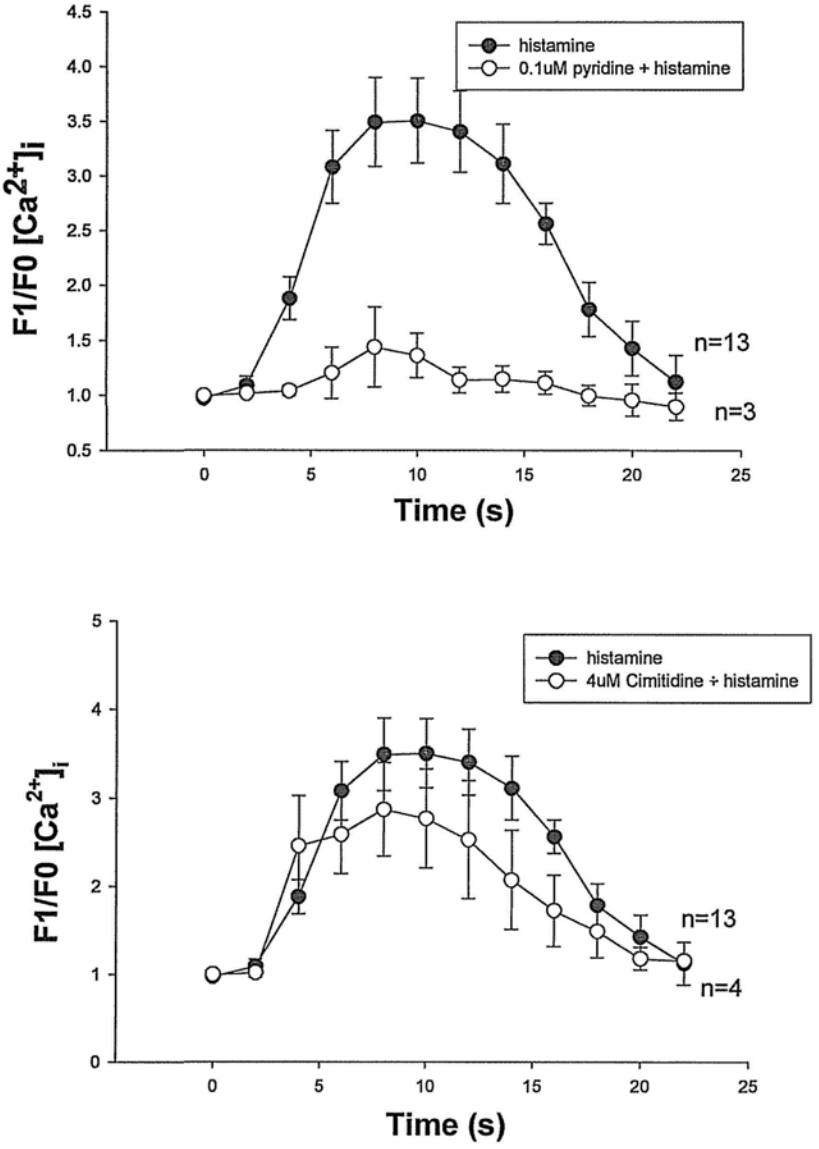

Figure 6-6. Effect of histamine receptor antagonists on the histamine induced calcium signal. **A.** 0.1 μM pyrilamine, H1R antagonist. **B.** 4 μM cimetidine, H2R antagonist

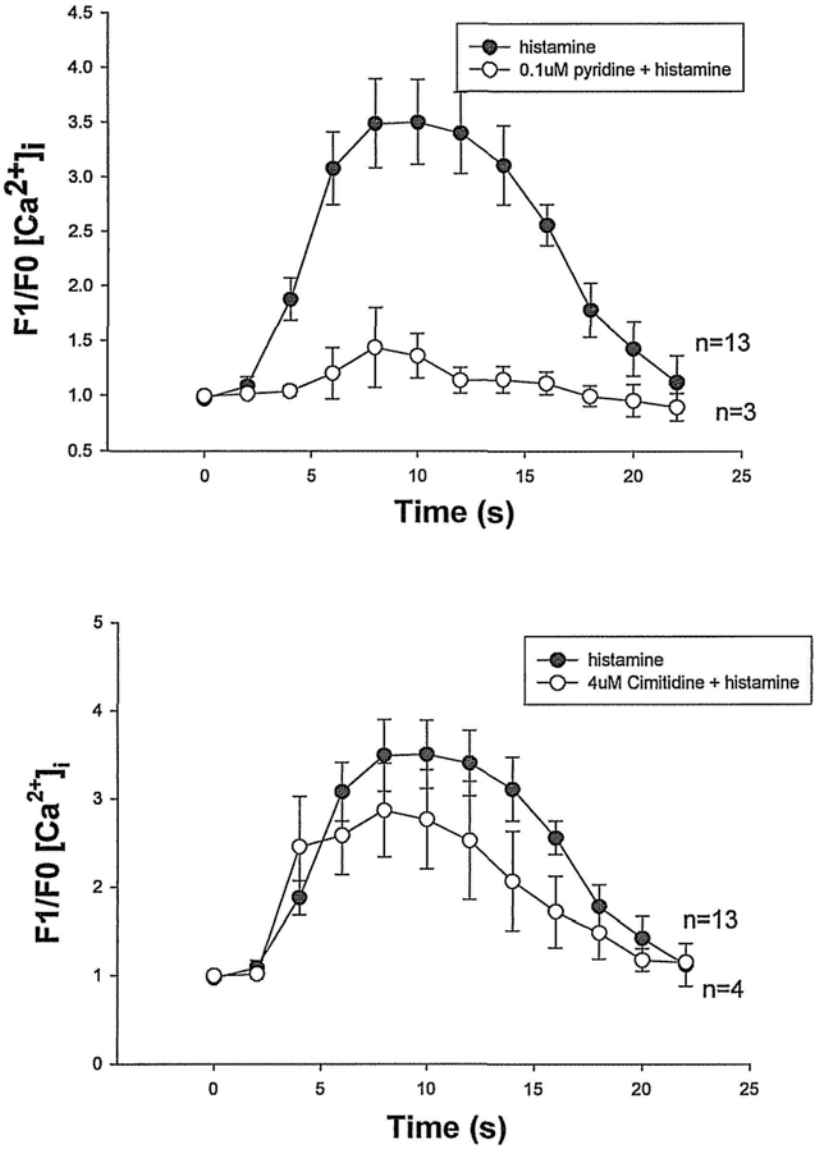

Figure 6-6. Effect of histamine receptor antagonists on the histamine induced calcium signal. **A**. 0.1 μM pyrilamine, H1R antagonist. **B**. 4 μM cimetidine, H2R antagonist

Chapter 7

General Discussion and Conclusion

7.1 General overview

The ubiquitous expression of adenylyl cyclase (AC), guanylyl cyclase (GC) and phosphodiesterase (PDE) make cyclic nucleotides (cGMP and cAMP) important signaling molecules in cells. A total of 9 AC isoforms, 2 types of GC and over 90 PDE isoforms have been identified, compounded with their differential expression in subcellular compartments and across cell types, enable accurate regulation of cyclic nucleotides level and their distinctive subsets of downstream targets. CNG channels are one of the many targets of cyclic nucleotides and their opening enables cation influx, causing membrane depolarization and/or resulting in intracellular calcium rise.

7.2 Possible role of CNG channels in endothelial and smooth muscle cells and future direction

My current work on endothelial cells suggested that CNGA2 channels play a key role in adenosine and epinephrine-induced vasorelaxation. However, the results that TP receptor agonist elicited smooth muscle contraction suggested that CNGA2 channel may be involved in the vasoconstriction. Most other studies in smooth muscle cells have linked cyclic nucleotides to vasorelaxation. Therefore, more work may need to be done to elucidate the detailed mechanism of how CNG channels are linked to vasocontraction in vascular smooth muscle cells. For examples, signaling pathway involved in the TP receptor stimulation of smooth muscle cells need to be clarified; AC and GC inhibitors may be used to confirm the involvement of cyclic nucleotides

in the signaling pathway; FRET-based imaging approach may be employed to visualize the increase in cAMP or cGMP level in response to the agonist and its subcellular localization. Another problem is that pharmacological CNG channel blockers in general can not differentiate different CNG isoforms. Thus siRNA against a specific CNG subtype may be needed to be utilized in future to study the subtype of CNG channel involved. CNG knockout mice offer another useful tool. Smooth muscle contraction studies using myograph can be used in CNG knockout mice to give clues on the roles of CNG isoforms in TP receptor agonist-induced contraction. One problem is that CNGA2 knockout mice can usually only survive for 1 day after birth. Thus specific baby mice feeding technique may need to be developed to raise CNGA2 knockout mice to adulthood before experiments may be conducted. Several other methods can also be developed. Emerging technique of *in vivo* siRNA transfection and tissue culture technique may enable knockdown of specific CNG subtype in blood vessel smooth muscle cells in the future and facilitate the study of gene functions in tissue. Immunoprecipitation may be performed to study the association, if any, of TP receptor with AC. Dorn and Becker (1993) suggested that stimulation of TP receptor causes a rise in IP_3 and Ca^{2+} release from intracellular Ca^{2+} stores. Cogolludo et al. (2003) suggested that simultaneous opening of calcium-sensitive chloride channels Cl_{Ca} and closing of potassium channels K_v, give rise to membrane depolarization which stimulates the opening of L-type Ca^{2+} channels and sustained Ca^{2+} influx for contraction. The currently available CNG channel blockers cannot analyse if CNG channel contribute to this membrane depolarization but knockout mice study may shed some light on it.

7.3 Role of cGMP in the inhibition of store-operated Ca^{2+} influx in Jurkat cells and future direction

Another important target of cNMPs is protein kinases, PKA or PKG. PKG in particular was shown to regulate intracellular Ca^{2+} level in a number of ways. The current study suggested that cGMP inhibits a store-operated Ca^{2+} channel in Jurkat cell through PKG but the identity of the channel and mechanism of inhibition are unknown. Although previous studies showed that TRPC3 channel, which is also expressed in Jurkat cells, may be opened by store depletion and inhibited by direct phosphorylation by cGMP (Kwan et al., 2004), there was also a report showing that knockdown of TRPC1 and TRPC3 did not affect SOCE in Jurkat cells but knockdown of Orai1 inhibited SOCE (Kim et al., 2009). Specific antibodies against TRPC3 or other Jurkat cell expressing TRP channel, or siRNA, may be used to confirm whether these channels are involved in the PKG-mediated inhibition of SOCE in Jurkat cells. Orai1 and STIM1 were also suggested to be key players in SOCE (Luik & Lewis, 2007), it would be interesting to explore the possible interaction between them and PKG.

PKG activation was shown to inhibit T cell receptor-stimulated human peripheral T cells proliferation and release of interleukin-2. Ca^{2+} release and the subsequent SOCE were found to be a major initial event in TCR-mediated immune response including T cell clonal expansion (Feske, 2007). The current experiments may provide a link between SOCE, PKG and T cell mediated immune response.

7.4 Spreading Ca^{2+} signal in vascular endothelial cells and future direction

Heterogeneity in endothelial cells and their response to different receptor agonists was shown in previous studies (Huang et al., 2000). Spreading of Ca^{2+} signals help to coordinate and synchronize the response along the vessel segment. The current study demonstrated that some endothelial cells or their underlying smooth muscle cells

may act as pacemaker cells in vessels generating spontaneous Ca^{2+} sparks and that the presence of Mg^{2+} ions greatly suppressed the sparks in endothelial cells. Extensive spreading of Ca^{2+} wave was observed upon the application of acetylcholine. Endothelial cell injury can induce Ca^{2+} increase in neighbouring cells which spread across 2-3 cells. Whether this elevation in $[Ca^{2+}]_i$ is related to subsequent tissue repair processes is yet to be confirmed. Further study with unidirectional flow of bathing medium may shed a light on whether the Ca^{2+} signal spread intracellularly through gap junctions or through the secretion of signaling molecules from the damaged cell. The role of cAMP, cGMP, PKA or PKG on the spreading of Ca^{2+} signal may also be assessed by pretreatment of the vessels with the appropriate activators or inhibitors, followed by measuring the difference in speed of wave propagation.

The development of more specific blockers of CNG channels and AC, GC subtypes, and advancement in biotech and imaging techniques would enable easier and more accurate determination of the physiological functions of these important signaling molecules and ion channels.

References

Adams DJ, Hill MA (2004) Potassium channels and membrane potential in the modulation of intracellular calcium in vascular endothelial cells. *J Cardiovasc Electrophysiol.* 15(5):598-610.

Akimoto Y, Horinouchi T, Shibano M, Matsushita M, Yamashita Y, Okamoto T, Yamaki F, Tanaka Y and Koike K (2002) Nitric oxide (NO) primarily accounts for endothelium-dependent component of beta-adrenoceptor-activated smooth muscle relaxation of mouse aorta in response to isoprenaline, *J. Smooth. Muscle. Res.* 38: 87–99

Alicia S, Angélica Z, Carlos S, Alfonso S, Vaca L. (2008) STIM1 converts TRPC1 from a receptor-operated to a store-operated channel: moving TRPC1 in and out of lipid rafts. *Cell Calcium* 44(5): 479–491

Arita H, Nakano T and Hanasaki K (1989) Thromboxane A2: its generation and role in platelet activation. *Progress Lipid Res.* 28: 273–301

Baraldi PG, Romagnoli R, Preti D, Fruttarolo F, Carrion MD, Tabrizi MA (2006) Ligands for A2B adenosine receptor subtype. *Curr Med Chem.*13(28):3467-3482.

Berridge MJ. (1993) Inositol trisphosphate and calcium signaling. *Nature* 361:315-325.

Bian X, Bird GS, Putney JW Jr. (1996) cGMP is not required for capacitative Ca2+ entry in Jurkat T-lymphocytes. *Cell Calcium* 19(4):351-354.

Bönigk W, Bradley J, Müller F, Sesti F, Boekhoff I, Ronnett GV, Kaupp UB, Frings S. (1999) The native rat olfactory cyclic nucleotide-gated channel is composed of three distinct subunits. *J Neurosci.* 19(13):5332-5347

Boo YC, Hwang J, Sykes M, Michell BJ, Kemp BE, Lum H, Jo H (2002) Shear stress stimulates phosphorylation of eNOS at Ser(635) by a protein kinase A-dependent mechanism. *Am J Physiol Heart Circ Physiol.* 283(5):H1819-1828.

Bradley J, Li J, Davidson N, Lester HA, Zinn K. (1994) Heteromeric olfactory cyclic nucleotide-gated channels: a subunit that confers increased sensitivity to cAMP. *Proc Natl Acad Sci U S A.* 91(19):8890-8894.

Brain SD, Grant AD (2003) Vascular actions of calcitonin gene-related peptide and adrenomedullin. *Physiol Rev.* 84: 903–934.

Braunstein TH, Inoue R, Cribbs L, Oike M, Ito Y, Holstein-Rathlou NH, Jensen LJ (2009) The Role of L- and T-Type Calcium Channels in Local and Remote Calcium Responses in Rat Mesenteric Terminal Arterioles. *J Vasc Res.* 46(2):138-151.

Brawley L, Shaw AM, MacDonald A (2000) Role of endothelium/nitric oxide in atypical beta-adrenoceptor-mediated relaxation in rat isolated aorta. *Eur. J. Pharmacol.* 398: 285–296.

Brock TA, Dennis PA, Griendling KK, Diehl TS, Davies PF. (1988) GTP gamma S loading of endothelial cells stimulates phospholipase C and uncouples ATP receptors, *Am. J. Physiol.* 255: C667–C673.

Buchan KW, Martin W. (1991) Modulation of agonist-induced calcium mobilisation in bovine aortic endothelial cells by phorbol myristate acetate and cyclic AMP but not cyclic GMP. *Br. J. Pharmacol.* 104: 361–366.

Busse R, Pohl U, Lückhoff A. (1989) Mechanisms controlling the production of endothelial autacoids. *Z. Kardiol.* 78 Suppl 6: 64–69.

Cassar SC, Chen J, Zhang D, Gopalakrishnan M. (2004) Tissue specific expression of alternative splice forms of human cyclic nucleotide gated channel subunit CNGA3. *Mol Vision* 10: 808-813

Chamorro A. (2009) TP Receptor Antagonism: A New Concept in Atherothrombosis and Stroke Prevention. *Cerebrovasc Dis* 27 (Suppl. 3):20-27

Chen H, Levine YC, Golan DE, Michel T, Lin AJ. (2008) Atrial natriuretic peptide-initiated cGMP pathways regulate vasodilator-stimulated phosphoprotein phosphorylation and angiogenesis in vascular endothelium. *J Biol Chem.* 283(7):4439-4447.

Chen J, Wang Y, Nakajima T, Iwasawa K, Hikiji H, Sunamoto M, Choi DK, Yoshida Y, Sakaki Y, Toyo-Oka T (2000) Autocrine action and its underlying mechanism of nitric oxide on intracellular Ca2+ homeostasis in vascular endothelial cells. *J Biol Chem.* 275(37):28739-28749.

Chen TY, Peng YW, Dhallan RS, Ahamed B, Reed RR, Yau KW. (1993) A new subunit of the cyclic nucleotide-gated cation channel in retinal rods. *Nature* 362(6422):764-767

Cheng KT, Chan FL, Huang Y, Chan WY, Yao X. (2003) Expression of olfactory-type cyclic nucleotide-gated channel (CNGA2) in vascular tissues. *Histochem Cell Biol.* 120(6):475-481.

Cheng KT, Liu X, Ong HL, Ambudkar IS. (2008) Functional requirement for Orai1 in store-operated TRPC1-STIM1 channels. *J. Biol. Chem.* 283:12935–12940

Cogolludo A, Moreno L, Bosca L, Tamargo J, Perez-Vizcaino F. (2003) Thromboxane A2-induced inhibition of voltage-gated K+ channels and pulmonary vasoconstriction. *Circ Res.* 93:656-663

Cohen RA, Weisbrod RM, Gericke M, Yaghoubi M, Bierl C, Bolotina VM. Mechanism of nitric oxide-induced vasodilatation: refilling of intracellular stores by sarcoplasmic reticulum Ca2+ ATPase and inhibition of store-operated Ca2+ influx. *Circ Res.* 1999 84(2):210-219.

Davis MJ, Donovitz JA, Hood JD. (1992) Stretch-activated single-channel and whole cell currents in vascular smooth muscle cells. *Am J Physiol.* 262(4 Pt 1):C1083-1088.

De Backer MD, Gommeren W, Moereels H, Nobels G, Van Gompel P, Leysen JE, Luyten WH (1993) Genomic cloning, heterologous expression and pharmacological characterization of a human histamine H1 receptors. *Biochem Biophys Res Commun.* 197(3):1601-1608.

DeWitt DL, Day JS, Sonnenburg WK, Smith WL. (1983) Concentrations of prostaglandin endoperoxide synthase and prostaglandin I2 synthase in the endothelium and smooth muscle of bovine aorta. *J Clin Invest.* 72(6):1882-1888.

Dimopoulos GJ, Semba S, Kitazawa K, Eto M, Kitazawa T (2007) Ca2+-dependent rapid Ca2+ sensitization of contraction in arterial smooth muscle. *Circ Res.* 100(1):121-129.

Ding C, Potter ED, Qiu W, Coon SL, Levine MA, Guggino SE (1997) Cloning and widespread distribution of the rat rod-type cyclic nucleotide-gated cation channel. *Am J Physiol* 272: C1335-C1344

Djellas Y, Manganello JM, Antonakis K, Le Breton GC. (1999) Indentification of Gα13 as one of the G-proteins that couple to human platelet thromboxane A2 receptors. *J Biol Chem* 274:14325–14330.

Dohlsten M, Sjögren HO, Carlsson R. (1987) Histamine acts directly on human T cells to inhibit interleukin-2 and interferon-gamma production. *Cell Immunol.* 109(1):65-74.

Dora KA, Garland CJ, Kwan HY, Yao X. Endothelial cell protein kinase G inhibits release of EDHF through a PKG-sensitive cation channel. *Am J Physiol Heart Circ Physiol.* 2001;280:H1272-H1277.

Dorn GW 2nd, Becker MW (1993) Thromboxane A2 stimulated signal transduction in vascular smooth muscle. *J Pharmacol Exp Ther.* 265(1):447-456

Duza T, Sarelius IH (2003) Conducted dilations initiated by purines in arterioles are endothelium dependent and require endothelial Ca2+. *Am J Physiol Heart Circ Physiol.* 285: H26–H37.

Duza T, Sarelius IH (2004) Increase in endothelial cell Ca2+ in response to mouse cremaster muscle contraction. *J Physiol.* 555: 459–469.

Fahim M, Hussain T, Mustafa SJ. (2001) Relaxation of rat aorta by adenosine in diabetes with and without hypertension: role of endothelium. *Eur J Pharmacol.* 412: 51–59.

Félétou M, Huang Y, Vanhoutte PM. (2010) Vasoconstrictor prostanoids. *Pflugers Arch.* 459(6):941-950.

Feng JF, Rhee SG, Im MJ. (1996) Evidence that phospholipase δ1 is the effector in the Gh (transglutaminase II)-mediated signaling. *J Biol Chem* 271:16451–16454.

Ferro A, Queen LR, Priest RM, Xu B, Ritter JM, Poston L, Ward JP. (1999) Activation of nitric oxide synthase by beta 2-adrenoceptors in human umbilical vein endothelium in vitro. *Br. J. Pharmacol.* 126:1872–1880.

Feske S, Gwack Y, Prakriya M, Srikanth S, Puppel SH, Tanasa B, Hogan PG, Lewis RS, Daly M, Rao A. (2006) A mutation in Orai1 causes immune deficiency by abrogating CRAC channel function. *Nature* 441:179–185

Feske S. (2007) Calcium signalling in lymphocyte activation and disease. *Nat Rev Immunol.* 7(9):690-702.

Frings S, Lynch JW, Lindemann B (1992) Properties of cyclic nucleotide-gated channels mediating olfactory transduction. Activation, selectivity, and blockage. *J Gen Physiol* 100(1): 45-67

Frings S, Seifert R, Godde M, Kaupp UB. (1995) Profoundly different calcium permeation and blockage determine the specific function of distinct cyclic nucleotide-gated channels. *Neuron* 15(1):169-179.

Gabella G. (1981) Structure of smooth muscle.In E Bulbring, AF Brading, AW Jones and T Tomita (Ed.), *Smooth Muscle: An Assessment of Current Knowledge* London: Arnold.

Gamberucci A, Giurisato E, Pizzo P, Tassi M, Giunti R, McIntosh DP, Benedetti A. (2002) Diacylglycerol activates the influx of extracellular cations in T-lymphocytes independently of intracellular calcium-store depletion and possibly involving endogenous TRP6 gene products. *Biochem J.* 364(Pt 1):245-254.

Gantz I, Munzert G, Tashiro T, Schäffer M, Wang L, DelValle J, Yamada T. (1991) Molecular cloning of the human histamine H2 receptor. *Biochem Biophys Res Commun.* 178(3):1386-1392.

Ginsberg MD (2008) Neuroprotection for ischemic stroke: past, present and future. *Neuropharmacology* 55(3):363-389.

Gluais P, Lonchampt M, Morrow JD, Vanhoutte PM, Feletou M. (2005) Acetylcholine-induced endothelium-dependent contractions in the SHR aorta: the Janus face of prostacyclin. *Br J Pharmacol.* 146(6):834-845.

Gordon SE, Downing-Park J and Zimmerman AL (1995) Modulation of the cGMP-gated ion channel in frog rods by calmodulin and an endogenous inhibitory factor. *J. Physiol.* 486:533–546

Graier WF, Groschner K, Schmidt K, Kukovetz WR. (1992) Increases in endothelial cyclic AMP levels amplify agonist-induced formation of endothelium-derived relaxing factor (EDRF). *Biochem. J.* 288:345–349.

Graier WF, Kukovetz WR, Groschner K. (1993) Cyclic AMP enhances agonist-induced Ca2+ entry into endothelial cells by activation of potassium channels and membrane hyperpolarization. *Biochem. J.* 291:263–267.

Gray DW, Marshall I. (1992) Novel signal transduction pathway mediating endothelium-dependent beta-adrenoceptor vasorelaxation in rat thoracic aorta. *Br. J. Pharmacol.* 107:637–684.

Guimarães S, Moura D. (2001) Vascular adrenoceptors: an update. *Physiol. Rev.* 53:319–356.

Hamberg M., Svensson J. and Samuelsson B. (1975) Thromboxanes: A new group of biologically active compounds derived from prostaglandin endoperoxides. *Proc Natl Acad Sci U S A* 72:2994–2998

Hartshorne DJ, Ito M, Erdödi F. (2004) Role of protein phosphatase type 1 in contractile functions: myosin phosphatase. *J Biol Chem.* 279(36):37211-37214.

Haynes LW. (1992) Block of the cyclic GMP-gated channel of vertebrate rod and cone photoreceptors by l-cis-diltiazem. *J Gen Physiol.* 100(5):783-801.

Heymes C, Habib A, Yang D, Mathieu E, Marotte F, Samuel J, Boulanger CM. (2000) Cyclo-oxygenase-1 and -2 contribution to endothelial dysfunction in ageing. *Br J Pharmacol.* 131(4):804-810.

Hirata M, Hayashi Y, Ushikubi F, Yokota Y, Kageyama R, Nakanishi S, Narumiya S. (1991) Cloning and expression of cDNA for a human thromboxane A2 receptor. *Nature* 349(6310):617-620

Hirata T, Ushikubi F, Kakizuka A, Okuma M, Narumiya S. (1996) Two thromboxane A2 receptor isoforms in human platelets. Opposite coupling to adenylyl cyclase with different sensitivity to Arg60 to Leu mutation. *J Clin Invest.* 97(4):949-956

Hla T, Neilson K. (1992) Human cyclooxygenase cDNA. *Proc Natl Acad Sci U S A.* 89(16):7384-7388

Huang GN, Zeng W, Kim JY, Yuan JP, Han L, Muallem S, and Worley PF (2006) STIM1 carboxyl-terminus activates native SOC, I(crac) and TRPC1 channels. *Nat. Cell Biol.* 8(9):1003–1010

Huang JS, Ramamurthy SK, Lin X, Le Breton GC. (2004) Cell signaling through thromboxane A2 receptors. *Cell Signal.* 16(5):521-533.

Huang TY, Chu TF, Chen HI, Jen CJ. (2000) Heterogeneity of [Ca2+]i signaling in intact rat aortic endothelium. *FASEB J.* 14:797–804

Hwang KC, Gray CD, Sivasubramanian N, Im MJ. (1995) Interaction Site of GTP Binding Gh (Transglutaminase II) with phospholipase C. *J Biol Chem* 270: 27058–27062.

Imboden JB & Stobo JD (1985) Transmembrane signalling by the T cell antigen receptor: Perturbation of the T3-antigen receptor complex generates inositol phosphates and releases calcium ions from intracellular stores. *J. Exp. Med.* 161:446–456.

Jaggar JH, Stevenson AS, Nelson MT. (1998) Voltage dependence of Ca2+ sparks in intact cerebral arteries. *Am J Physiol.* 274(6 Pt 1):C1755-1761.

Jutel M, Watanabe T, Klunker S, Akdis M, Thomet OA, Malolepszy J, Zak-Nejmark T, Koga R, Kobayashi T, Blaser K, Akdis CA. (2001) Histamine regulates T-cell and antibody responses by differential expression of H1 and H2 receptors. *Nature.* 413(6854):420-425.

Kansui Y, Garland CJ, Dora KA. (2008) Enhanced spontaneous Ca2+ events in endothelial cells reflect signalling through myoendothelial gap junctions in pressurized mesenteric arteries. *Cell Calcium* 44(2):135-146.

Kaupp UB, Seifert R (2002) Cyclic nucleotide-gated ion channels. *Physiol Rev.* 82(3):769-824.

Kawano Y, Fukata Y, Oshiro N, Amano M, Nakamura T, Ito M, Matsumura F, Inagaki M, Kaibuchi K. (1999) Phosphorylation of myosin-binding subunit (MBS) of myosin phosphatase by Rho-kinase in vivo. *J Cell Biol.* 147(5):1023-1038.

Kawasaki T, Lange I, Feske S. (2009) A minimal regulatory domain in the C terminus of STIM1 binds to and activates ORAI1 CRAC channels. *Biochem. Biophys. Res. Commun.* 385:49–54

Kim MS, Zeng W, Yuan JP, Shin DM, Worley PF, Muallem S. (2009) Native store-operated Ca2+ influx requires the channel function of Orai1 and TRPC1. *J Biol Chem.* 284(15):9733-9741

Kinsella BT, O'Mahony DJ, Fitzgerald GA. (1997) The human thromboxane A2 receptor α isoform (TPα) functionally couples to the G proteins Gq and G11 in vivo and is activated by the isoprostane 8-epi progstaglandin F2α. *J Pharmacol Exp Therap* 281:957–964.

Kitamura Y, Arima T, Kitayama Y, Nomura Y. (1996) Regulation of [Ca2+]i rise activated by doxepin-sensitive H1-histamine receptors in Jurkat cells, cloned human T lymphocytes. *Gen Pharmacol.* 27(2):285-291.

Kleene SJ, Gesteland RC. (1991) Calcium-activated chloride conductance in frog olfactory cilia. *J Neurosci.* 11(11):3624-3629.

Kruse LS, Sandholdt NTH, Gammeltoft S, Olesen J, Kruuse C. (2006) Phosphodiesterase 3 and 5 and cyclic nucleotide-gated ion channel expression in rat trigeminovascular system. *Neurosci Lett* 404: 202-207

Kwan HY, Huang Y, Yao X. (2000) Store-operated calcium entry in vascular endothelial cells is inhibited by cGMP via a protein kinase G-dependent mechanism. *J Biol Chem.* 275(10):6758-6763.

Kwan HY, Huang Y, Yao X. (2004) Regulation of canonical transient receptor potential isoform 3 (TRPC3) channel by protein kinase G. *Proc Natl Acad Sci U S A.* 101(8):2625-2630.

Kwan HY, Huang Y, Yao X. (2007) Cyclic nucleotides and Ca2+ influx pathways in vascular endothelial cells. *Clin Hemorheol Microcirc.*37(1-2):63-70.

Kwan HY, Wong CO, Chen ZY, Dominic Chan TW, Huang Y, Yao X. (2009) Stimulation of histamine H2 receptors activates TRPC3 channels through both phospholipase C and phospholipase D. *Eur J Pharmacol.*602(2-3):181-187.

Lau KL, Kong SK, Ko WH, Kwan HY, Huang Y, Yao X. (2003) cGMP stimulates endoplasmic reticulum Ca(2+)-ATPase in vascular endothelial cells. *Life Sci.* 73(16):2019-2028.

Leinders-Zufall T, Rand MN, Shepherd GM, Greer CA, Zufall F. (1997) Calcium

entry through cyclic nucleotide-gated channels in individual cilia of olfactory receptor cells: spatiotemporal dynamics. *J Neurosci* 17: 4136-4148

Leopoldt D, Harteneck C, Nürnberg B. (1997) G proteins endogenously expressed in Sf 9 cells: interactions with mammalian histamine receptors. Naunyn Schmiedebergs Arch Pharmacol. 356(2):216-224.

Lewis RS. (2003) Calcium oscillations in T-cells: mechanisms and consequences for gene expression. *Biochem Soc Trans.* 31(Pt 5):925-929.

Liao, Y., Erxleben, C., Abramowitz, J., Flockerzi, V., Zhu, M. X., Armstrong, D. L., and Birnbaumer, L. (2008) Functional interactions among Orai1, TRPCs, and STIM1 suggest a STIM-regulated heteromeric Orai/TRPC model for SOCE/Icrac channels. *Proc. Natl. Acad. Sci. U. S. A.* 105:2895–2900

Liao Y, Erxleben C, Yildirim E, Abramowitz J, Armstrong DL, and Birnbaumer L (2007) Orai proteins interact with TRPC channels and confer responsiveness to store depletion. *Proc. Natl. Acad. Sci. U. S. A.* 104:4682–4687

Liman ER, Buck LB (1994) A second subunit of the olfactory cyclic nucleotide-gated channel confers high sensitivity to cAMP. *Neuron* 13(3):611-621.

Lincoln TM, Dey N, Sellak H. (2001) cGMP-dependent protein kinase signaling mechanisms in smooth muscle: from the regulation of tone to gene expression. *J Appl Physiol.* 91:1421–1430.

Liu CQ, Leung FP, Wong SL, Wong WT, Lau CW, Lu L, Yao X, Yao T, Huang Y. (2009) Thromboxane prostanoid receptor activation impairs endothelial nitric oxide-dependent vasorelaxations: the role of Rho kinase. *Biochem Pharmacol.* 78(4):374-381.

Lovenberg TW, Roland BL, Wilson SJ, Jiang X, Pyati J, Huvar A, Jackson MR, Erlander MG. (1999) Cloning and functional expression of the human histamine H3 receptor. *Mol Pharmacol.* 55(6):1101-1107.

Luik RM, Lewis RS. (2007) New insights into the molecular mechanisms of store-operated Ca2+ signaling in T cells. *Trends Mol Med.* 13(3):103-107.

Mark AL, Abboud FM, Schmid PG, Heistad DD, Mayer HE. (1972) Differences in direct effects of adrenergic stimuli on coronary, cutaneous, and muscular vessels, *J.*

Clin. Invest. 51:279–287.

McKenzie C, MacDonald A, Shaw AM (2009) Mechanisms of U46619-induced contraction of rat pulmonary arteries in the presence and absence of the endothelium *Br J Pharmacol.* 157(4):581-596

Miggin SM and Kinsella BT (1998) Expression and tissue distribution of the mRNAs encoding the human thromboxane A2 receptor (TP) α and β isoforms. *Biochim biophys Acta* 1425(3):543-559

Morita H, Cousins H, Onoue H, Ito Y, Inoue R (1999) Predominant distribution of nifedipine-insensitive, high voltage-activated Ca2+ channels in the terminal mesenteric artery of guinea pig. *Circ Res.* 85:596-605.

Muck S, Weber AA, Meyer-Kirchrath J, Schrör K. (1998) The bovine thromboxane A2 receptor: molecular cloning, expression, and functional characterization. *Naunyn Schmiedebergs Arch Pharmacol.* 357(1):10-16

Muik M, Fahrner M, Derler I, Schindl R, Bergsmann J, et al. (2009) A cytosolic homomerization and a modulatory domain within STIM1 C terminus determine coupling to ORAI1 channels. *J. Biol. Chem.* 284:8421–8426

Musso CG. (2009) Magnesium metabolism in health and disease. *Int Urol Nephrol.* 41(2):357-362.

Nakahata N (2008) Thromboxane A2: physiology/pathophysiology, cellular signal transduction and pharmacology. *Pharmacol Ther.* 118(1):18-35

Nakamura T, Gold GH. (1987) A cyclic nucleotide-gated conductance in olfactory receptor cilia. *Nature.* 325(6103):442-444.

Nilius B and Groogman G. (2001) Ion channels and their functional role in vascular endothelium, *Physiol. Rev.* 81:1415–1459.

Oda T, Morikawa N, Saito Y, Masuho Y, Matsumoto S. (2000) Molecular cloning and characterization of a novel type of histamine receptor preferentially expressed in leukocytes. *J Biol Chem.* Nov 24;275(47):36781-36786.

Offermans S, Laugwitz KL, Spicher K and Schultz G. (1994) G proteins of the G12

family are activated via thromboxane A2 and thrombin receptors in human platelets. *Proc Natl Acad Sci* 91:504–508.

Ogletree ML. (1987) Overview of physiological and pathophysiological effects of thromboxane A2. *Fed Proc* 46:133-138

Oh-hora M. (2009) Calcium signaling in the development and function of T-lineage cells. *Immunol Rev.* 231(1):210-224

Ong HL, Cheng KT, Liu X, Bandyopadhyay BC, Paria BC, Soboloff J, Pani B, Gwack Y, Srikanth S, Singh BB, Gill DL, Ambudkar IS. (2007) Dynamic assembly of TRPC1-STIM1-Orai1 ternary complex is involved in store-operated calcium influx. Evidence for similarities in store-operated and calcium release-activated calcium channel components. *J. Biol. Chem.* 282:9105–9116

Pani B, Ong HL, Liu X, Rauser K, Ambudkar IS, Singh BB. (2008) Lipid rafts determine clustering of STIM1 in endoplasmic reticulum-plasma membrane junctions and regulation of store-operated Ca2+ entry (SOCE). *J. Biol. Chem.* 283:17333–17340

Park CY, Hoover PJ, Mullins FM, Bachhawat P, Covington ED, et al. (2009). STIM1 clusters and activates CRAC channels via direct binding of a cytosolic domain to Orai1. *Cell* 136:876–890

Philipp S, Strauss B, Hirnet D, Wissenbach U, Mery L, Flockerzi V, Hoth M. (2003) TRPC3 mediates T-cell receptor-dependent calcium entry in human T-lymphocytes. *J Biol Chem.* 278(29):26629-38.

Phillis JW. (2004) Adenosine and adenine nucleotides as regulators of cerebral blood flow: roles of acidosis, cell swelling, and KATP channels. *Crit Rev Neurobiol.* 16(4):237-270

Priest RM, Hucks D, Ward JP. (1997) Noradrenaline, beta-adrenoceptor mediated vasorelaxation and nitric oxide in large and small pulmonary arteries of the rat. *Br. J. Pharmacol.* 122:1375–1384.

Radvány Z, Darvas Z, Kerekes K, Prechl J, Szalai C, Pállinger E, Valéria L, Varga VL, Sandor M, Erdei A, Falus A. (2000) H1 histamine receptor antagonist inhibits constitutive growth of Jurkat T cells and antigen-specific proliferation of ovalbumin-specific murine T cells. *Semin Cancer Biol.* 10(1):41-45.

Ray CJ, Marshall JM. (2006) The cellular mechanisms by which adenosine evokes release of nitric oxide from rat aortic endothelium. *J Physiol.* 570: 85–96.

Raychowdhury MK, Yukawa M, Collins LJ, McGrail SH, Kent KC, Ware JA. (1994) Alternative splicing produces a divergent cytoplasmic tail in the human endothelial thromboxane A2 receptor. *J Biol Chem.* 269(30):19256-19261

Rispoli G, Menini A. (1988) The blocking effect of l-cis-diltiazem on the light-sensitive current of isolated rods of the tiger salamander. *Eur Biophys J.* 16(2): 65-71

Ristimäki A, Garfinkel S, Wessendorf J, Maciag T, Hla T. (1994) Induction of cyclooxygenase-2 by interleukin-1 alpha. Evidence for post-transcriptional regulation. *J Biol Chem.* 269(16):11769-11775

Sakariassen KS, Alberts P, Fontana P, Mann J, Bounameaux H, Sorensen AS. (2009) Effect of pharmaceutical interventions targeting thromboxane receptors and thromboxane synthase in cardiovascular and renal diseases. *Future Cardiol* 5(5): 479-493

Sakurada S, Takuwa N, Sugimoto N, Wang Y, Seto M, Sasaki Y, Takuwa Y. (2003) Ca2+-dependent activation of Rho and Rho kinase in membrane depolarization-induced and receptor stimulation-induced vascular smooth muscle contraction. *Circ Res.* 93:548-556

Satake K, Lee JD, Shimizu H, Uzui H, Mitsuke Y, Yue H, Ueda T. (2004) Effects of magnesium on prostacyclin synthesis and intracellular free calcium concentration in vascular cells. *Magnes Res.* 17(1):20-27.

Shen B, Cheng KT, Leung YK, Kwok YC, Kwan HY, Wong CO, Chen ZY, Huang Y, Yao X. (2008) Epinephrine-induced Ca2+ influx in vascular endothelial cells is mediated by CNGA2 channels. *J Mol Cell Cardiol.* 45(3):437-45.

Shen HM, Dong SY, Ong CN. (2001) Critical role of calcium overloading in cadmium-induced apoptosis in mouse thymocytes. *Toxicol Appl Pharmacol.* 171(1):12-9

Shenker, P. Goldsmith, C.G. Unson and A.M. Spiegel (1991) The G protein coupled to the thromboxane A2 receptor in human platelets is a member of the novel Gq

family. *J Biol Chem* 266:9309–9313.

Shore SA, Austen KF, and Drazen JM. (1989) Eicosanoids and the lung. In Massaro D (Ed.), *Lung Cell Biology*. New York: Dekker. vol. 41: 1012-1089

Smith WL, DeWitt DL, Garavito RM. (2000) Cyclooxygenases: structural, cellular, and molecular biology. *Annu Rev Biochem.* 69:145-182.

Somlyo AP, Somlyo AV. (2003) Ca2+ sensitivity of smooth muscle and nonmuscle myosin II: modulated by G proteins, kinases, and myosin phosphatase. *Physiol Rev.* 83(4):1325-58.

Song Y, Cygnar KD, Sagdullaev B, Valley M, Hirsh S, Stephan A, Reisert J, Zhao H. (2008) Olfactory CNG channel desensitization by Ca2+/CaM via the B1b subunit affects response termination but not sensitivity to recurring stimulation. *Neuron.* 58(3):374-386

Sontia B, Touyz RM. (2007) Role of magnesium in hypertension. *Arch Biochem Biophys.* 458(1):33-39.

Stern JH, Kaupp UB, Macleish PR. (1986) Control of the light-regulated current in rod photoreceptors by cyclic GMP, calcium, and l-cis-diltiazem. *Proc Natl Acad Sci USA* 83: 1163-1167

Tabrizchi R, Bedi S. (2001) Pharmacology of adenosine receptors in the vasculature. *Pharmacol Ther* 91:133–147

Takano H, Dora KA, Garland CJ. (2005) Spreading vasodilatation in resistance arteries. *J. Smooth Muscle Res.* 41(6):303-311

Tang EH, Vanhoutte PM (2009) Prostanoids and reactive oxygen species: Team players in endothelium-dependent contractions. *Pharmacol Ther.* 122(2):140-149.

Teragawa H, Matsuura H, Chayama K, Oshima T. (2002) Mechanisms responsible for vasodilation upon magnesium infusion in vivo: clinical evidence. *Magnes Res.* 15(3-4):241-246.

Topper JN, Cai J, Falb D, Gimbrone MA Jr. (1996) Identification of vascular

endothelial genes differentially responsive to fluid mechanical stimuli: cyclooxygenase-2, manganese superoxide dismutase, and endothelial cell nitric oxide synthase are selectively up-regulated by steady laminar shear stress. *Proc Natl Acad Sci U S A.* 93(19):10417-10422.

Tosun M, Paul RJ, Rapoport RM. (1998) Role of extracellular Ca++ influx via L-type and non-L-type Ca++ channels in thromboxane A2 receptor-mediated contraction in rat aorta. *J Pharmacol Exp Ther.* 284(3):921-928.

Trochu JN, Leblais V, Rautureau Y, Bévérelli F, Le Marec H, Berdeaux A, Gauthier C. (1999) Beta3-adrenoceptor stimulation induces vasorelaxation mediated essentially by endothelium-derived nitric oxide in rat thoracic aorta. *Br. J. Pharmacol.* 128:69–76.

Vane JR, Mitchell JA, Appleton I, Tomlinson A, Bishop-Bailey D, Croxtall J, Willoughby DA. (1994) Inducible isoforms of cyclooxygenase and nitric-oxide synthase in inflammation. *Proc Natl Acad Sci U S A.* 91(6):2046-2050.

Vanhoutte PM. (2009) COX-1 and vascular disease. *Clin Pharmacol Ther.* 86(2):212-5

Vanhoutte, PM, Feletou M & Taddei S. (2005) Endothelium-dependent contractions in hypertension. *Br. J. Pharmacol.* 144:449-458

Vanhoutte PM, Tang EH. (2008) Endothelium-dependent contractions: when a good guy turns bad! J Physiol. 586(Pt 22):5295-5304.

Vezza R, Habib A, FitzGerald GA. (1999) Differential signaling by the thromboxane receptor isoforms via the novel GTP-binding protein, Gh. *J Biol Chem* 274:12774–12779.

Vig M, Peinelt C, Beck A, Koomoa DL, Rabah D, Koblan-Huberson M, Kraft S, Turner H, Fleig A, Penner R, Kinet JP. (2006) CRACM1 is a plasma membrane protein essential for store-operated Ca2+ entry. *Science* 312:1220–1223

Villalba N, Stankevicius E, Simonsen U, Prieto D. (2008) Rho kinase is involved in Ca2+ entry of rat penile small arteries. *Am J Physiol Heart Circ Physiol.* 294(4):H1923-1932.

Wang C, Li JF, Zhao L, Liu J, Wan J, Wang YX, Wang J, Wang C. (2009) Inhibition of SOC/Ca2+/NFAT pathway is involved in the anti-proliferative effect of sildenafil on pulmonary artery smooth muscle cells. *Respir Res.* 10(1):123.

Wang LD, Hoeltzel M, Gantz I, Hunter R, Del Valle J. (1998) Characterization of the histamine H2 receptor structural components involved in dual signaling. *J Pharmacol Exp Ther.* 285(2):573-578.

Willoughby D & Cooper DM. (2006) Ca2+ stimulation of adenylyl cyclase generates dynamic oscillations in cyclic AMP. *J Cell Sci.* 119(Pt 5):828-36.

Wilson DP, Susnjar M, Kiss E, Sutherland C, Walsh MP (2005) Thromboxane A2-induced contraction of rat caudal arterial smooth muscle involves activation of Ca2+ entry and Ca2+ sensitization: Rho-associated kinase-mediated phosphorylation of MYPT1 at Thr-855, but not Thr-697. *Biochem J.* 389(Pt 3):763-774

Wray S, Burdyga T. (2010) Sarcoplasmic reticulum function in smooth muscle. *Physiol Rev.* 90(1):113-178.

Wu S, Moore TM, Brough GH, Whitt SR, Chinkers M, Li M, Stevens T. (2002) Cyclic nucleotide-gated channels mediate membrane depolarization following activation of store-operated calcium entry in endothelial cells. *J Biol Chem.* 275: 18887–18896.

Wyatt AW, Steinert JR, Wheeler-Jones CP, Morgan AJ, Sugden D, Pearson JD, Sobrevia L, Mann GE. (2002) Early activation of the p42/p44MAPK pathway mediates adenosine-induced nitric oxide production in human endothelial cells: a novel calcium-insensitive mechanism. *FASEB J.* 16:1584–1594.

Xu B, Li J, Gao L, Ferro A. (2000) Nitric oxide-dependent vasodilatation of rabbit femoral artery by beta(2)-adrenergic stimulation or cyclic AMP elevation in vivo. *Br. J. Pharmacol.* 129:969–974.

Yao X (2007) TRPC, cGMP-dependent protein kinases and cytosolic Ca2+. *Handb Exp Pharmacol.* 179:527-540

Yao X, Huang Y. (2003) From nitric oxide to endothelial cytosolic Ca2+: a negative feedback control. *Trends Pharmacol Sci.* 24(6):263-266.

Yao X, Leung PS, Kwan HY, Wong TP, Fong MW. (1999) Rod-type cyclic

nucleotide-gated cation channel is expressed in vascular endothelium and vascular smooth muscle cells. *Cardiovasc Res.* 41(1):282-290

Yashiro Y, Duling BR (2000) Integrated Ca(2+) signaling between smooth muscle and endothelium of resistance vessels. *Circ Res.* 87(11):1048-1054

Ye CL, Shen B, Ren XD, Luo RJ, Ding SY, Yan FM, Jiang JH. (2004) An increase in opening of BK(Ca) channels in smooth muscle cells in streptozotocin-induced diabetic mice. *Acta Pharmacol Sin* 25(6): 744-750

Ying X, Minamiya Y, Fu C, Bhattacharya J. (1996) Ca2+ waves in lung capillary endothelium. *Circ Res.* 79(4):898-908.

Yuan JP, Zeng W, Dorwart MR, Choi YJ, Worley PF, Muallem S. (2009) SOAR and the polybasic STIM1 domains gate and regulate Orai channels. *Nat. Cell Biol.* 11:337–343

Yuan JP, Zeng W, Huang GN, Worley PF, Muallem S. (2007) STIM1 heteromultimerizes TRPC channels to determine their function as store-operated channels. *Nat Cell Biol.* 9(6):636–645

Zaccolo M, Movsesian MA (2007) cAMP and cGMP signaling cross-talk: role of phosphodiesterases and implications for cardiac pathophysiology. *Circ Res.* 100(11):1569-1578.

Zembowicz A, Jones SL, Wu KK. (1995) Induction of cyclooxygenase-2 in human umbilical vein endothelial cells by lysophosphatidylcholine. *J Clin Invest.* 96(3):1688-1692.

Zhang J, Xia SL, Block ER, Patel JM. (2002) NO upregulation of a cyclic nucleotide-gated channel contributes to calcium elevation in endothelial cells. *Am J Physiol Cell Physiol.* 283: C1080–C1089.

Zhang SL, Yeromin AV, Zhang XH, Yu Y, Safrina O, Penna A, Roos J, Stauderman KA, Cahalan MD. (2006) Genome-wide RNAi screen of Ca(2+) influx identifies genes that regulate Ca(2+) release-activated Ca(2+) channel activity. *Proc. Natl. Acad. Sci. U. S. A.* 103:9357–9362

Zheng J, Zagotta WN. (2004) Stoichiometry and assembly of olfactory cyclic nucleotide-gated channels. *Neuron* 42:411–421.

Zhou C, Wu S. (2006) T-type calcium channels in pulmonary vascular endothelium. *Microcirculation.* 13(8):645-656.

Zhou Y, Meraner P, Kwon HT, Machnes D, Oh-hora M, et al. (2010) Minimal requirement for store-operated calcium entry: STIM1 gates ORAI1 channels in vitro. *Nat. Struct. Mol. Biol.* 17:112–116

Zolle O, Lawrie AM, Simpson AW. (2000) Activation of the particulate and not the soluble guanylate cyclase leads to the inhibition of Ca2+ extrusion through localized elevation of cGMP. *J Biol Chem.* 275(34):25892-25899.